KINETIC STUDIES OF B/HLH/Z TRANSCRIPTION FACTORS MYC/MAX/MAD

by

OZGUR ECEVIT

A dissertation submitted to the Graduate Faculty in Chemistry in partial fulfillment of the requirements for the degree of Doctor of Philosophy,

The City University of New York

2008

This manuscript has been read and accepted for the
Graduate Faculty in Chemistry in satisfaction of the
dissertation requirement for the degree of Doctor of Philosophy.

Prof. Dixie J. Goss

Date **Chair of Examining Committee**

Prof. Mahesh K. Lakshman

Date **Executive Officer**

Prof. Ruth Stark

Date

Prof. Yujia Xu

Date **Supervisory Committee**

THE CITY UNIVERSITY OF NEW YORK

Abstract

KINETIC STUDIES OF B/HLH/Z TRANSCRIPTION FACTORS MYC/MAX/MAD

by

Ozgur Ecevit

Adviser: Professor Dixie J. Goss

Myc, Mad and Max proteins belong to the basic helix-loop-helix leucine zipper family of transcription factors. They bind to a specific hexanucleotide element of DNA, the E-box (CACGTG). In order to be biologically active, Myc and Mad require dimerization with Max. For the route of complex assembly of these dimers, there are two proposed pathways. Monomer pathway: Two monomers bind DNA sequentially and assemble their dimerization interface while bound to DNA. Dimer pathway: Two monomers form a dimer first, and then associate with DNA.

Stopped flow polarization was utilized to determine the rate of the individual steps in the assembly pathway. Individual rate constants were assigned to dimer formation, DNA binding of dimeric Max-Max, Myc-Max and Mad-Max and DNA binding of monomeric transcription factors. The kinetic effects of Myc-Max, Mad-Max and Max-Max dimerization and the temperature dependence of these reactions were measured and compared. Stopped-flow anisotropy data showed that Myc-Max dimerization had ~5-fold and ~2-fold higher rate constant than Max-Max and Mad-Max, respectively. The Myc, Max and Mad dimerization rates were found to be

concentration independent suggesting conformational changes were rate limiting. There was no significant difference in the Arrhenius activation energies calculated for the dimerization of Myc, Max and Mad.

The rate constants for the DNA binding of Max-Max homodimer, Myc-Max and Mad-Max heterodimers were also studied as a function of temperature and concentration. Results showed that the average rate constants for the Max-Max-DNA and Myc-Max-DNA are 1.7 and 1.5 fold higher than for the Mad-Max-DNA, respectively. Concentration dependence revealed that the interactions between the protein dimers Max-Max, Myc-Max, Mad-Max and the E-box DNA are concentration independent.

To compare the monomer and dimer pathways, the DNA binding rates of monomeric Max and Myc were studied. Results showed that both monomeric and dimeric transcription factors recognize the palindromic E-Box at similar rates. Since the rate of dimer formation is slower than the DNA binding rates, the monomer pathway was kinetically favored over the dimer pathway.

ACKNOWLEDGEMENTS

This dissertation was the culmination of a long process that required the help and support of many.

To start with, I must express my deepest gratitude to my thesis mentor, Professor Dixie Goss, for her endless patience, great support and encouragement. It has been my good fortune to work under her guidance. Without her advisement and support, it would have been impossible to accomplish what is in my hands today. I owe her my lifelong indebtedness.

I thank to the members of my thesis committee, Professor Ruth Stark and Professor Yujia Xu for their most valuable guidance and suggestions to make this thesis a success.

I would like to acknowledge the presence of Professor John Trujillo for his helpful comments and support.

I would also like to express my heartiest gratitude to Professor Klaus Grohmann who was always there whenever I needed him throughout this whole process.

I owe the maximum to Dr. Mateen Khan. Without his help, encouragement and moral support, my completion of the program would not have been accomplished.

I would like to express my sincerest thankfulness to my friends as well as colleagues, Hasan and Sumeyra Yumak, for giving me inspiration to keep going through the ups and downs of a Ph.D.

I am grateful to my former colleagues Dr.Sibnath Ray, Dr.Diana Friedland, Dr.Anamika Banerjee, Dr.Jianzhong Hu and Artem Domashevskiy for their generous help.

Without the love, support and patience of my parents and sisters to whom I owe more than anybody else in my life, it would not have been possible to sustain this project.

To all those I have mentioned as well as those I may have inadvertently forgotten I give my hearty thanks and appreciation for helping me to make this thesis success.

TABLE OF CONTENTS

LIST OF TABLES

LIST OF FIGURES

LIST OF ABBREVIATIONS

Myc: Myc Proto-oncogene Protein (gene name: v-myc myelocytomatosis viral oncogene homolog)

Max: Myc-Associated Factor X

Mad: Max Dimerization Protein

b/HLH/Z: basic/helix-loop-helix/leucine zipper

E-Box: Enhancer Box

AP-2: Activating Enhancer-binding Protein 2

Miz-1: Myc-interacting Zinc Finger Protein

Nmi: N-myc-interactor

TAD: Trans Activation Domain

Mxi1: MAX-interacting Protein 1

Mnt: Max-binding Protein (Myc Antagonist)

HDAC: Histone Deacetylase

TRRAP: Transformation/Transcription Domain-associated Protein

hGCN5: Histone Acetyltransferase

GCN4: General Control Protein

Mlx: Max-like Protein X

MondoA: Mlx Interactor Protein

WBSCR14: Williams-Beuren Syndrome Chromosome Region 14 Protein

IgH: Immunoglobin Heavy Chain

USF: Upstream Stimulatory Factor

TFE3: Transcription Factor E3

TFEB: Transcription Factor EB

TFEC: Transcription Factor EC

LB: Luria-Bertani Broth (Lysogeny Broth)

IPTG: Isopropyl β-D-1-thiogalactopyranoside

HEPES: 4-(2-hydroxyethyl)-1-piperazineethanesulfonic acid

PMSF: Phenylmethanesulphonylfluoride

DTT: Dithiothreitol

PBS: Phosphate-buffered Saline

GST: Glutathione-S-transferase

SDS-PAGE: Sodium Dodecyl Sulfate Polyacrylamide Gel Electrophoresis

FITC: Fluorescein Isothiocyanate

DMSO: Dimethyl Sulfoxide

CF: Correction Factor

IgG: Immunoglobulin G

MLP: Major Late Promoter

1.0 INTRODUCTION

Gene expression is controlled and modulated by transcription factors-proteins that bind to the promoter elements upstream of genes and either activate or repress transcription. Transcription factors contain two essential functional regions: a trans-activating domain and a DNA binding domain. They can be categorized into five major family groups based on the structure of their DNA binding domains: zinc fingers, helix-turn-helix, helix-loop-helix, leucine zipper and high mobility groups [1, 2]. A large number of biologically important proteins contain a conserved basic region (b) facilitating DNA binding, helix-loop-helix region (HLH) which is the primary contact area for dimerization and a leucine zipper region (Z) supporting dimerization through hydrophobic interactions [3].

Myc, Max and Mad are members of the basic helix-loop-helix leucine zipper family of transcription factors. Myc was first discovered as the proto-oncogene of avian retroviruses inducing lymphoid tumors [4]. Deregulation of Myc is associated with the development of many human cancers such as Burkitt lymphoma, neuroblastomas, small cell lung cancers, breast cancers and colon cancers [11]. The Myc family proteins, c-Myc, n-Myc and l-Myc, have been implicated in cell proliferation, differentiation and neoplasia [5]. Since Myc family proteins dimerize poorly and do not bind DNA except at very high concentrations a search for Myc interacting proteins lead to the identification of Max protein. Max protein, Myc-associated factor X, is a b/HLH/Z family protein similar to Myc, but lacks the transactivation domain. Max can also form homodimers. Some studies showed that it

may act as a transcription repressor in this homodimeric form [6]. All biological functions of Myc require dimerization with Max. The Myc-Max transcription activator is involved in the transcriptional regulation of target genes associated with cellular growth, proliferation, metabolism and differentiation [7].

The fact that Max is expressed in the absence of Myc lead to searches for other Max-interacting partners. Mad family proteins were first discovered by Ayer by screening a lambda gt11 expression library with radiolabeled Max protein [8-10] [34]. Mad like Myc homodimerizes poorly but interacts with Max, forming a sequence-specific DNA binding complex similar to Myc-Max heterodimer. Unlike Myc, Mad acts as a transcriptional repressor. Overexpression of Mad in a wide range of cell types is associated with terminal differentiation. Mad also blocks proliferation and inhibits transformation [7]. Mad and Myc compete for binding Max.

The x-ray structures of the b/HLH/Z domains of Myc-Max and Mad-Max at 1.9 Å and 2.0 Å resolution, respectively, reveal that both heterodimers bind to their common DNA target, the enhancer box (E-Box) hexanucleotide (5-prime-CACGTG-3-prime) [11]. E-boxes are located in the proximal region of class II nuclear gene promoters, between 50 and 200 base pairs upstream of the transcription sites. Binding of these structurally similar transcription factor dimers to the E-Box determines whether a cell will divide and proliferate (Myc-Max) or differentiate and become quiescent (Mad-Max) [11].

Many transcriptional factors form dimeric complexes with DNA [12, 13]. In the absence of DNA, they may be found either as monomers [14] or dimers [15]. It has been shown that dimers have more advantages than monomers [16]. The diversity

of the interacting partners in the heterodimeric complexes provides a number of different target site recognition and function [17].

Kinetic analysis of some members of b/HLH/Z and b/Z family proteins (Max, ATF) has shown that assembly of the dimeric transcription factors and specific DNA sites follows a pathway in which two protein monomers bind DNA sequentially and form their dimerization interface while bound to DNA (monomer pathway) [18]. An alternative model is formation of a protein dimer and subsequent binding to DNA (dimer pathway).

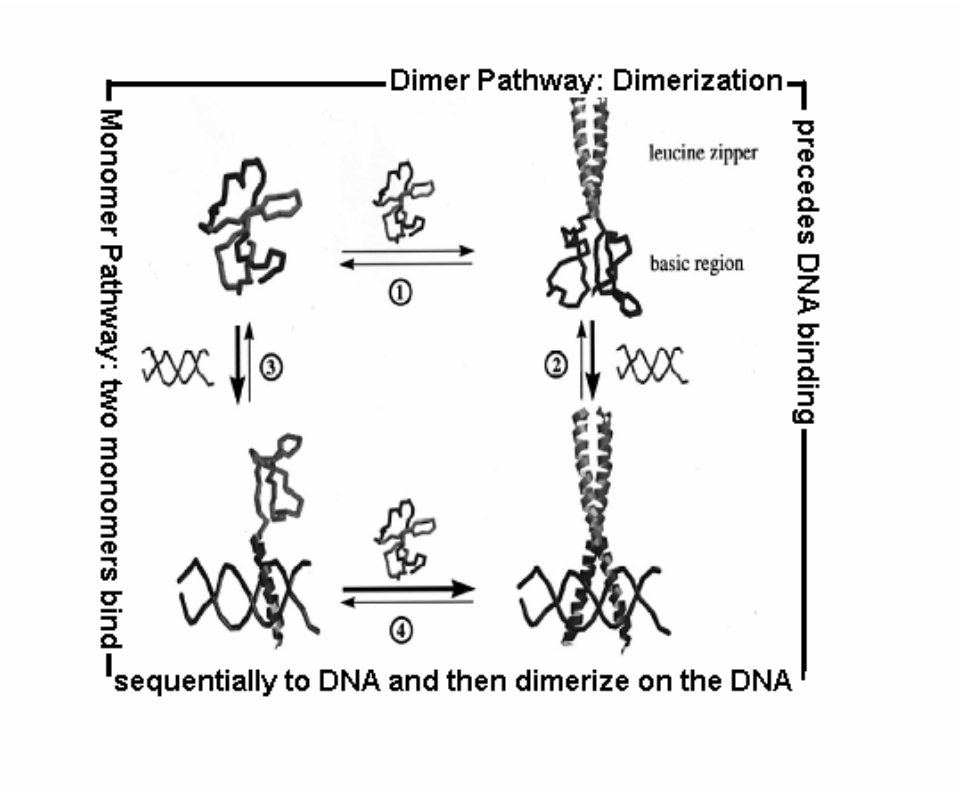

Figure 1: Monomer and dimer pathways for the binding of b/HLH/Z proteins to DNA [49]

The monomer and dimer pathways form a thermodynamic cycle. It does not matter which pathway is followed, monomer or dimer, the equilibrium affinity will be the same for either path. However, the rate at which the final complex is formed will be different for each pathway. Different intermediates in each pathway can interact at different rates with other proteins and non-specific DNA. This kinetic control allows for discriminating between specific and non-specific DNA. Therefore, it is important to determine the rate limiting steps and kinetic mechanism of assembly in order to understand regulation of transcription by cellular and viral proteins and other pharmacological agents.

Our working hypothesis is that differences in the rate of assembly of dimer-DNA complex will determine whether Myc or Mad competes to form a heterodimer with Max at the DNA E-Box. In order to test this hypothesis, we determined the rate of the individual steps in the assembly pathway.

In this work, we utilized stopped-flow fluorescence anisotropy to study the kinetics of each step in Figure 1. We were able to assign individual rate constants to dimer formation (step 1), DNA binding of dimeric Max-Max, Myc-Max and Mad-Max (step 2) and DNA binding of monomeric transcription factors (step 3&4). The temperature and concentration dependence of these reactions were measured and compared.

Our results show that both monomeric and dimeric transcription factors recognize E-Box at similar rates. Since the rate of dimer formation (step 1 in fig.1) is slower than the DNA binding rates (steps 2, 3 and 4), the monomer pathway is more rapid than the dimer pathway.

1.1 Myc

Myc genes were discovered almost 30 years ago as the transforming sequences of chicken retroviruses inducing lymphoid tumors [19]. Later, cellular homologs (c-myc) were found also in other vertebrae species such as chicken, mice and humans. Myc is involved in a wide range of cellular functions. Overexpression of Myc is observed in human tumors including lymphoid malignancies, lung cancer, breast cancer and colon cancer [20]. Myc family proteins are found mostly in the cell nucleus and have been implicated in cell proliferation, differentiation and neoplasia [7]. Myc protein has a short half-life of 20-30 min [21] and is rapidly degraded. Since Myc family proteins dimerize poorly and do not bind DNA except at very high concentrations a search for Myc interacting proteins lead to the identification of Max protein. For all the biological functions, Myc requires dimerization with Max [22]. For the activation of genes containing an E-Box binding site, Myc interacts with Max protein. Myc-Max heterodimers activate transcription by recruiting histone acetyltransferase via TRRAP (transformation/transcription associated domain protein) which leads to the acetylation of histone tails and the opening of local chromatin structure [23]. Myc activity could be controlled by Myc-Max heterodimer antagonists by inhibiting the dimerization of Myc with Max. Consequently, Myc activated cancers could be prevented. Some of the other Myc interacting proteins are AP-2 [24], Miz-1 [25], and Nmi [26]. Myc-Max heterodimers have been observed to interact with Miz-1, but other interactions have not been characterized. In all of these interactions, the b/HLH/Z region of the Myc-Max heterodimer plays an important

role. This region targets the proteins to particular promoter regions and may also have a structural function in protein-DNA interactions.

Figure 2: X-Ray structure of Myc-Max heterodimer recognizing DNA.
PDB file: 1NKP

1.2 Max

The biological functions of Myc such as activating transcription, promoting cell proliferation, transformation or apoptosis and the ability to bind to its cognate DNA recognition E-Box site (CACGTG) require dimerization with a structurally similar b/HLH/Z binding partner. This search led Blackwood and Eisenmann [27] to discover Max protein. In 1991 they screened a complimentary DNA(c-DNA) expression library using the b/HLH/Z region of c-Myc protein and identified a new b/HLH/Z protein, Max. Max is a stably expressed b/HLH/Z family protein that forms homodimers and heterodimers with Myc oncoprotein. These dimers bind DNA under physiologic conditions. Max also forms heterodimers with another b/HLH/Z protein, Mad [28-30]. In vivo, Max is found in at least three dimeric states: Myc-Max, Mad-Max and Max-Max of which the exact function is still unclear [3, 31, 32, 33]. These structurally similar dimers, i.e Max-Max homodimer, Myc-Max and Mad-Max heterodimers bind the sequence 5'CACGTG3' (E-Box) with different affinities. The main difference of Max from Myc and Mad is that it does not contain a functional transactivation domain (TAD). Hence, it acts as a transcriptional repressor in the homodimeric form by sequestering the DNA targets normally recognized by b/HLH/Z activators. Since Max does not contain a transactivation domain, Myc is the part of the Myc-Max heterodimer responsible for activation and transcription through its TAD. In recent years, different types of Max proteins have been identified with alternative splicing. Among these, p21 and p22 are the predominant ones [3, 27].

Since the expression of Max protein is ubiquitous [32], a search for Max-interacting proteins led to the discovery of Mad protein.

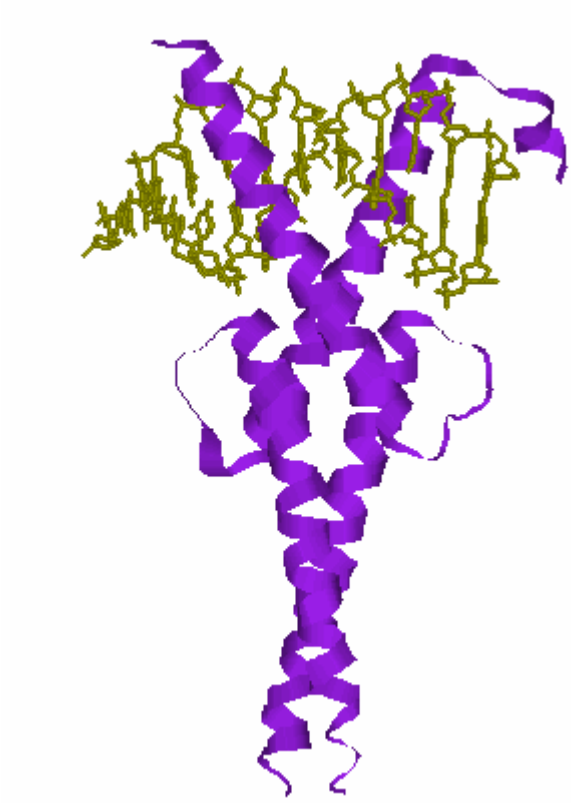

Figure 3: X-Ray structure of Max-Max homodimer recognizing DNA.
PDB file: 1HLO

1.3 Mad

Myc protein is not the only dimerization partner of Max. There are other b/HLH/Z family proteins which also interact with Max protein, i.e Mad1, Mxi1, Mad3, Mad4 and Mnt. Mad protein was first discovered by Ayer by screening a lambda gt11 expression library with radiolabeled Max protein [8-10] [34]. All these Mad family proteins specifically bind with Max and form heterodimers. This makes Max the most essential component of the Myc/Max/Mad network of transcriptional factors. Mad protein is structurally similar to Myc protein. Its biological function shows similarities to Myc as well. Mad like Myc homodimerizes poorly but forms heterodimers with Max. Mad protein affects cell growth negatively and antagonizes Myc functions. Mad-Max heterodimers recognize the E-Box sequence as do Myc-Max heterodimers [35]. In contrast to Myc, Mad acts to repress E-Box dependent expression of synthetic reporter genes [8, 9, 36]. Overexpression of Mad in a wide range of cell types is associated with terminal differentiation. Mad also blocks proliferation and inhibits transformation [7, 8, 10, 37, 38]. Mad mutants that do not interact with Max or bind DNA are found to be inactive in biological assays. [9, 30, 36]. Mad-Max heterodimers repress gene transcription by interacting with mSin3 corepressor via histone deacetylation [39].

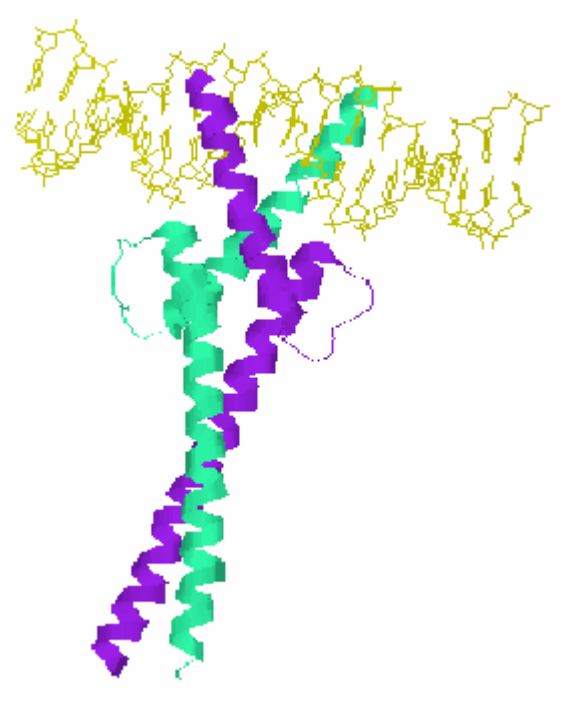

Figure 4: X-Ray structure of Mad-Max heterodimer recognizing DNA.
PDB file: 1NLW

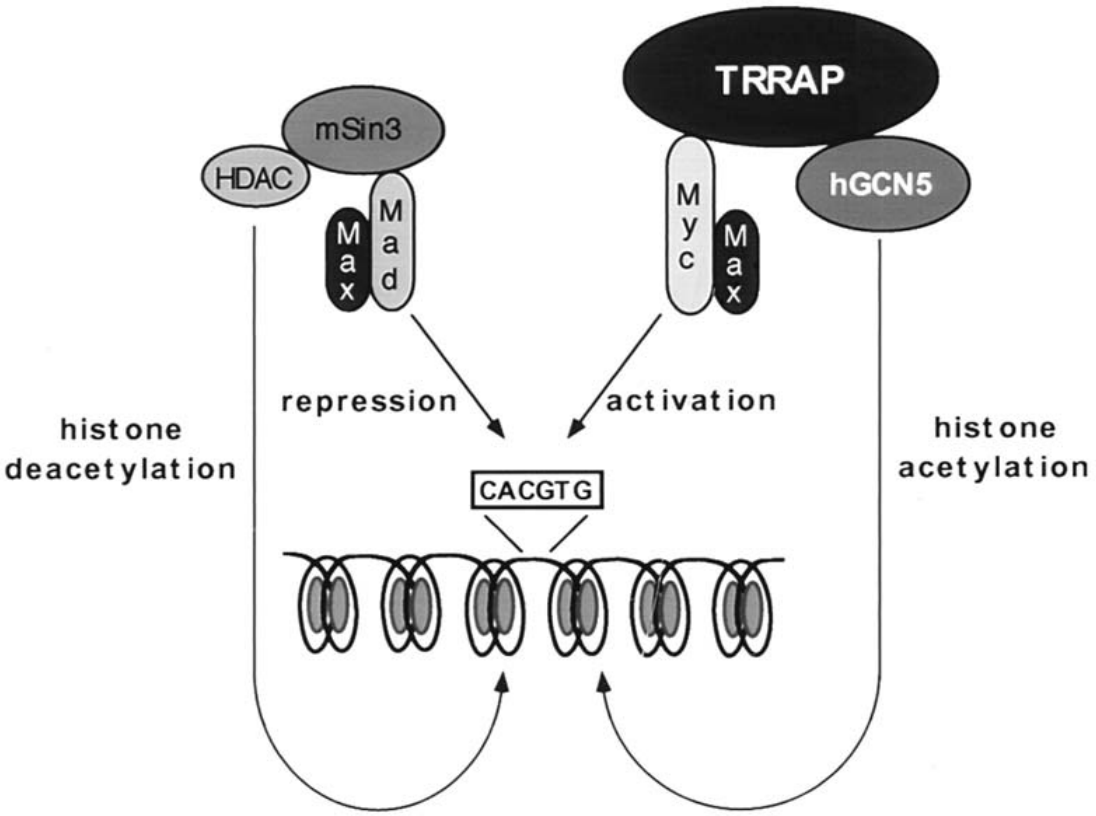

Figure 5: Model of the opposing biochemical functions of c-Myc and Mad
by S.B. McMahon et. al. Mol. Cell Bio. 2000 January, 20(2): 556-562

1.4 Structural Aspects of Myc-Max-Mad Network

Twenty years ago, HLH and Zip domains were identified as protein-protein interaction motifs [40]. Structural analyses and protein modeling studies revealed that the HLH domains contain two amphipathic helices connected by a loop and the Zip domains are formed of one amphipathic helix [40]. The X-ray structure of the b/HLH/Z domain of Max homodimer bound to an E-Box, derived from the Adenovirus major late promoter, provided the structural bases for DNA recognition by b/HLH/Z family proteins [41]. The structure revealed that Max-Max homodimer forms a left-handed, four helix bundle with a well-defined hydrophobic core. Two pairs of α-helices project in opposite directions from the bundle. The two basic regions project into the major groove of the DNA like scissors and make a number of contacts with the bases and backbone of the DNA. The other pair of alpha helices forms the leucine zipper region of the molecule. The two α-helical segments of each Max monomer are composed of the basic region plus helix 1 of the HLH region and helix 2 plus the leucine zipper region, respectively. The two α-helices are connected by the loop. Therefore, the basic region and helix 1 as well as helix 2 and leucine zipper form continuous α-helices. The four helix bundle appears to confer rigidity such that the orientation of the basic regions is such that these proteins recognize palindromic sequences without spacing between the repeated elements. The zipper region supports dimerization through hydrophobic interactions. The N-terminal α-helix containing the basic region is the area of interaction with the major grooves of the target DNA. By making base contacts, the basic region determines the specificity

of DNA binding. The helix-loop-helix region is the primary area of contact for dimerization.

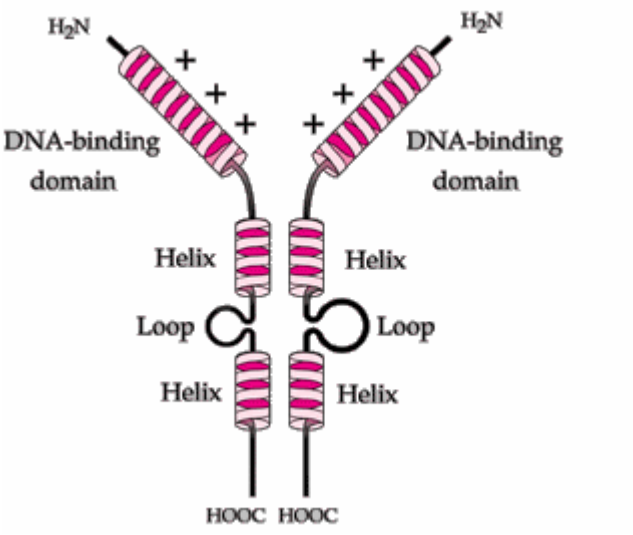

Figure 6: Domains of the basic helix-loop-helix transcription factors

In 2003, Nair and Burley were able to crystallize the Myc-Max and Mad-Max proteins recognizing DNA. The X-Ray structures of these heterodimers with DNA showed similar secondary structural elements. The main difference in these structures from the Max-Max homodimer was in the leucine zipper region. The Max-Max homodimer structure had a Gln 91-Asn 92-Gln91-Asn92 tetrad near the C-terminal end of the zipper region. However, the leucine zipper of Myc-Max and Mad-Max structures had tighter intermolecular packing due to hydrogen bond formation [42].

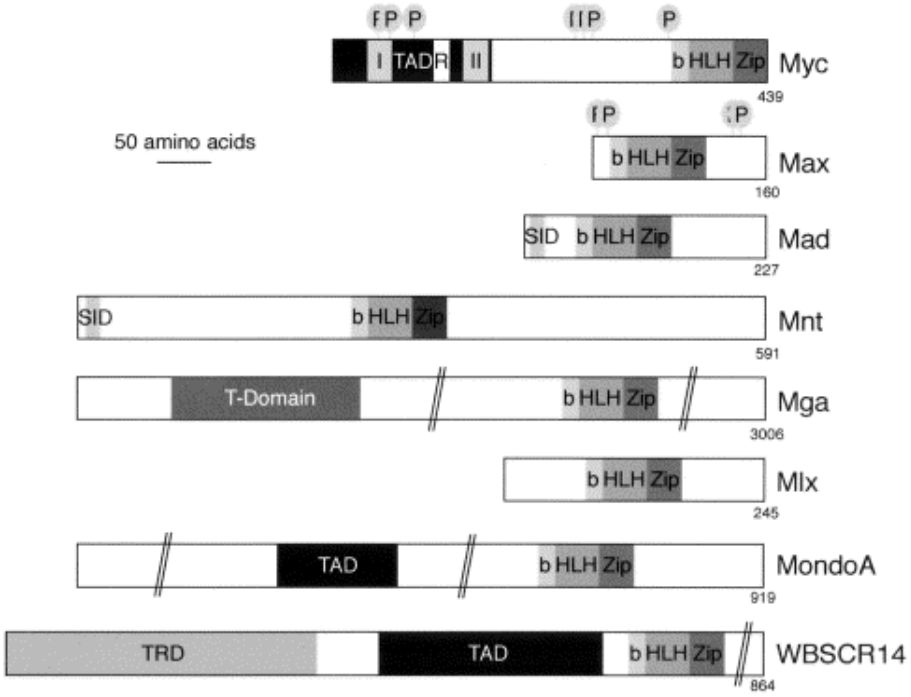

Figure 7: Structure-function schematic of Myc/Max/Mad network components.

TAD: transactivation domain;
I: Myc box I;
II: Myc box II;
b: basic region;
R: region involved in repression;
HLH: helix-loop-helix domain;
Zip: leucine zipper domain;
SID: mSin3-interaction domain;
T-Domain: T-box DNA binding domain;
TRD: transrepression domain;
P: position of known phosphorylation sites.

The numbers refer to amino acids of the human proteins

1.5 E-Box Recognition

After the identification of the b/HLH/Z in Myc and Max proteins as the likely domains responsible for interaction with DNA, a search for specific binding sites started. A sequence with the core 5'CACGTG was discovered and termed as Myc E-Box.

E-Boxes are cis-acting DNA elements, IgH enhancers, regulating the transcription of immunoglobin heavy chain (IgH) gene. Using in vivo methylation, a number of such elements were discovered in IgH and kappa-light chain enhancers, which shared a hexanucleotide core signature sequence CANNTG.

There are two subclasses of E-Box binding proteins. Two central amino acid residues in the hexanucleotide E-Box element are responsible for b/HLH/Z family proteins distinguishing class A from class B E-Boxes. Subclass A proteins recognize 5'CAGCTG whereas subclass B proteins recognize 5'CACGTG [43]. Since Myc-Max, Mad-Max and Max-Max dimers all bind specifically to 5'CACGTG sequence; they fall into the subclass B which in addition contains several other transcription factors including USF, TFE3, TFEB and TFEC.

As mentioned above, Myc/Max/Mad network proteins recognize DNA with the contact of their basic regions. Since the amino acids in these basic regions are conserved, the Myc-Max and Mad-Max heterodimers and Max-Max homodimer bind the same DNA elements. Therefore it is important to determine whether these proteins compete for binding to the same E-Box and affect gene regulation or whether

there are mechanisms that differentiate between the binding of these transcription factors to their specific target.

1.6 Fluorescence Polarization

Polarization and anisotropy measurements are widely used techniques in biochemical research. In recent years, the sensitivity of this approach has been significantly increased such that it is now applicable to study protein denaturation, protein ligand association reactions and the rotational rates of proteins.

If fluorescent samples are excited with polarized light, their emission is also polarized. The reason why these fluorophores are polarized lies in their orientation relative to the direction of the polarized excitation. Polarization depends on the angle between absorption and emission transition dipoles. Depending on the fluorophores, the emission can be depolarized due to the rotational diffusion. In addition to depolarization, local rotational motion, energy transfer and reabsorbtion can be observed during the lifetime of the excited state. The angle between absorption and emission transition dipoles, the angular displacement, depends on the rate and extent of this rotational motion of the fluorophores. These motions in turn depend on the viscosity of the solvent and the size and shape of the fluorophores.

Figure 8 shows a schematic diagram for fluorescence anisotropy measurements. The instrument consists of a light source, excitation monochromator, excitation polarizer, sample chamber, emission polarizer, emission monochromator (or replaced by a filter) and a detector. To make the anisotropy measurement, the

emission channel must be corrected for effects of polarization on the detected signal with a gain-factor (G-factor). This is collected with the excitation polarizer in the horizontal position and intensity is measured with the emission polarizer in horizontal (I_{HH}), then the vertical (I_{HV}) position. The G-factor is defined as the ratio of vertical to horizontal intensities. After the sample is excited with vertically polarized light, the intensity of the emission is measured through a polarizer. I_{VV} is the light intensity with excitation and emission polarizers mounted vertically, whereas I_{HH} is the light intensity with excitation and emission polarizers mounted horizontally. I_{HV} uses an excitation polarizer horizontal and the emission polarizer vertical and I_{VH} requires the excitation polarizer vertical and emission polarizer horizontal.

The anisotropy (**r**) is defined as

$$r = \frac{I_{VV} - GI_{VH}}{I_{VV} + 2GI_{VH}} \qquad \textbf{(1)}$$

Where the G-factor is

$$G = \frac{I_{HV}}{I_{HH}} \qquad \textbf{(2)}$$

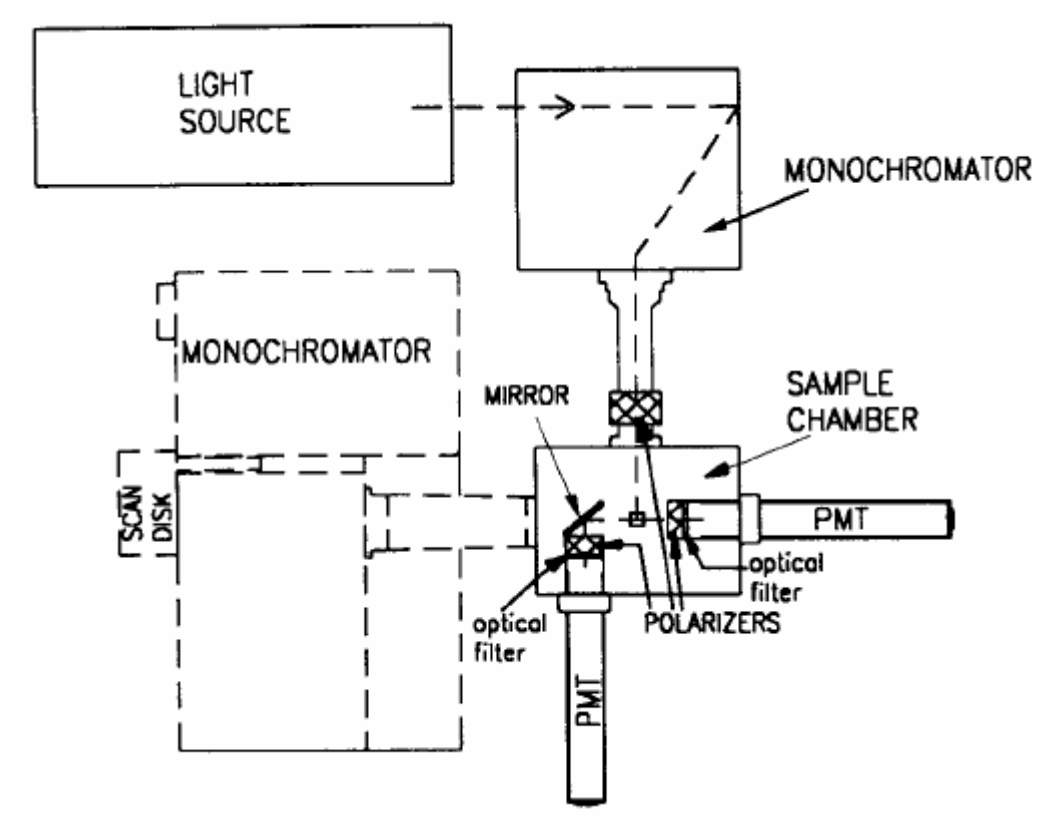

Figure 8: Schematic diagram for fluorescence anisotropy measurement

1.7 Stopped-Flow Spectrophotometry

Stopped-flow spectrophotometry is one of the methods to study the chemical kinetics of a reaction in a solution. In a stopped-flow instrument, the samples in two separate syringes are rapidly fired into a mixing chamber. This rapid shot causes the flow actuator to push the plunger block which in turn triggers the drive syringe plungers. Upon the movement of the drive syringe plungers, the desired amount of each sample is delivered into the mixing chamber. Then, the freshly mixed solutions flow into the observation cell and move the previous contents into the waste syringe. A light source illuminates the mixed samples in the observation cell. The flow of the solutions is stopped by the stop syringe. The stop syringe also adjusts how much sample is consumed per stopped-flow shot. As soon as the flow of solution is stopped by the stop syringe, the stop syringe plunger initiates the data collection. The change in the desired optical property is recorded as a function of time. Depending on the detectors of the stopped-flow instrument, the change in the sample can be measured in fluorescence intensity, polarization, anisotropy, absorbance, light scattering etc.

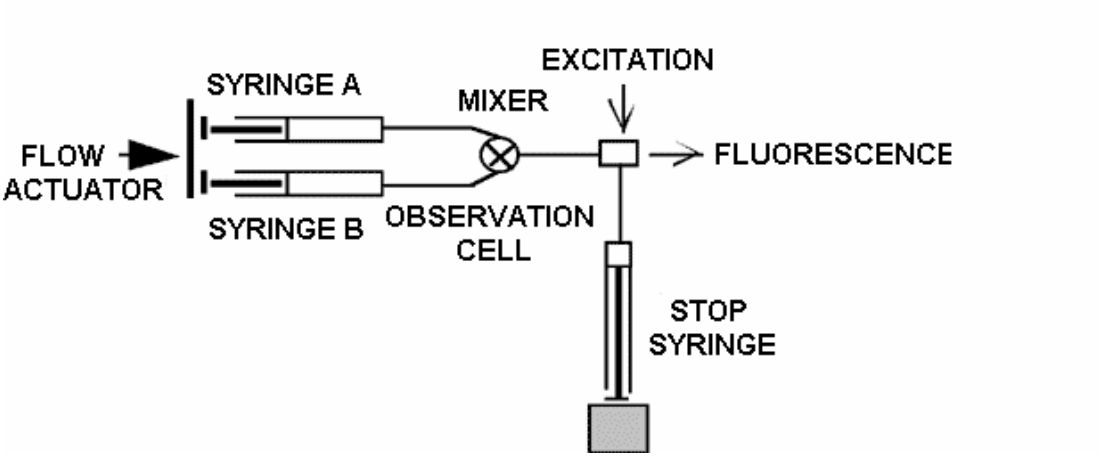

Figure 9: Schematic diagram for stopped-flow instrument

The dead-time of a stopped-flow instrument is an important property for a kinetic measurement because it affects the time resolution of a stopped-flow kinetic method. After the samples are mixed in the mixing chamber, they are delivered into the observation cell. The time which is passed between these two moments is called the dead time. Dead time is also defined as the age of the reaction mixture when it is first available for measurement.

With stopped-flow kinetic methods, first order rate constants can be observed up to the order of 500 s^{-1}. The ease of varying and controlling the temperature is another advantage of stopped-flow instrument.

2.0 MATERIALS AND METHODS

2.1 Protein Expression and Purification

Expression vectors Max/PET3a and c-Myc/PGex2T were kindly provided by S.K.Burley, Rockefeller University. The cloning vector pET30a containing the full-length Mad cDNA was purchased from Open Biosystems, Huntsville, AL. All three vectors were transformed into Escherichia Coli (E.Coli) BL21-pLys cells containing the DE3 promoter. Truncated proteins Max and c-Myc consisting of amino acids 22 to 113 and 347 to 439, respectively and the full-length Mad1 contained the functional b/HLH/Z domains.

PROTEIN	***VECTOR***	***AMINO ACID RESIDUES***	***MW OF THE PURIFIED PROTEIN***	***METHOD OF PURIFICATION***
Max	pET23	22-113	11 kDa	Cation Exchange Chromatography
c-Myc	pGEX2T	347-439	11 kDa	Affinity Chromatography
Mad	pET30a	1-220	26 kDa	Affinity Chromatography

Table 1: Vectors, molecular weights and purification methods of Max, c-Myc and Mad proteins

Bacterial storage cultures used for inoculation were prepared as follows. A total of 1-2 µl of storage culture was transferred on the agar plate containing 100 µg/ml ampicillin and grown at 37°C.The single colony was transferred to a 2.8 L flask containing 1L of LB media with 100 µg/ml ampicillin and grown at 37°C until the OD600 reaches 0.5-1. The culture was induced with 1 mM IPTG and the culture growth was allowed to continue for 6h at 37°C. Cells were harvested by centrifugation for 20 min, 6000 rpm and frozen -80°C. Frozen cell pellets were thawed on ice, resuspended in lysis buffer (20 mM HEPES buffer, pH 7.6, 0.5 mM PMSF, 10% glycerol, protease inhibitor cocktail and lysozyme) and sonicated for 2 min. The lysed cells were centrifuged at 18000 rpm for 10 min to separate soluble proteins from inclusion bodies (Myc and Mad1). The supernatant was used for chromatography and purification of the proteins (Max).

The inclusion bodies for Mad1 were isolated from cell lysates, washed twice with 10 ml of 20 mM HEPES buffer (pH 7.6) containing 1% Triton X-100. After centrifugation at 18000 rpm for 30 min, the inclusion bodies were dissolved in 2 ml of 50 mM HEPES buffer (pH 7.6), 6 M guanidine hydrochloride and 25 mM DTT and incubated for 1h at 4°C. To pellet the insoluble material, the sample was centrifuged at 18000 rpm at 10 min and the supernatant was diluted into 20 ml of 50 mM HEPES (pH 7.6).

The inclusion bodies for c-Myc were washed as described above for Mad1. The inclusion bodies were solubilized with 10 ml of PBS buffer, pH 7.4, containing 1% Triton X-100 and incubated overnight with gentle stirring. After removal of the

insoluble material by centrifugation, the soluble protein was diluted into 20 ml of cold 20 mM PBS, pH 7.4.

HiTrap SP-ion exchange chromatography was used for the purification of Max. c-Myc was purified by GST affinity chromatography using 20 mM PBS, pH 7.4 as the wash buffer and 50 mM glutathione and 200 mM Tris-HCl, pH 8.5 as the elution buffer. The purification of Mad1 was performed on a Ni^{2+}-His trap affinity column. The column was prepared according to the manufacturer's instructions and washed with 10 volumes of binding buffer (0.5 M NaCl, 20 mM Tris-HCl, 5 mM imidazole, pH 7.9). The supernatant containing the Mad protein was loaded on the washed column. The column was washed with additional binding buffer and 10 volumes of wash buffer (0.5 M NaCl, 20 mM Tris-HCl, 60 mM imidazole, pH 7.9), and the bound protein was eluted with the elution buffer (0.5 M NaCl, 20 mM Tris-HCl, 1 M imidazole, pH 7.9). The protein fractions were collected and dialyzed against HEPES buffer pH 7.6. The purity of all three proteins was determined by 10% SDS-PAGE gel. After the proteins were concentrated with Centricon YM filters (Amicon Co.), the concentrations were determined by a Bradford assay with bovine serum albumin as the standard using a Bio-Rad protein assay reagent (Bio-Rad Laboratories, Hercules, CA).

2.2 Fluorescent Labeling of Max

Fluorescein isothiocyanate (FITC) reacts only with primary amines of proteins to form dye-protein conjugates. Therefore, the N-terminus of Max was labeled with FITC as follows. The absorption and fluorescence emission maxima of FITC-labeled proteins are approximately 494 and 518 nm, respectively.

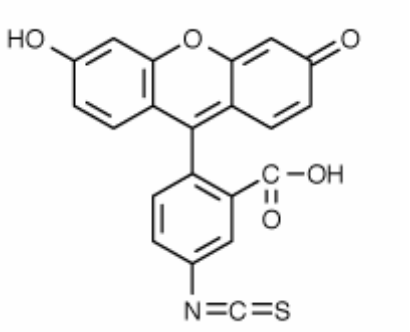

Figure 10: Structure of fluorescein-5-isothiocyanate (FITC)

The concentration of purified Max was adjusted to 1mg/ml in HEPES buffer. In the labeling procedure, 100 µl of 1.5 mg/ml reactive dye stock solution (dissolved in anhydrous DMSO) is added to 1ml of protein solution. The FITC-Max mixture was incubated overnight at 4°C with gentle agitation, protected from light. FITC-labeled Max was purified on a Sephadex G25 column equilibrated with HEPES buffer. The FITC conjugated protein fractions were collected in the void volume and concentrated with Centricon YM filters (Amicon Co) by centrifugation for 6h at 4000 rpm. To determine the concentration, the purified protein was diluted into HEPES buffer and the absorbance at both 280 nm (A_{280}) and 494nm (A_{494}) were measured.

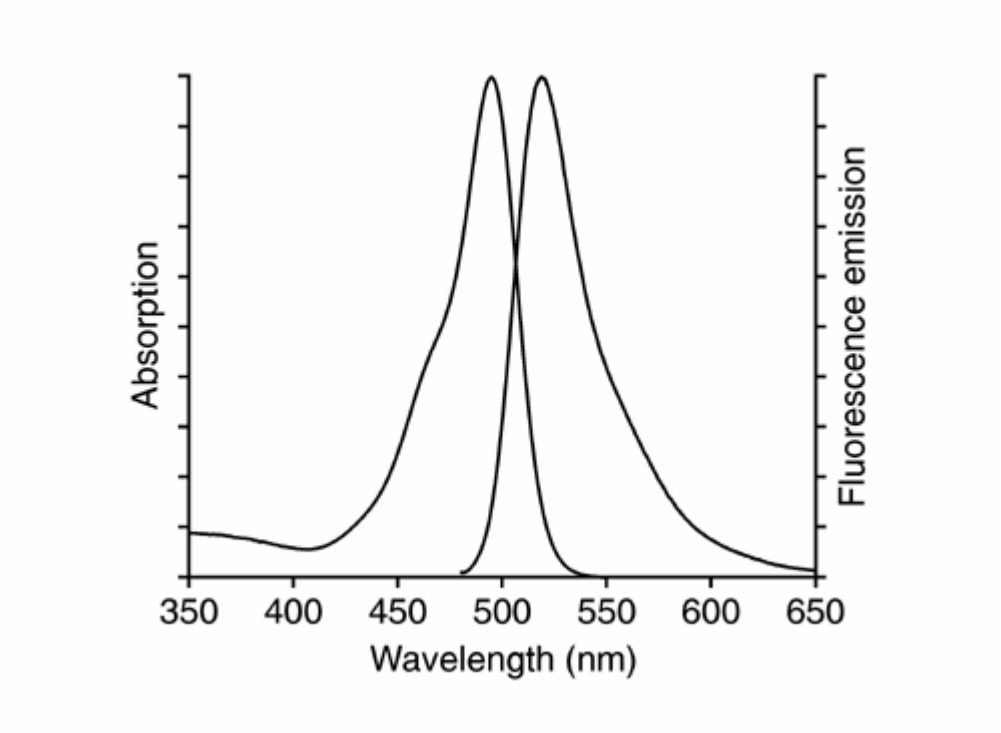

Figure 11: Absorption and fluorescence emission spectra of fluorescein-5-isothiocyanate–labeled goat anti–mouse IgG antibody in pH 8.0 buffer (from The Handbook — A Guide to Fluorescent Probes and Labeling Technologies)

The final protein concentration was calculated according to the formula:

$$\text{Protein concentration} = \frac{[A_{280} - (A_{494} \times 0.30)] \times \text{dilution factor}}{\varepsilon} \quad \textbf{(3)}$$

where 0.30 is a correction factor(CF) and ε is the molar extinction coefficient of the protein at 280 nm. CF= (A_{280} free dye) / (A_{494} free dye) = 0.30 for FITC

The CF is included to compensate for absorption of the dye at 280 nm.

The following formula was used to obtain the degree of labeling:

$$\text{dye per protein molecule} = \frac{A_{494} \text{ x dilution factor}}{68000 \text{ x protein concentration}} \quad \textbf{(4)}$$

where 68000 $cm^{-1}M^{-1}$ is the molar extinction coefficient of the dye at pH 8.0 at 494 nm. The site of the protein labeling was confirmed by enzymatic digestion. Approximately 90% of the protein was labeled (1 dye/monomer). Labeling at sites other than the N-terminus was not detected [46].

2.3 DNA Oligonucleotides

The oligonucleotides used in this stopped-flow study were synthesized on a 200 nm scale by GeneLink (Hawthorne, NY). Fluorescein was attached at the 5' end of the 16-mer oligonucleotides during the synthesis. Crude oligonucleotides were purified by polyacrylamide gel electrophoresis. Complementary strands were annealed together to form duplex DNA. 20 μM of each DNA strand (labeled oligonucleotide and unlabeled complement) were dissolved in nuclease-free water, heated to 75-80°C for 30 min, and allowed to cool at room temperature overnight. The DNA duplex used in this study contained the following sequence: 5'TAGGCCACGTGACCGG3' and its complementary strand. 16bp oligonucleotide contained the sequence derived from the adenovirus major late promoter (MLP) containing the E-Box (CACGTG).

2.4 Stopped-Flow Fluorescence Anisotropy Measurements

Stopped-Flow fluorescence anisotropy experiments were made with an OLIS RSM 1000 stopped-flow spectrophotometer equipped with a fluorescence polarization module. The dead time of the stopped-flow system, the age of the mixture when it is first available for measurement, is 1ms. The instrument was configured in T-format, and emission was collected through 495 nm cut-on filters (provided by ORIEL Corporation, Stratford, CT) placed in front of each photomultiplier tube.

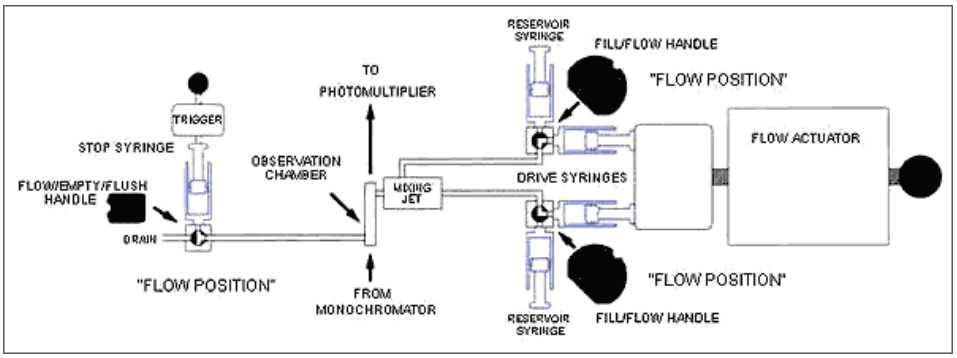

Figure 12: Block diagram of an OLIS stopped-flow instrument

A 450 W Xe arc lamp with a single grating monochromator was used for excitation of Max-FITC with 490 nm light. A temperature–controlled circulating water bath was used to maintain the temperature of the flow cell and solution reservoirs. After rapid mixing of samples, the time course of fluorescence anisotropy change was recorded by computer data acquisition. 1000 data points were collected

per rapid-mix shot. For each experiment, the data from 6-10 consecutive shots were averaged. Each averaged set of stopped-flow data was then analyzed by nonlinear least squares fitting using Kaleidagraph (Synergy Software, West Palm Beach, FL) and the following single-exponential equation.

$$r_t = r_{final} - r_{initial} \times \exp(-k_{obs}t) \quad \textbf{(5)}$$

r_t is the anisotropy observed at any time t, r_{final} is the anisotropy when the reaction reaches the equilibrium and $r_{initial}$ is the anisotropy at time zero. k_{obs} is the observed first-order rate constant. All the reactions in this study were consistent with a single-exponential process. Arrhenius plots were constructed by using the observed rate constants according to the Arrhenius equation.

$$\ln k = (-E_a/ RT) + \ln A \quad \textbf{(6)}$$

where k is the rate constant, E_a is the activation energy and A is the Arrhenius pre-exponential factor. Activation energies were calculated using the slopes of ln k versus 1/T plots. The average rate constants were obtained as the reciprocal of the y-intercept of $1/k_{obs}$ versus 1/[C] kinetic plots.

3.0 RESULTS

3.1 Monomer-dimer kinetics

The stopped-flow data for the dimerization of the transcription factors Max, Myc and Mad with FITC labeled Max were plotted as the anisotropy change versus time as shown in figures 13-33. Stopped-flow kinetic traces were fitted to a single exponential equation using nonlinear regression analysis. In all temperature dependence experiments, the final concentration of FITC labeled Max protein was 50 nM. 400 nM of unlabeled Max and 4 μM of unlabeled Myc and Mad proteins were rapidly mixed with 50 nM of FITC labeled Max protein in the stopped flow instrument at 13, 21, 27 and 32°C. A temperature -controlled circulating water bath was used to maintain the temperature of the flow cell and solution reservoirs.

Table 2 shows the rate constants of the dimerization of Max, Myc and Mad with FITC labeled Max at increasing temperatures. For all the three protein-protein interactions, Max-Max, Myc-Max and Mad-Max, an increase in the rate constants were observed with an increase in temperature. The stopped-flow kinetic data revealed that at all four different temperatures Myc-Max dimerization had the highest rate constants compared to the other two transcription factor dimerizations. Myc-Max interaction had a 1.7 to 2 times higher rate constant than Mad-Max dimerization and 3.2 to 5 times higher than Max-Max homodimerization.

The rate constants in table 2 were used to construct Arrhenius plots (fig.34) according to the Arrhenius equation. The activation energies were obtained from the

slope of linear fit of ln k versus 1/T plots. The activation energies for the dimerization of Max-Max, Myc-Max and Mad-Max, determined from the temperature dependence of the rate constants are represented in Table 2. Our results show that the activation energy for the heterodimerization of Mad-Max and Myc-Max is 2.2 and 1.9 fold higher than for the homodimerization of Max-Max, respectively.

Under the pseudo-first order conditions, where unlabeled protein (Max, Myc or Mad) was in excess, the observed pseudo-first -order rate constant is predicted to be a linear function of the concentration of FITC-labeled Max. To confirm this prediction, Myc-Max and Mad-Max dimerization experiments were performed over a concentration range of 2-5 μM, 40-100 fold excess. For Max-Max dimerization experiment, the concentrations of unlabeled Max proteins were 200-500 nM. In all these experiments, the concentration of the FITC-labeled Max was kept constant at 50 nM. The concentrations of the unlabeled Myc and Mad were 2, 3, 4 and 5 μM. Table 3 shows the rate constants of the Max-Max, Myc-Max and Mad-Max interactions at different concentrations. The Max, Myc and Mad dimerization rates were found to be concentration independent suggesting conformational changes are rate limiting.

The dimerization rates have a relationship with the concentration of substrate, $1/k_{obs} = 1/k_2 + k_1/k_2[C]$, where k_{obs} is the observed first-order rate constant, k_2 is the forward rate constant for the second step, and [C] is the concentration of the unlabeled protein Max, Myc or Mad.

The $1/k_{obs}$ versus 1/[C] plots shown in figures 35 and 36 for Max-Max, Myc-Max and Mad-Max dimerizations confirm the predicted linear relationship. k_2 values, obtained from the intercept of $1/k_2$, were found to be 19.2, 93.2 and 42.5 s^{-1} for Max-

Max, Myc-Max and Mad-Max dimerizations, respectively.

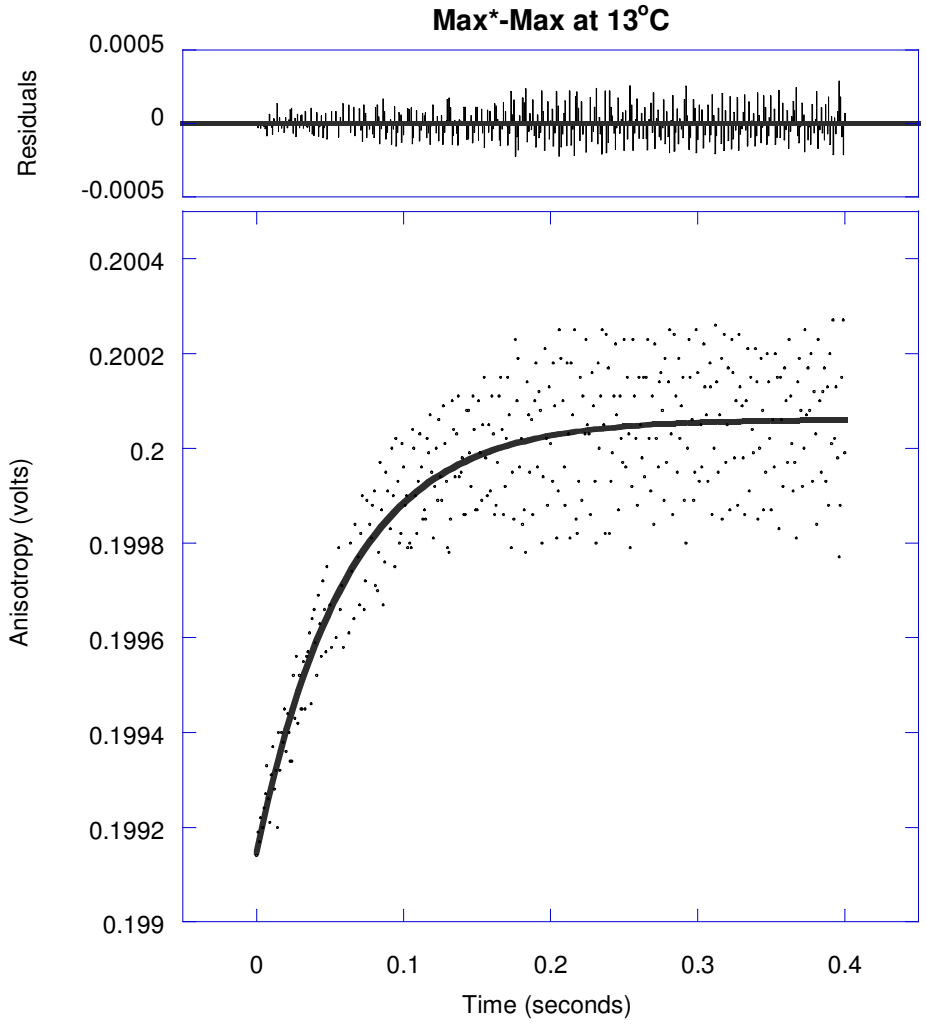

Figure 13: Stopped- flow kinetic binding measurement of Max to FITC labeled Max

Kinetic data shows the time dependent increase in anisotropy after mixing 50 nM FITC labeled Max with 400 nM unlabeled Max at 13 °C. All measurements were performed in 20 mM HEPES-KOH, 50 mM KCl, 0.5 mM $MgCl_2$ and 1 mM DTT buffer, pH 7.6

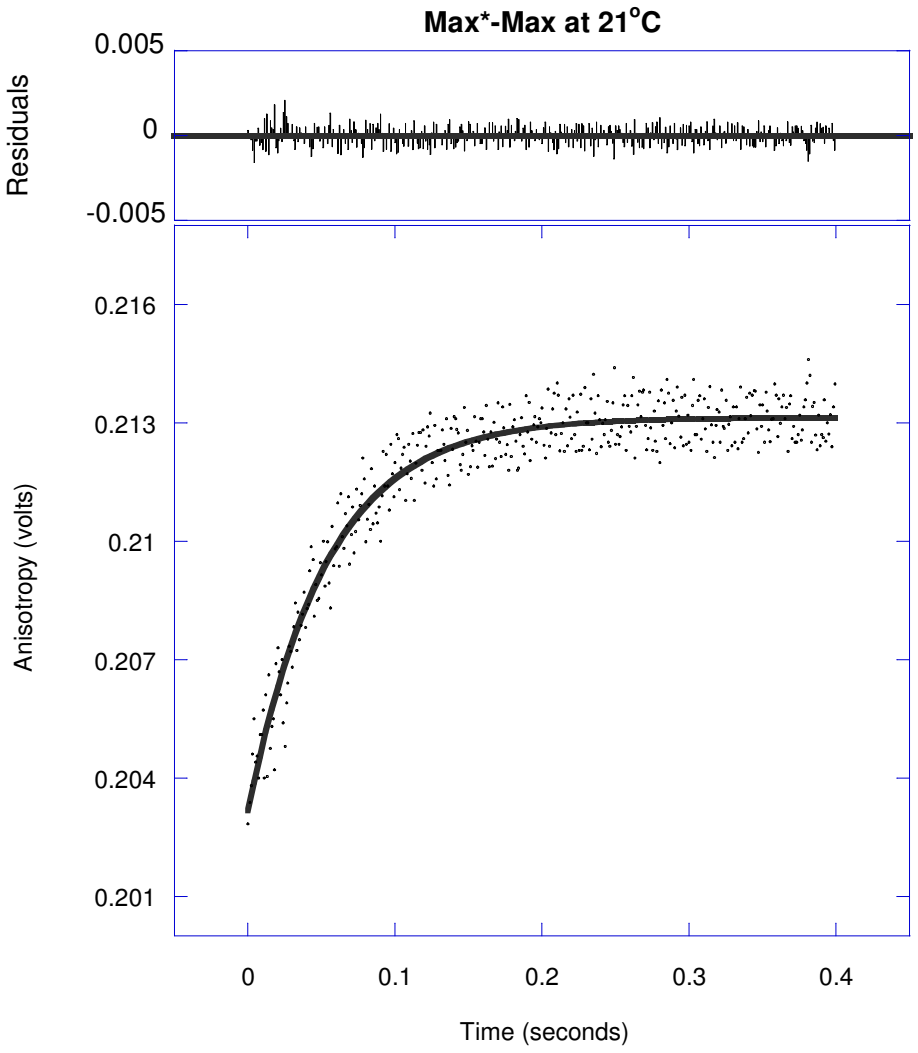

Figure 14: Stopped- flow kinetic binding measurement of Max to FITC labeled Max

Kinetic data shows the time dependent increase in anisotropy after mixing 50 nM FITC labeled Max with 400 nM unlabeled Max at 21 °C

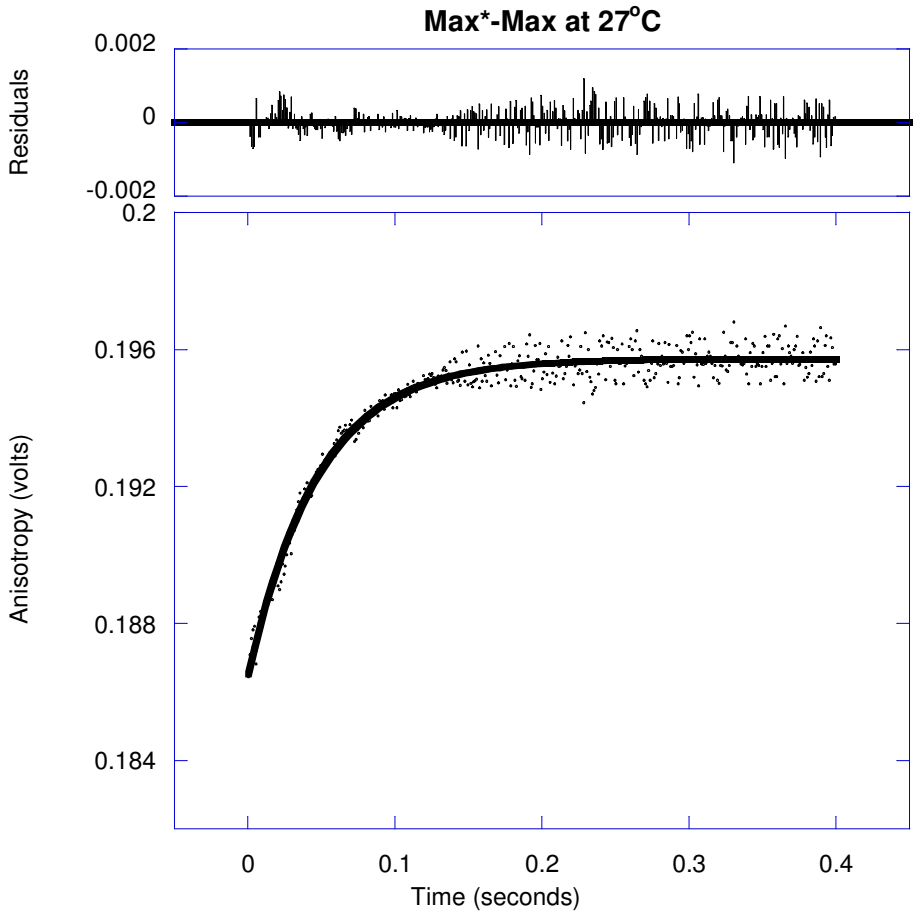

Figure 15: Stopped- flow kinetic binding measurement of Max to FITC labeled Max

Kinetic data shows the time dependent increase in anisotropy after mixing 50 nM FITC labeled Max with 400 nM unlabeled Max at 27 °C

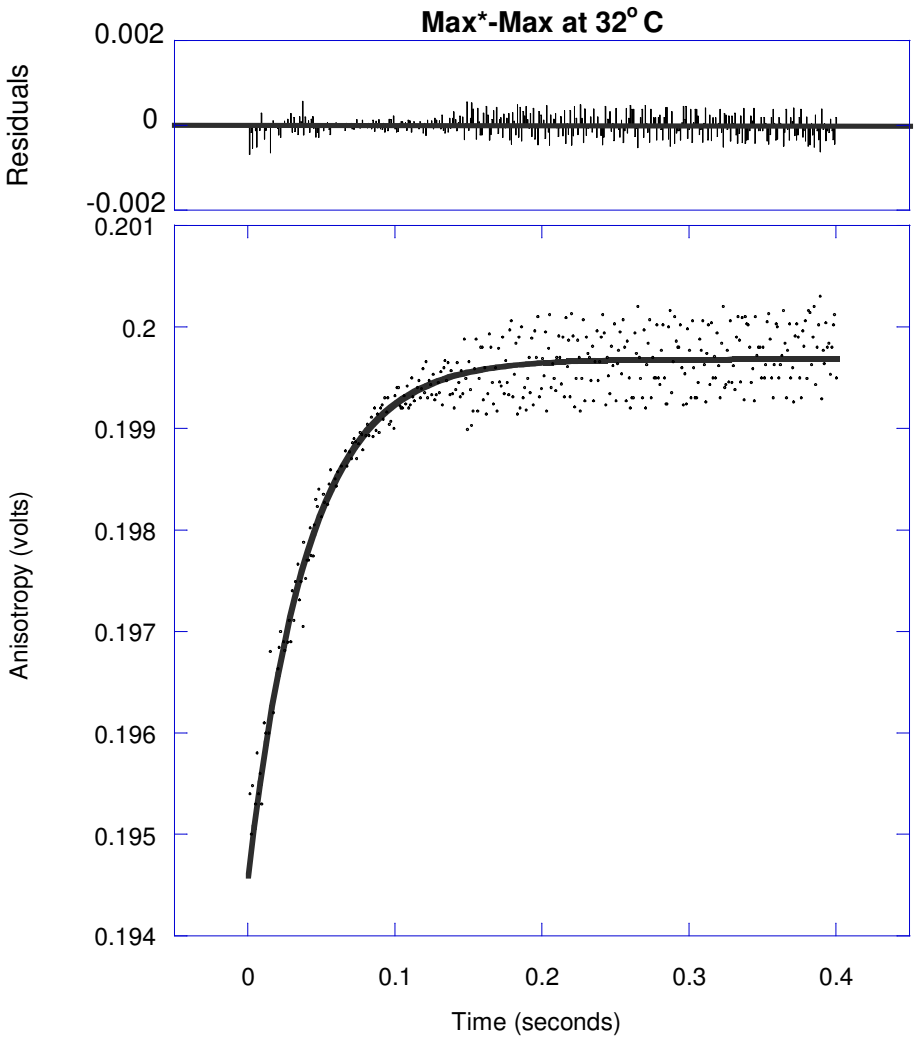

Figure 16: Stopped- flow kinetic binding measurement of Max to FITC labeled Max

Kinetic data shows the time dependent increase in anisotropy after mixing 50 nM FITC labeled Max with 400 nM unlabeled Max at 32 °C

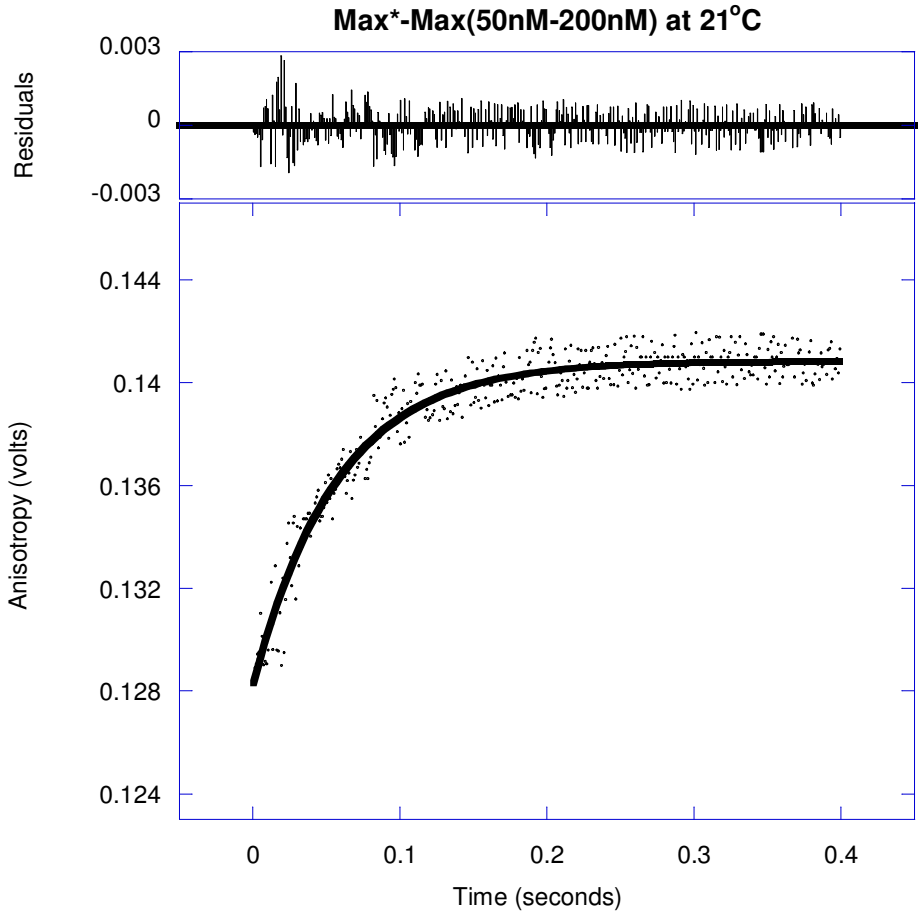

Figure 17: Stopped- flow kinetic binding measurement of Max to FITC labeled Max

Kinetic data shows the time dependent increase in anisotropy after mixing 50 nM FITC labeled Max with 200 nM unlabeled Max at 21 °C

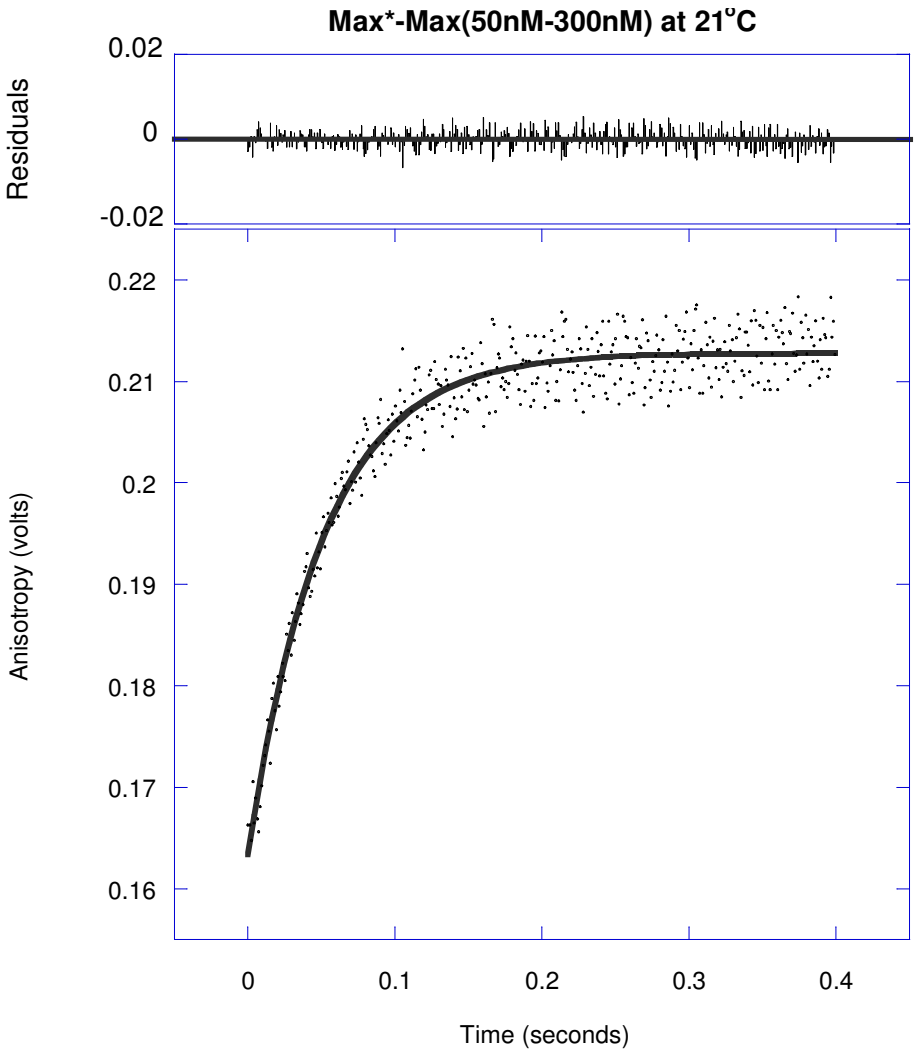

Figure 18: Stopped- flow kinetic binding measurement of Max to FITC labeled Max

Kinetic data shows the time dependent increase in anisotropy after mixing 50 nM FITC labeled Max with 300 nM unlabeled Max at 21 °C

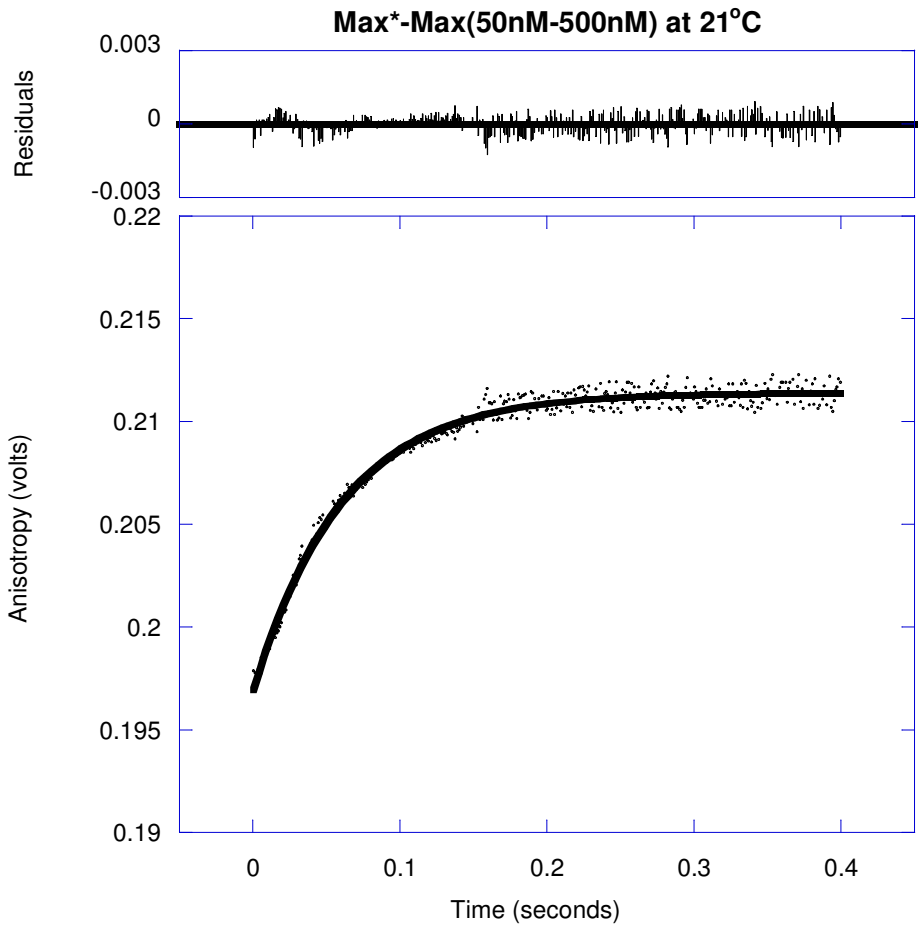

Figure 19: Stopped- flow kinetic binding measurement of Max to FITC labeled Max

Kinetic data shows the time dependent increase in anisotropy after mixing 50 nM FITC labeled Max with 500 nM unlabeled Max at 21 °C

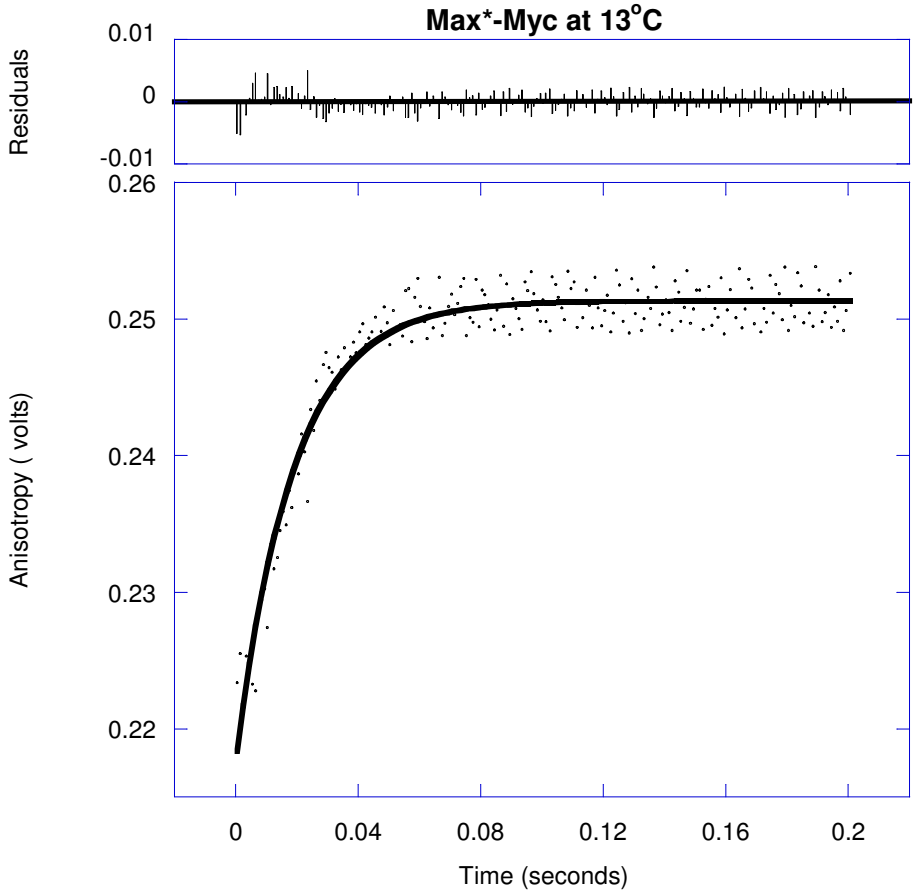

Figure 20: Stopped- flow kinetic binding measurement of Myc to FITC labeled Max

Kinetic data shows the time dependent increase in anisotropy after mixing 50 nM FITC labeled Max with 4 µM unlabeled Myc at 13 °C

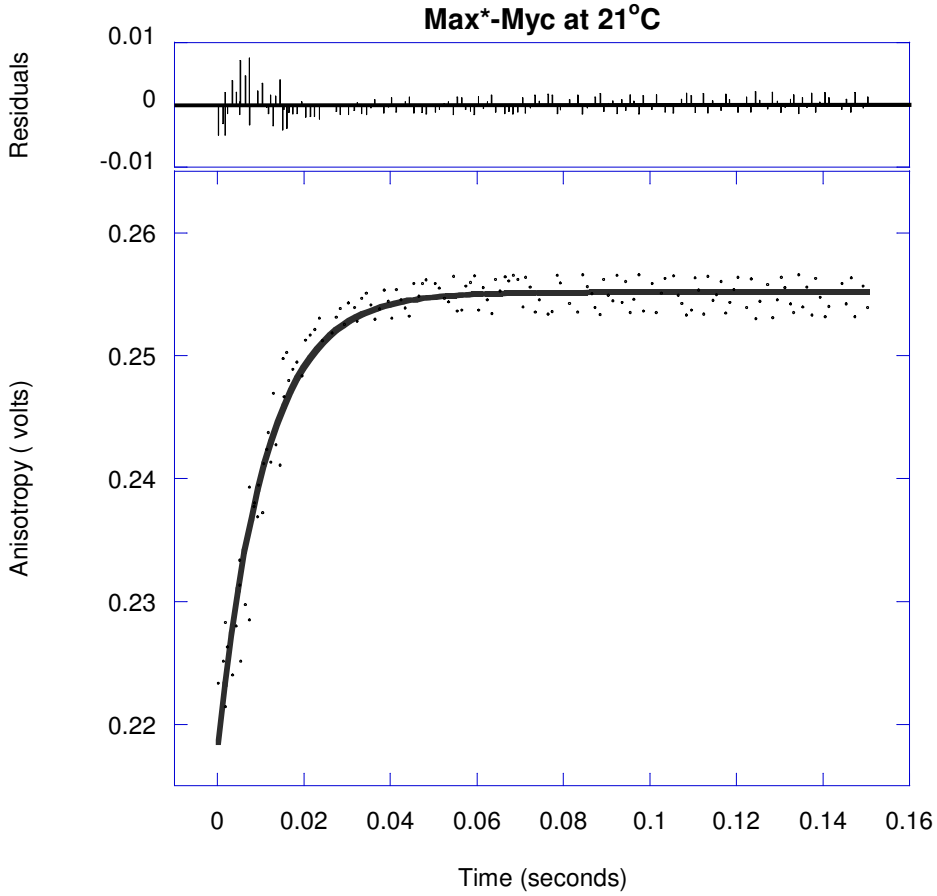

Figure 21: Stopped- flow kinetic binding measurement of Myc to FITC labeled Max

Kinetic data shows the time dependent increase in anisotropy after mixing 50 nM FITC labeled Max with 4 µM unlabeled Myc at 21 °C

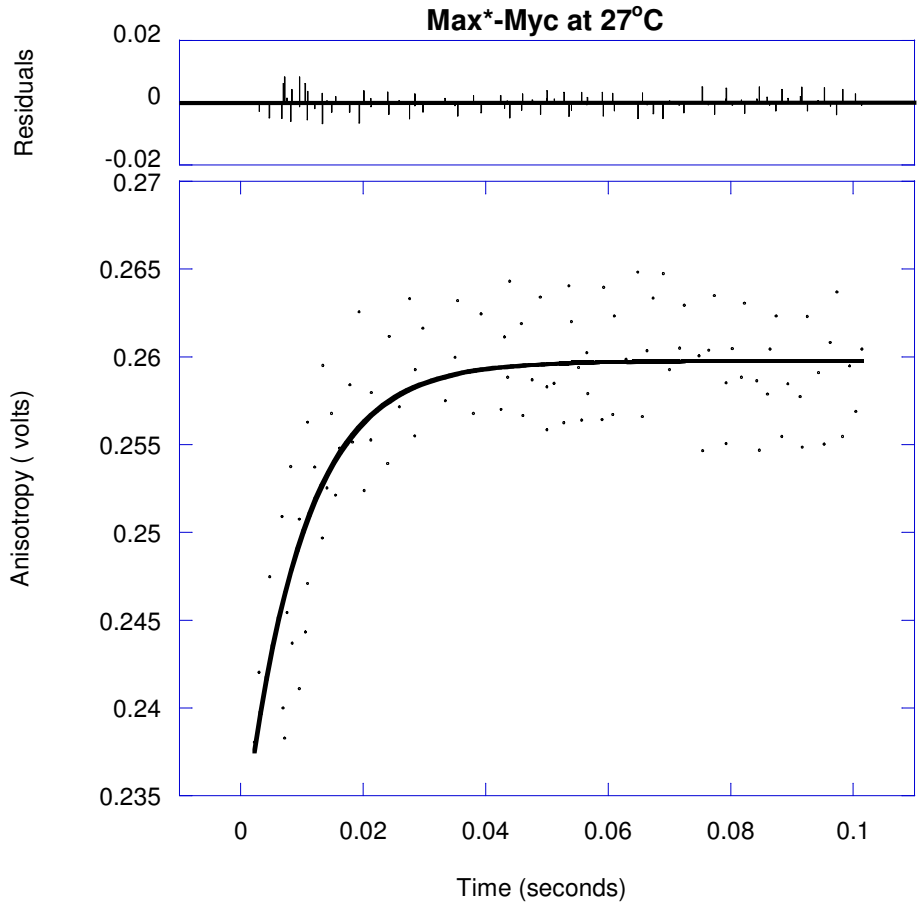

Figure 22: Stopped- flow kinetic binding measurement of Myc to FITC labeled Max

Kinetic data shows the time dependent increase in anisotropy after mixing 50 nM FITC labeled Max with 4 µM unlabeled Myc at 27 °C

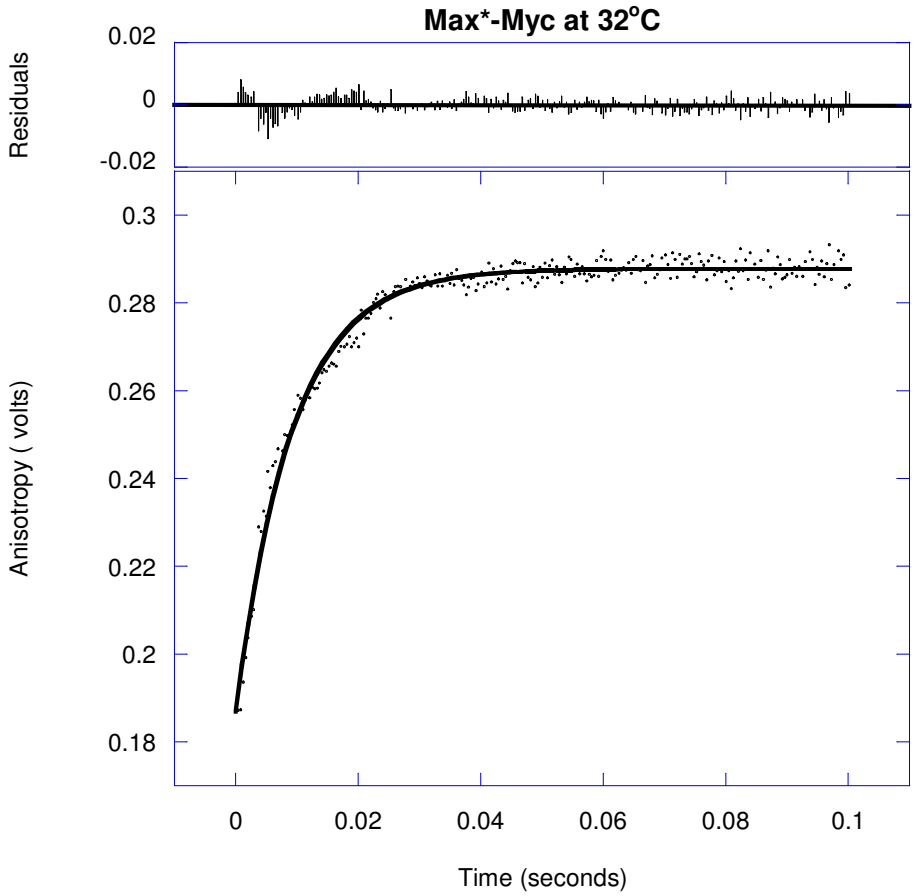

Figure 23: Stopped- flow kinetic binding measurement of Myc to FITC labeled Max

Kinetic data shows the time dependent increase in anisotropy after mixing 50 nM FITC labeled Max with 4 µM unlabeled Myc at 32 °C

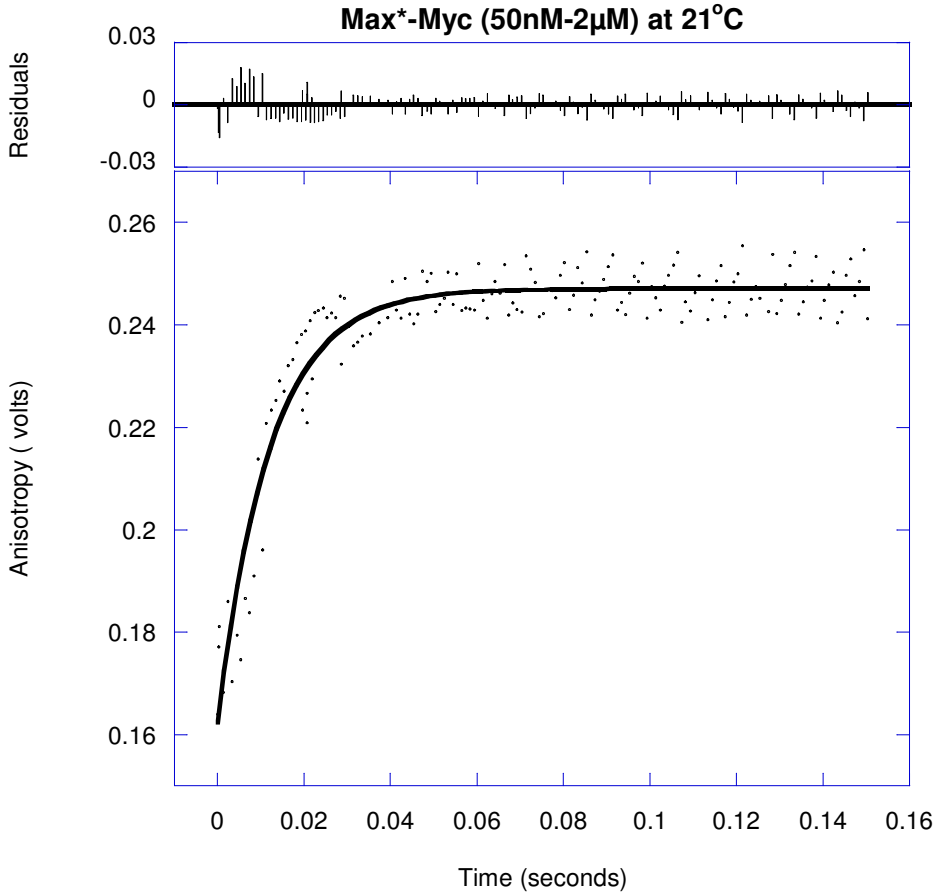

Figure 24: Stopped- flow kinetic binding measurement of Myc to FITC labeled Max

Kinetic data shows the time dependent increase in anisotropy after mixing 50 nM FITC labeled Max with 2 µM unlabeled Myc at 21 °C

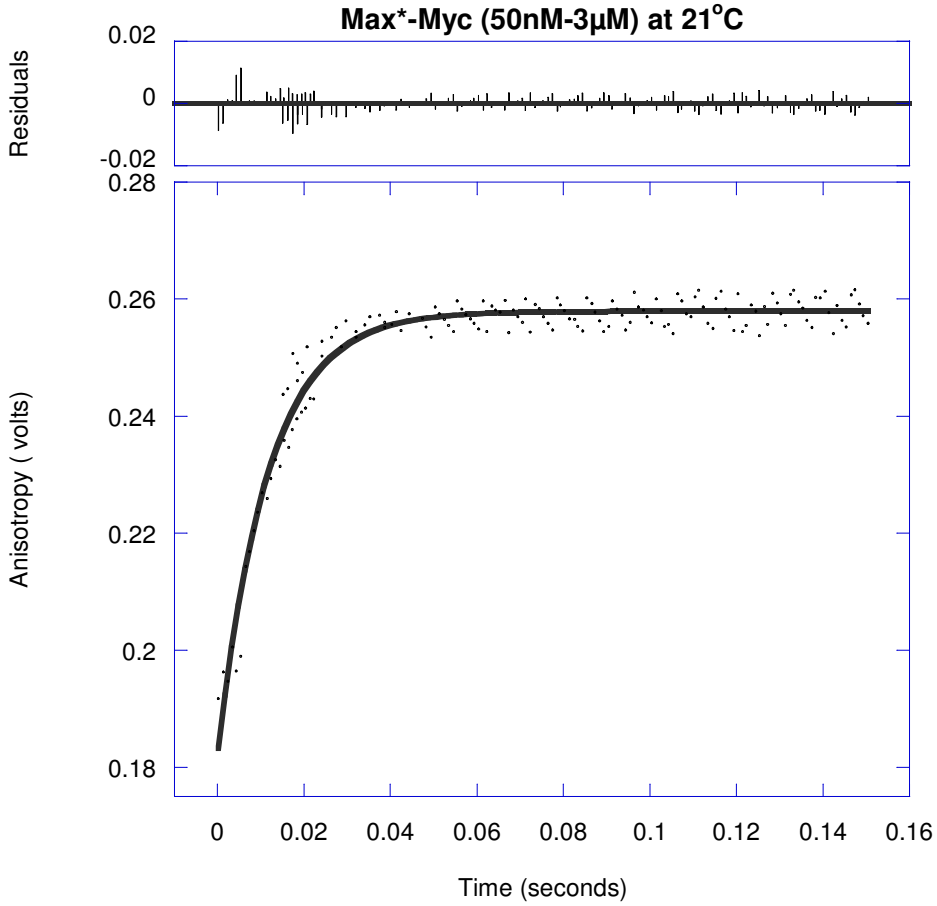

Figure 25: Stopped- flow kinetic binding measurement of Myc to FITC labeled Max

Kinetic data shows the time dependent increase in anisotropy after mixing 50 nM FITC labeled Max with 3 µM unlabeled Myc at 21 °C

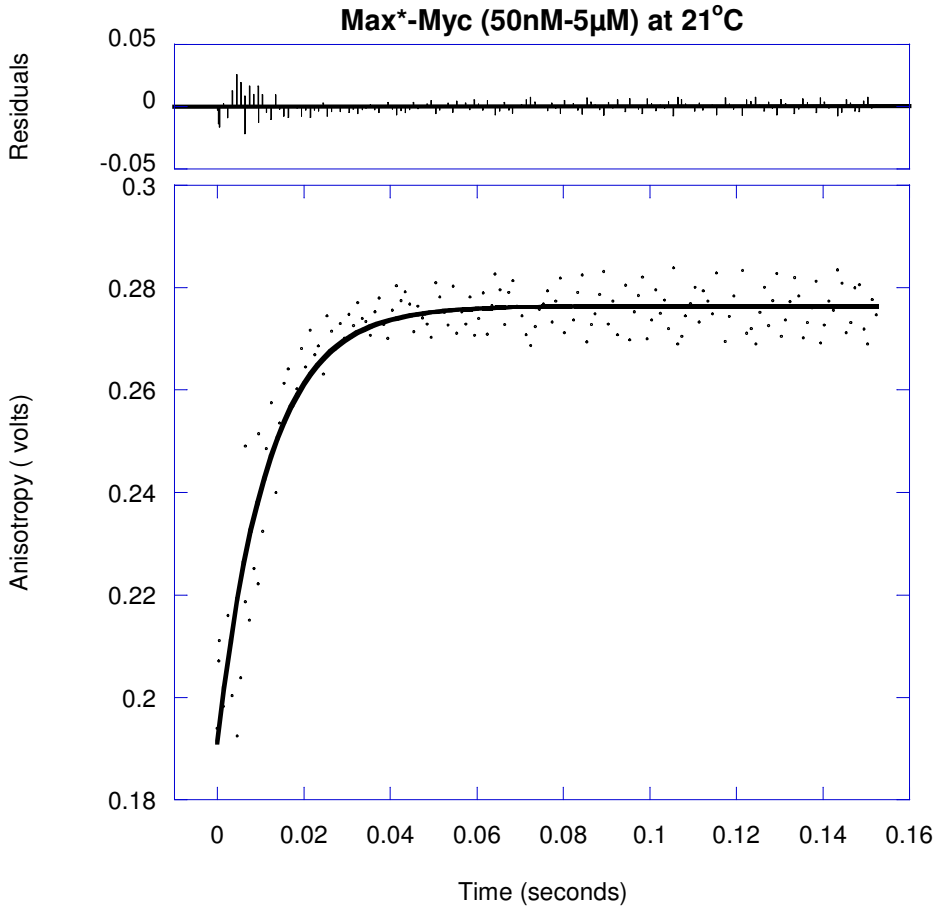

Figure 26: Stopped- flow kinetic binding measurement of Myc to FITC labeled Max

Kinetic data shows the time dependent increase in anisotropy after mixing 50 nM FITC labeled Max with 5 µM unlabeled Myc at 21 °C

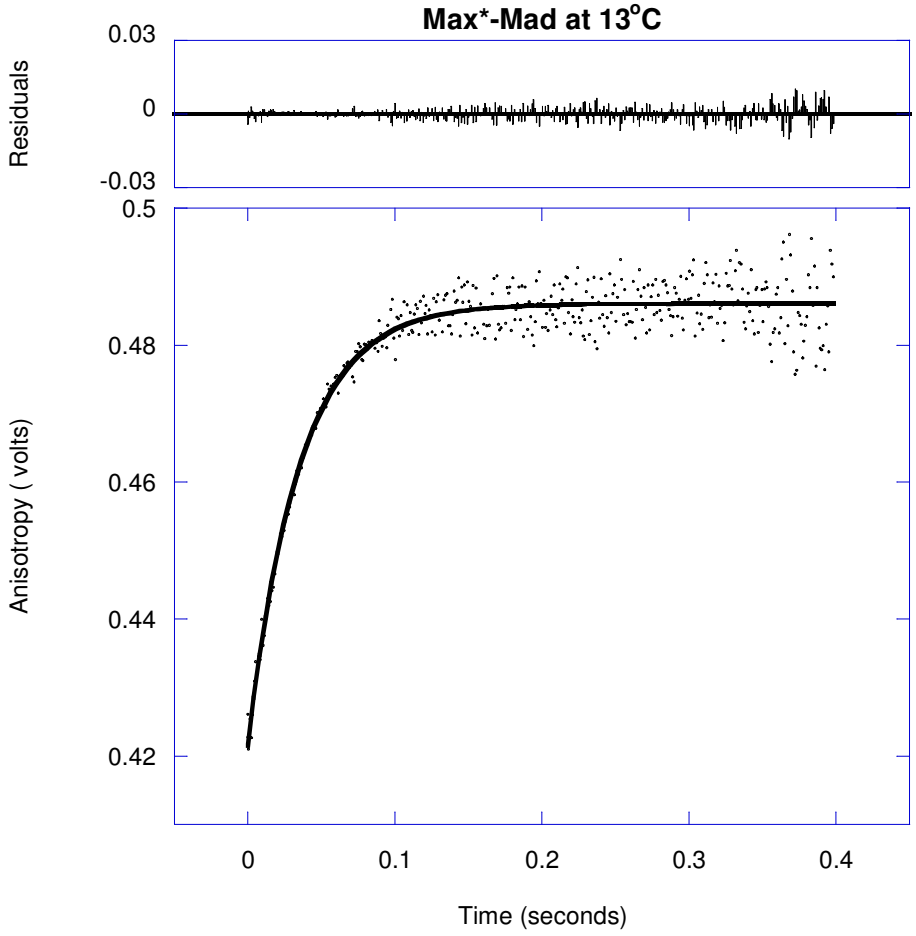

Figure 27: Stopped- flow kinetic binding measurement of Mad to FITC labeled Max

Kinetic data shows the time dependent increase in anisotropy after mixing 50 nM FITC labeled Max with 4 µM unlabeled Mad at 13 °C

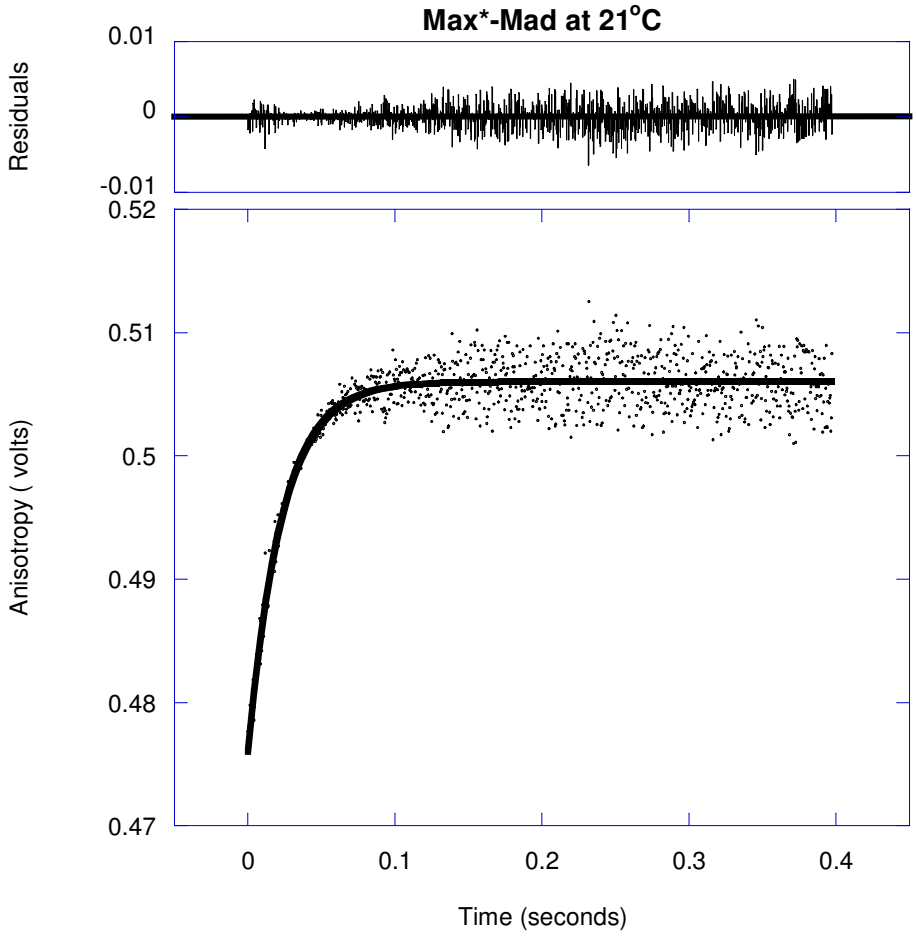

Figure 28: Stopped- flow kinetic binding measurement of Mad to FITC labeled Max

Kinetic data shows the time dependent increase in anisotropy after mixing 50 nM FITC labeled Max with 4 µM unlabeled Mad at 21 °C

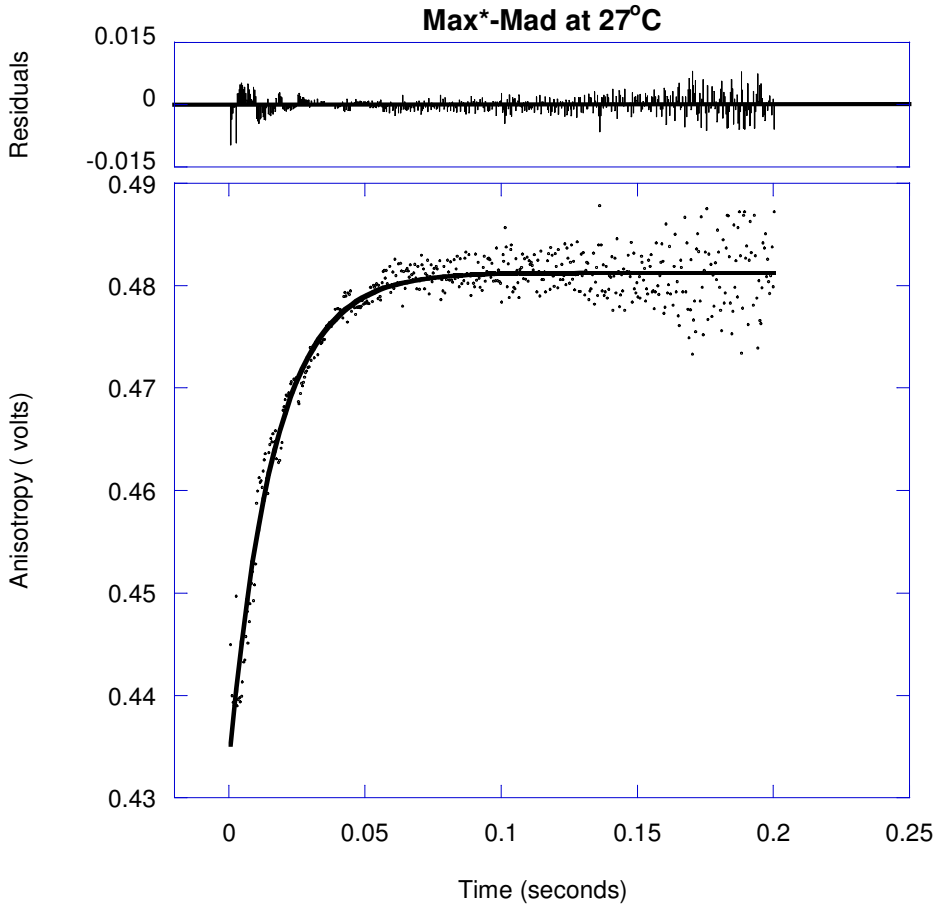

Figure 29: Stopped- flow kinetic binding measurement of Mad to FITC labeled Max

Kinetic data shows the time dependent increase in anisotropy after mixing 50 nM FITC labeled Max with 4 µM unlabeled Mad at 27 °C

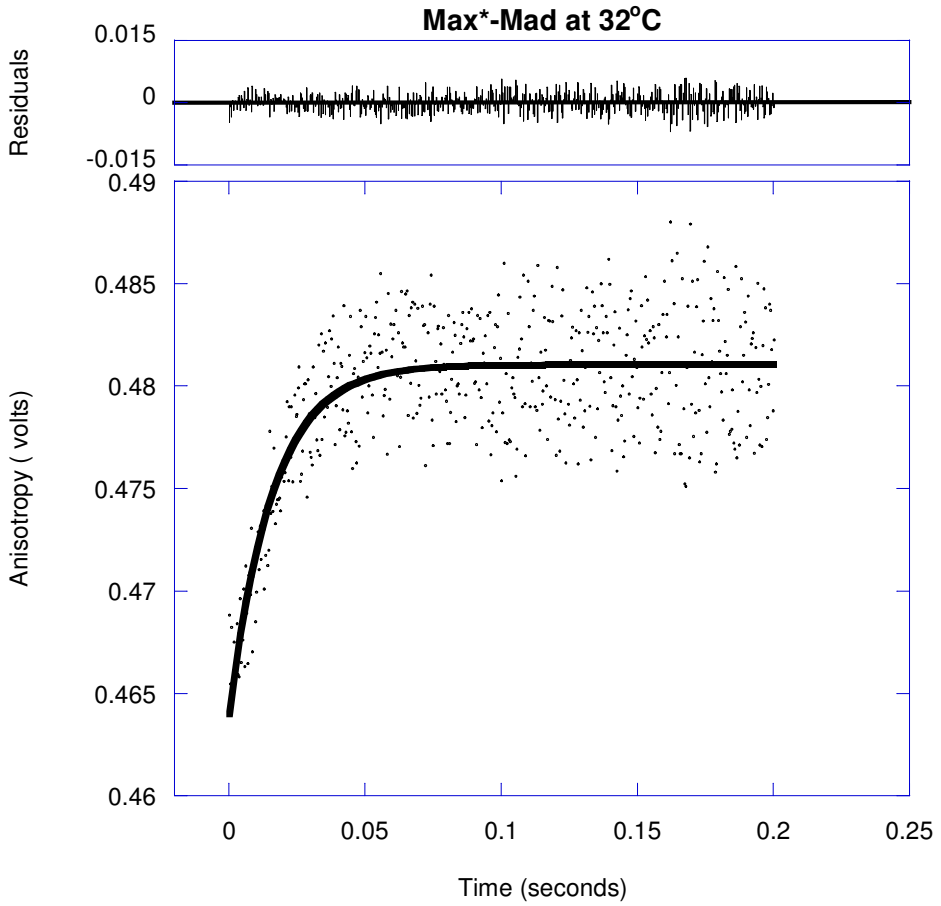

Figure 30: Stopped- flow kinetic binding measurement of Mad to FITC labeled Max

Kinetic data shows the time dependent increase in anisotropy after mixing 50 nM FITC labeled Max with 4 µM unlabeled Mad at 32 °C

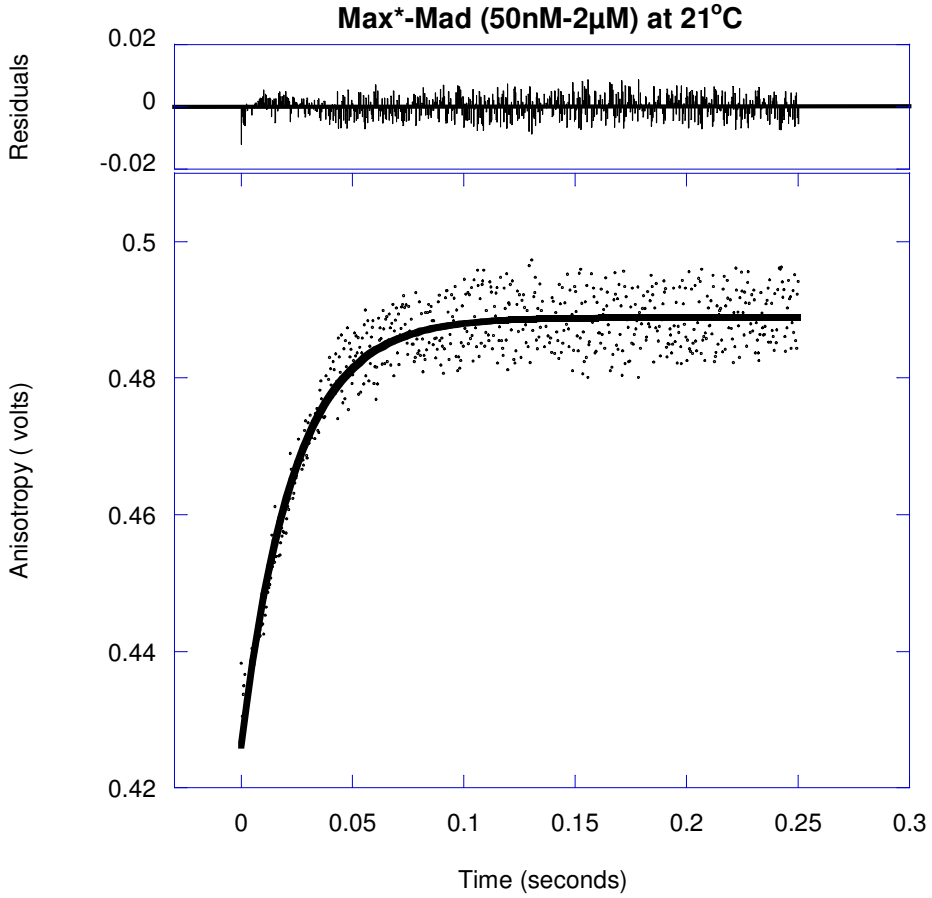

Figure 31: Stopped- flow kinetic binding measurement of Mad to FITC labeled Max

Kinetic data shows the time dependent increase in anisotropy after mixing 50 nM FITC labeled Max with 2 µM unlabeled Mad at 21 °C

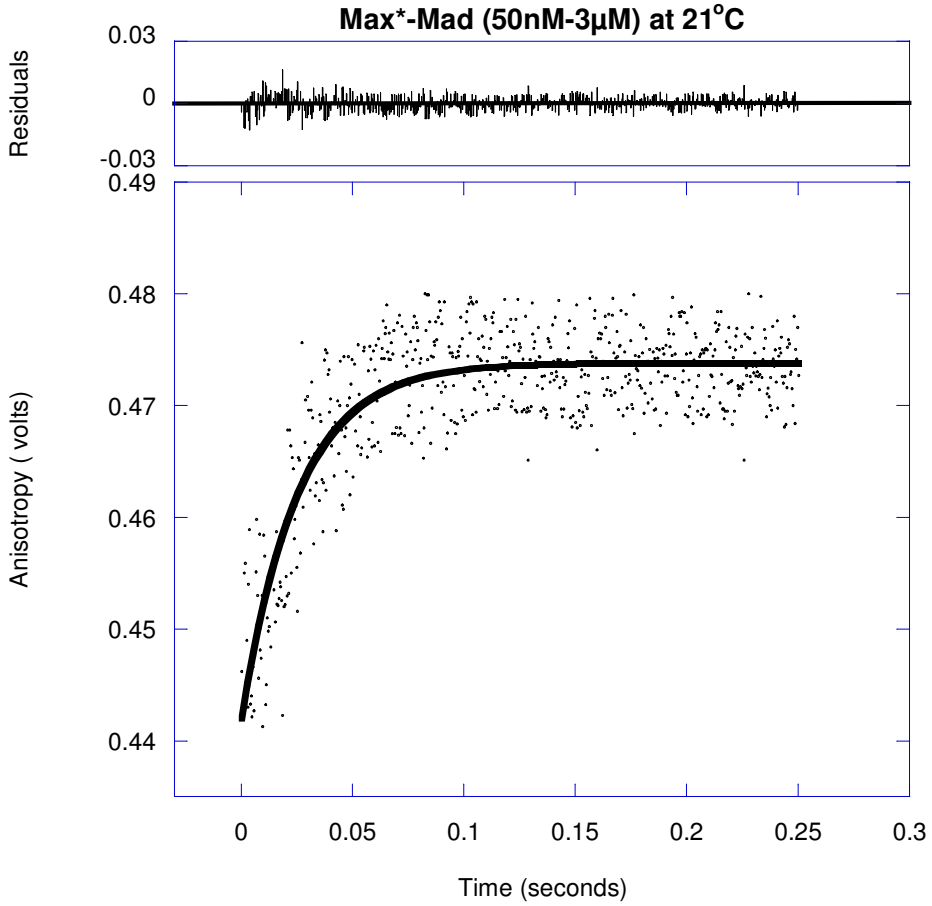

Figure 32: Stopped- flow kinetic binding measurement of Mad to FITC labeled Max

Kinetic data shows the time dependent increase in anisotropy after mixing 50 nM FITC labeled Max with 3 µM unlabeled Mad at 21 °C

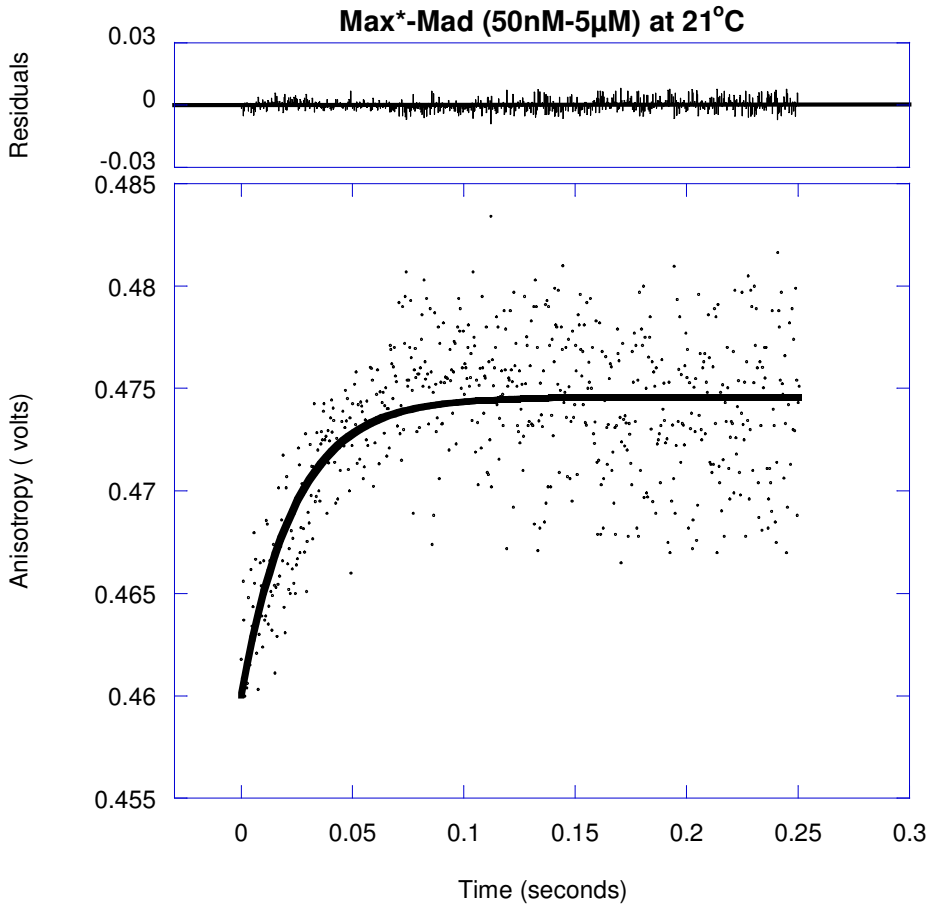

Figure 33: Stopped- flow kinetic binding measurement of Mad to FITC labeled Max

Kinetic data shows the time dependent increase in anisotropy after mixing 50 nM FITC labeled Max with 5 µM unlabeled Mad at 21 °C

Table 2: Kinetic binding constants for the interaction of Max, Myc and Mad with FITC labeled Max

Rate Constants $k_2(s^{-1})$

Temp	Max-Max	Myc-Max	Mad-Max
13°C	16.4±1.0	53.3±1.9	28.5±0.7
21°C	18.7±0.5	90.7±3.6	43.7±1.1
27°C	21.1±0.4	104±4.0	60.4±1.5
32°C	24.4±0.7	109±1.9	63.1±4.7
E_a(kJ/mol)	***14.8±0.2***	***27.6±0.8***	***31.9±0.6***

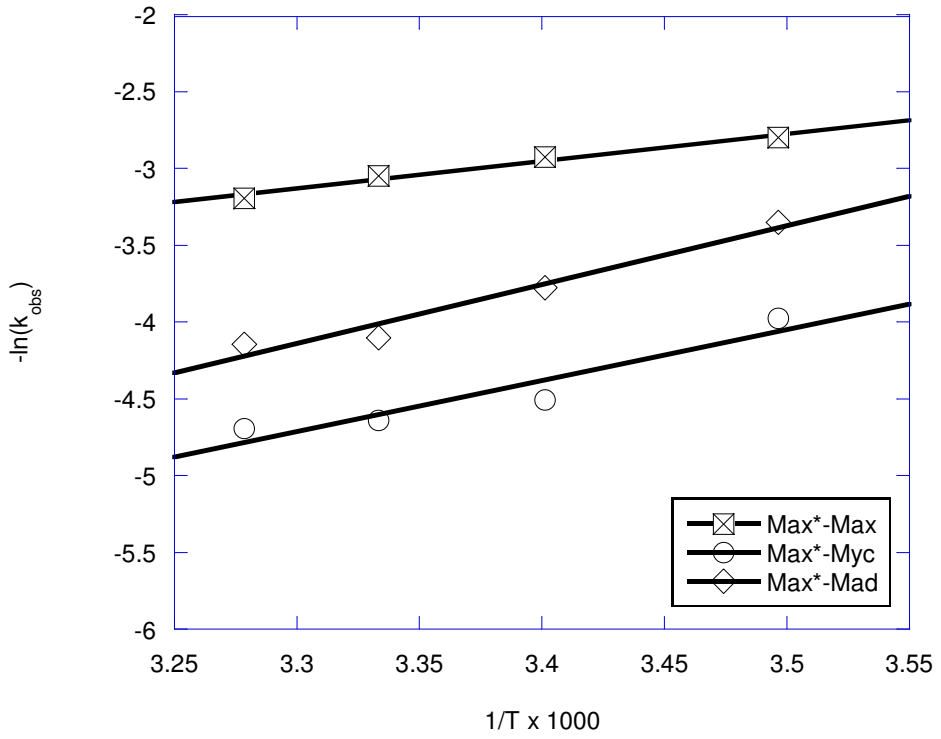

Figure 34: Arrhenius plots for the interaction of Max, Myc and Mad with FITC labeled Max

Table 3: Kinetic binding constants for the interaction of Max, Myc and Mad with FITC labeled Max

Rate Constants $k_2(s^{-1})$

[C] of unlabeled Myc and Mad [µM]	Myc-Max	Mad-Max
2	82.4±4.3	42.5±1.1
3	86.5±2.8	39.6±2.0
4	90.7±3.6	43.7±1.1
5	86.3±5.1	42.2±3.7

[C] of unlabeled Max [µM]	Max-Max
0.2	18.1±0.5
0.3	19.6±0.5
0.4	18.7±0.5
0.5	18.6±0.2

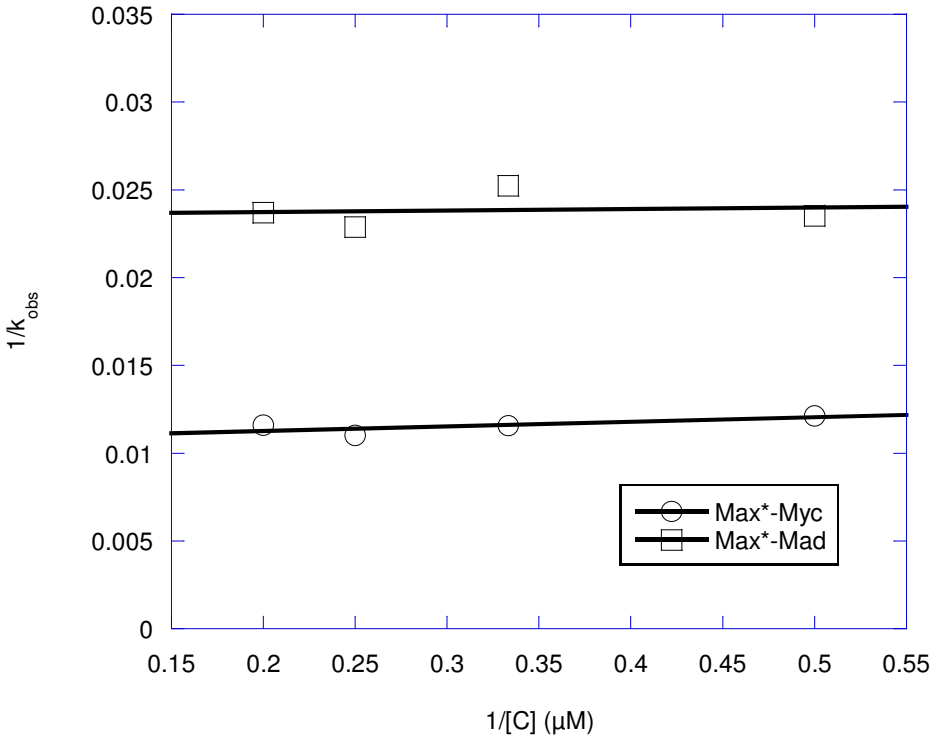

Figure 35: Kinetic plots of 1/ k_{obs} versus 1/ [C] for the interaction of Myc and Mad with FITC labeled Max

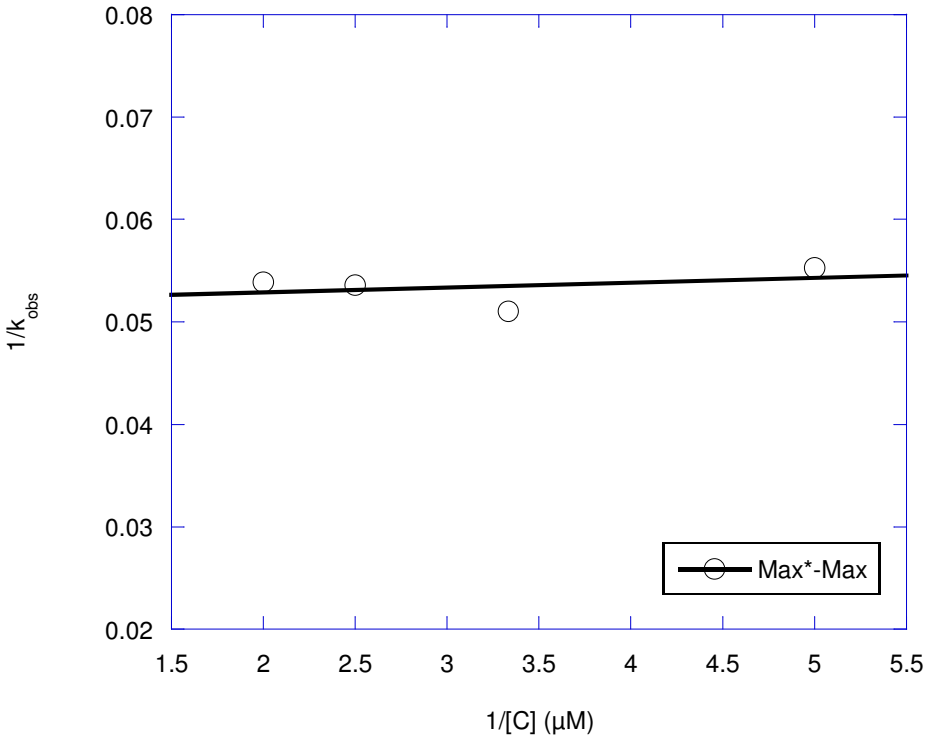

Figure 36: Kinetic plots of 1/ k_{obs} versus 1/ [C] for the interaction of Max with FITC labeled Max

3.2 Dimer-DNA Kinetics

To determine the DNA binding rate constants of Max-Max homodimer, Myc-Max and Mad-Max heterodimers, stopped-flow anisotropy experiments were performed using 16mer 5'FITC labeled E-Box DNA oligonucleotide. In all these kinetic studies, the final concentration of the 5' FITC labeled 16mer DNA oligonucleotide was kept constant at 50 nM. Increasing concentrations of the unlabeled Max-Max, Myc-Max and Mad-Max protein dimers (for each case, the final concentrations were: 2, 3, 4 and 5 μM) were injected into the mixing chamber of the stopped-flow instrument. All these concentration dependence studies were performed at 21°C. Max was preincubated with Myc or Mad protein at room temperature for 30 min to dimerize prior to the reaction with the E-Box DNA. The changes in the anisotropy as a function of time for the four different concentrations of the protein dimers were recorded and fitted using equation 5 given above (fig. 37-57).

The kinetic rate constants for the interaction of Max-Max, Myc-Max and Mad-Max with the DNA-E-Box at four different concentrations of protein dimers are shown in Table 5. The rate constants calculated for the Myc-Max -DNA were found to be very similar to the rate constants of Max-Max-DNA. Among all the three interactions, the Mad-Max-DNA has the lowest rate constants at all four different concentrations. Our results show that the average rate constants for the Max-Max-DNA and Myc-Max-DNA are 1.6 and 1.5 fold higher than for the Mad-Max-DNA, respectively.

To determine whether protein dimer-DNA rates are concentration dependent,

$1/k_{obs}$ versus 1/[C] graphs were plotted. Figure 59 representing $1/k_{obs}$ versus 1/[C] kinetic plots, reveals that the interactions between the protein dimers Max-Max, Myc-Max, Mad-Max and the E-box DNA are concentration independent. k_2 values, obtained from the y-intercept , were calculated to be 128, 122 and 80 s^{-1} for Max-Max-DNA, Myc-Max-DNA and Mad-Max-DNA interactions, respectively.

The interactions between Max-Max, Myc-Max and Mad-Max protein dimers and FITC labeled E-box DNA oligonucleotide were also investigated at different temperatures using stopped-flow polarization methods. The effects of the temperature on the rate constants of these protein dimer-DNA reactions are shown in table 4. Anisotropy change upon the interaction was measured by rapidly mixing unlabeled Max-Max, Myc-Max, Mad-Max dimers and FITC-labeled DNA-E-box oligonucleotide. The final concentration of the protein dimers and DNA E-Box in the mixing chamber of the stopped-flow instrument were 3 μM and 50 nM, respectively. Stopped-flow data traces for four increasing temperatures (13, 21, 27 and 32°C) are presented in figures 37-57. For all the three protein-dimer-DNA interactions, an increase in the observed rate constants was observed with increasing temperatures. The observed rate constants for Mad-Max-DNA at all four temperatures are the lowest, whereas Max-Max-DNA and Myc-Max-DNA interactions have similar rate constants. The rate for the reaction of Max-Max and Myc-Max dimers with DNA is approximately 1.6 times faster than that of Mad-Max.

From the temperature dependence of the rate constants of these dimer-DNA interactions, Arrhenius plots (fig. 58) were obtained and activation energies, E_a, were evaluated from their slopes. Analysis of the Arrhenius plots show that the activation

energies for Max-Max-DNA and Mad-Max-DNA are very close to each other (~12 kJ/mol). The activation energy for the interaction of Myc-Max dimer with DNA E-Box is slightly lower than for Mad-Max and Max-Max dimers (~10 kJ/mol).

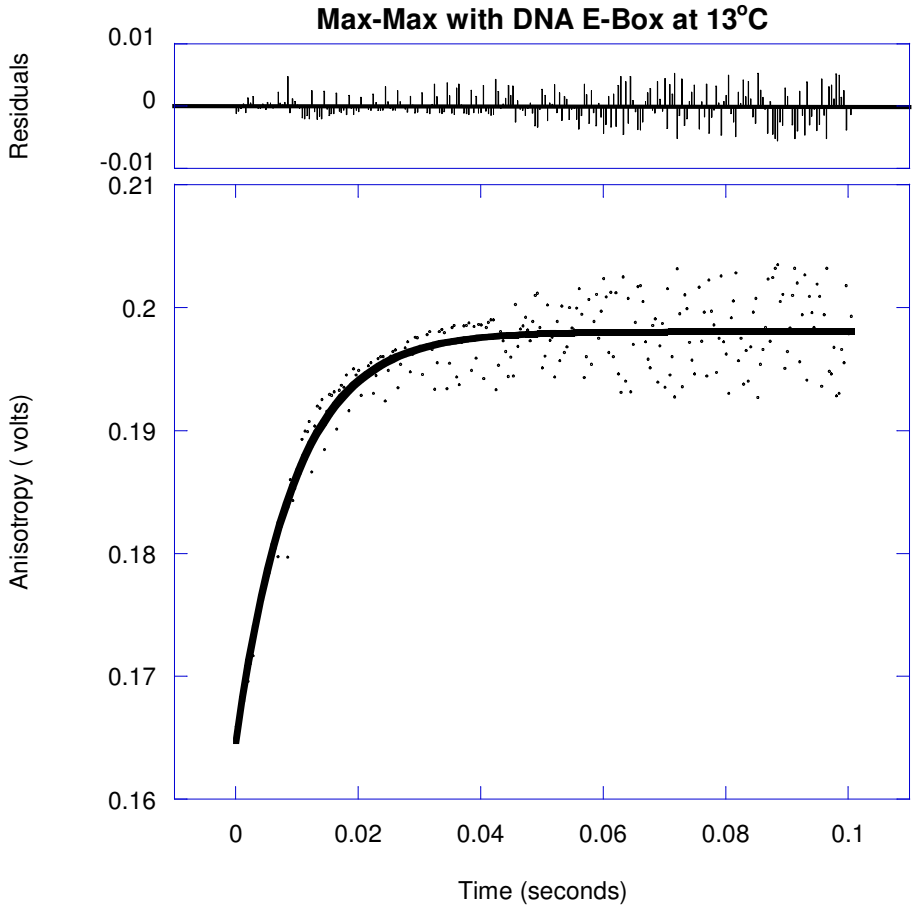

Figure 37: Stopped- flow kinetic binding measurement of Max-Max to DNA E-Box

Kinetic data shows the time dependent increase in anisotropy after mixing 50 nM DNA oligonucleotide with 3 µM Max-Max homodimer at 13 °C

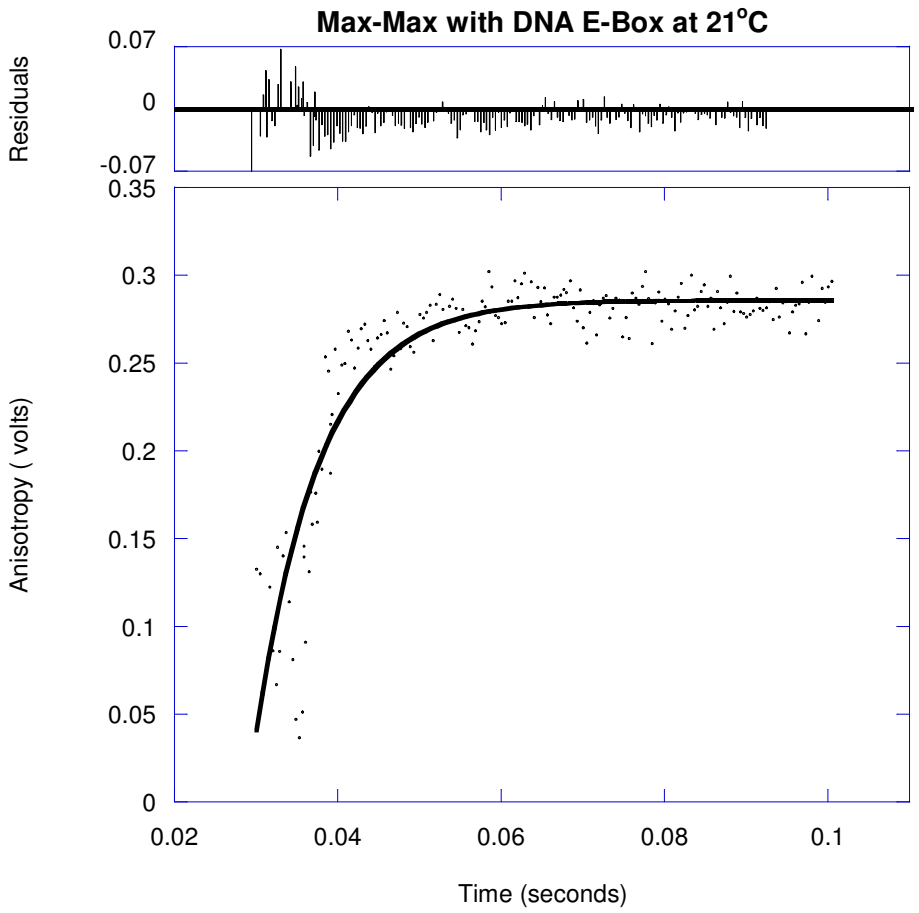

Figure 38: Stopped- flow kinetic binding measurement of Max-Max to DNA E-Box

Kinetic data shows the time dependent increase in anisotropy after mixing 50 nM DNA oligonucleotide with 3 µM Max-Max homodimer at 21 °C

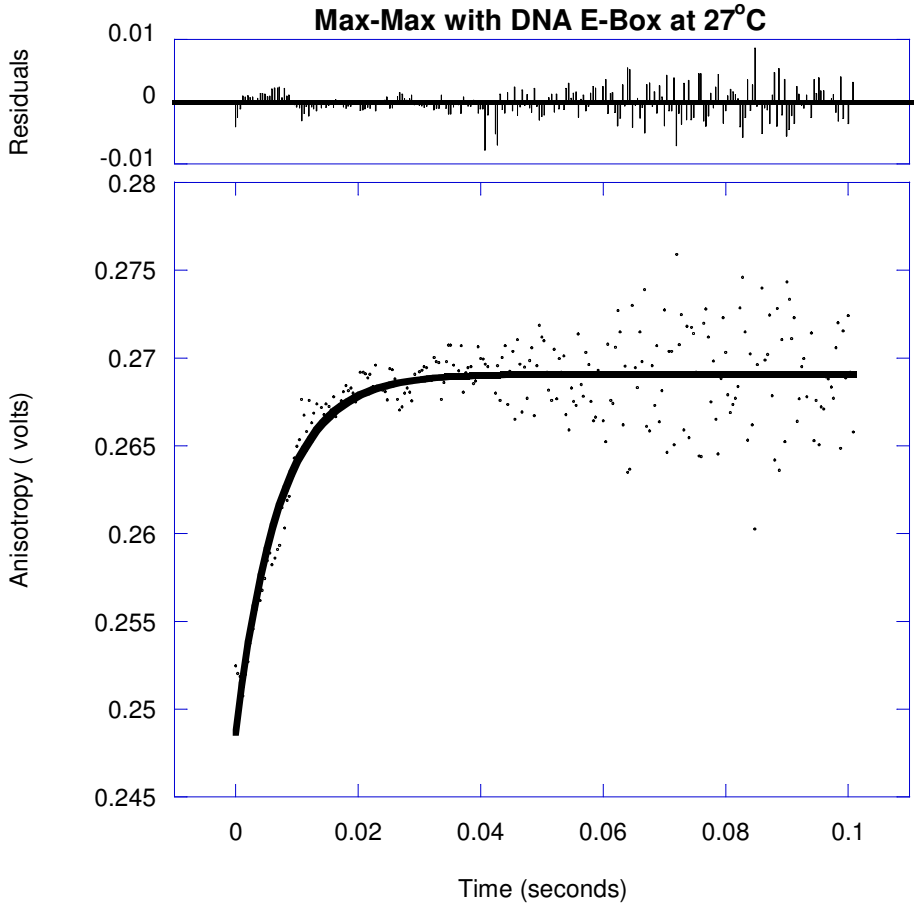

Figure 39: Stopped- flow kinetic binding measurement of Max-Max to DNA E-Box

Kinetic data shows the time dependent increase in anisotropy after mixing 50 nM DNA oligonucleotide with 3 µM Max-Max homodimer at 27 °C

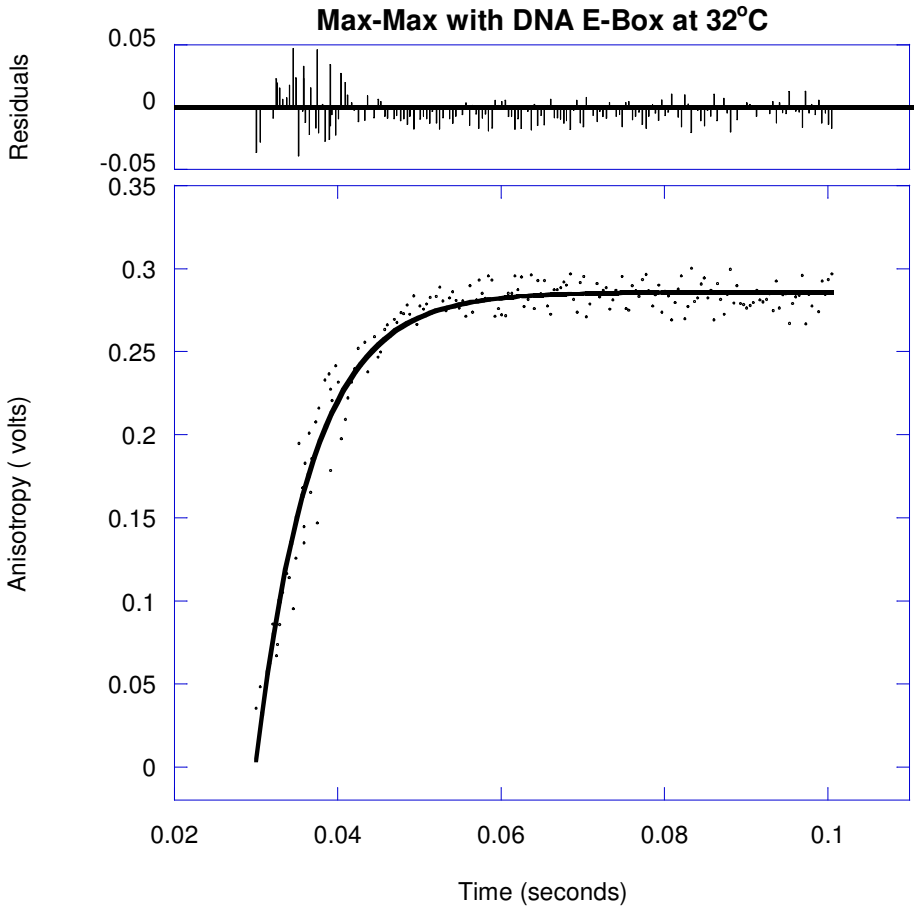

Figure 40: Stopped- flow kinetic binding measurement of Max-Max to DNA E-Box

Kinetic data shows the time dependent increase in anisotropy after mixing 50 nM DNA oligonucleotide with 3 µM Max-Max homodimer at 32 °C

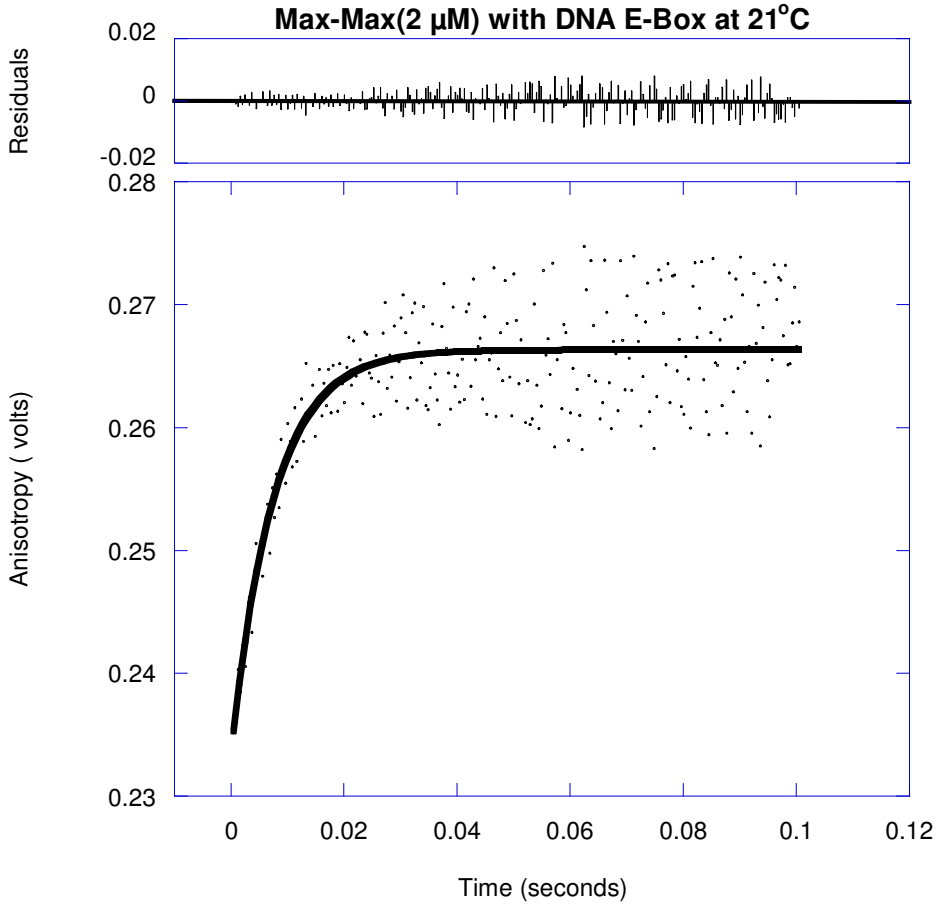

Figure 41: Stopped- flow kinetic binding measurement of Max-Max to DNA E-Box

Kinetic data shows the time dependent increase in anisotropy after mixing 50 nM DNA oligonucleotide with 2 µM Max-Max homodimer at 21 °C

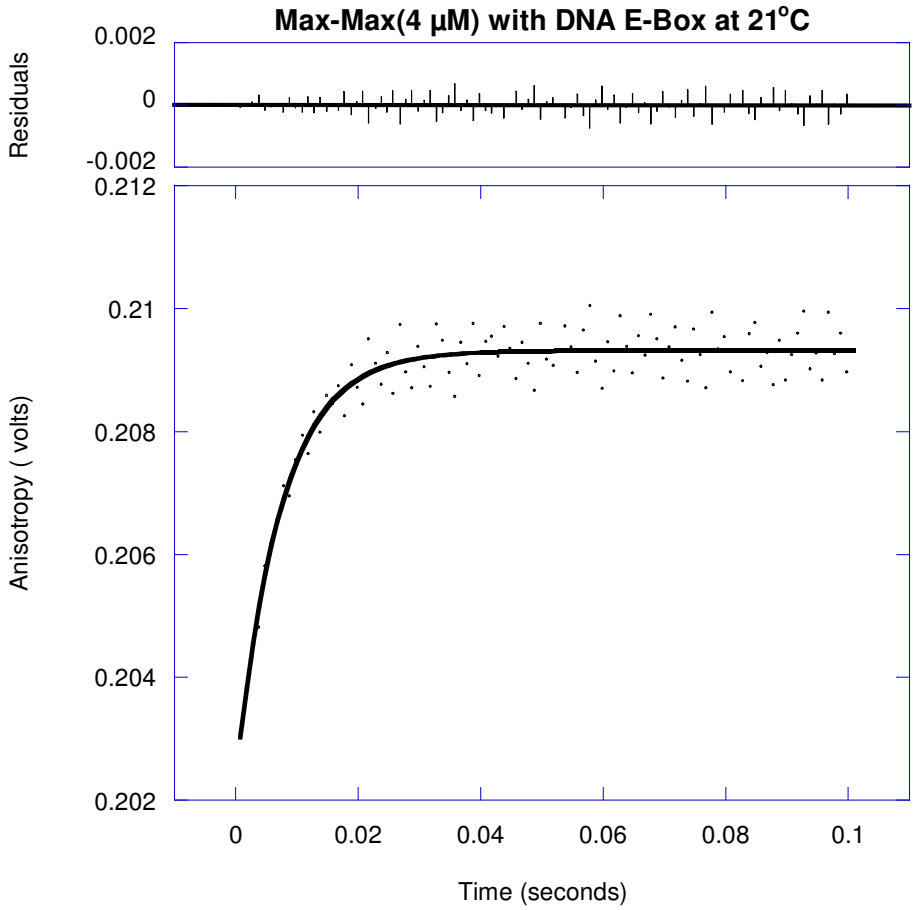

Figure 42: Stopped- flow kinetic binding measurement of Max-Max to DNA E-Box

Kinetic data shows the time dependent increase in anisotropy after mixing 50 nM DNA oligonucleotide with 4 µM Max-Max homodimer at 21 °C

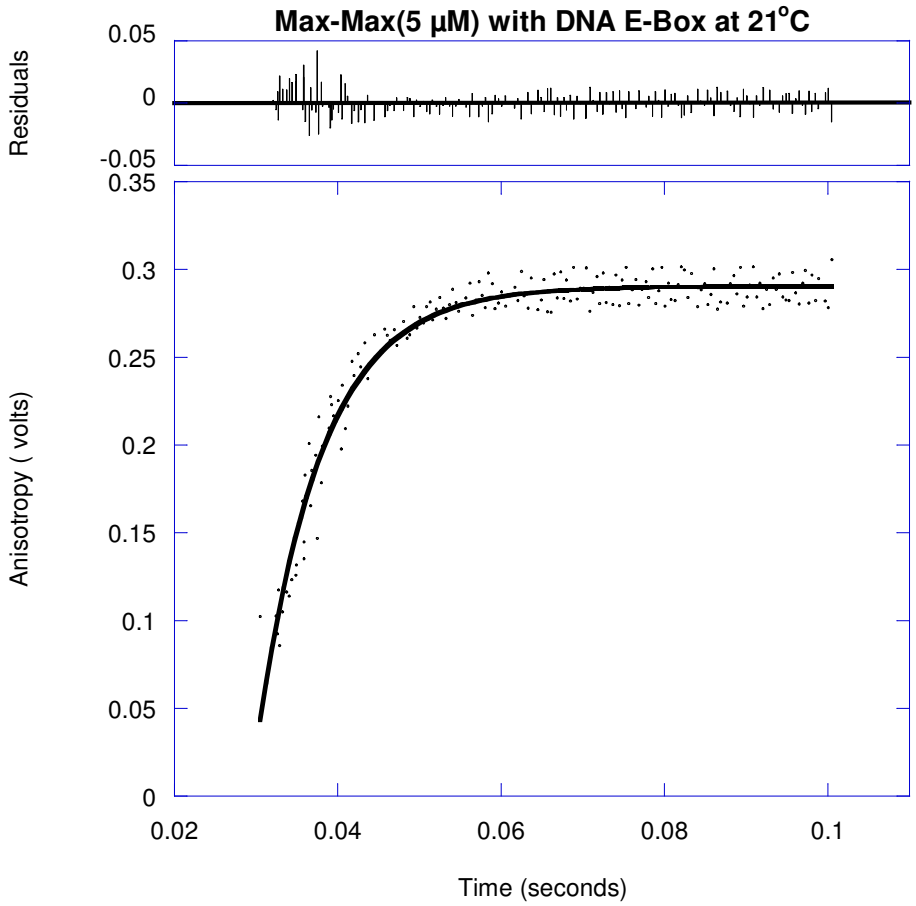

Figure 43: Stopped- flow kinetic binding measurement of Max-Max to DNA E-Box

Kinetic data shows the time dependent increase in anisotropy after mixing 50 nM DNA oligonucleotide with 5 µM Max-Max homodimer at 21 °C

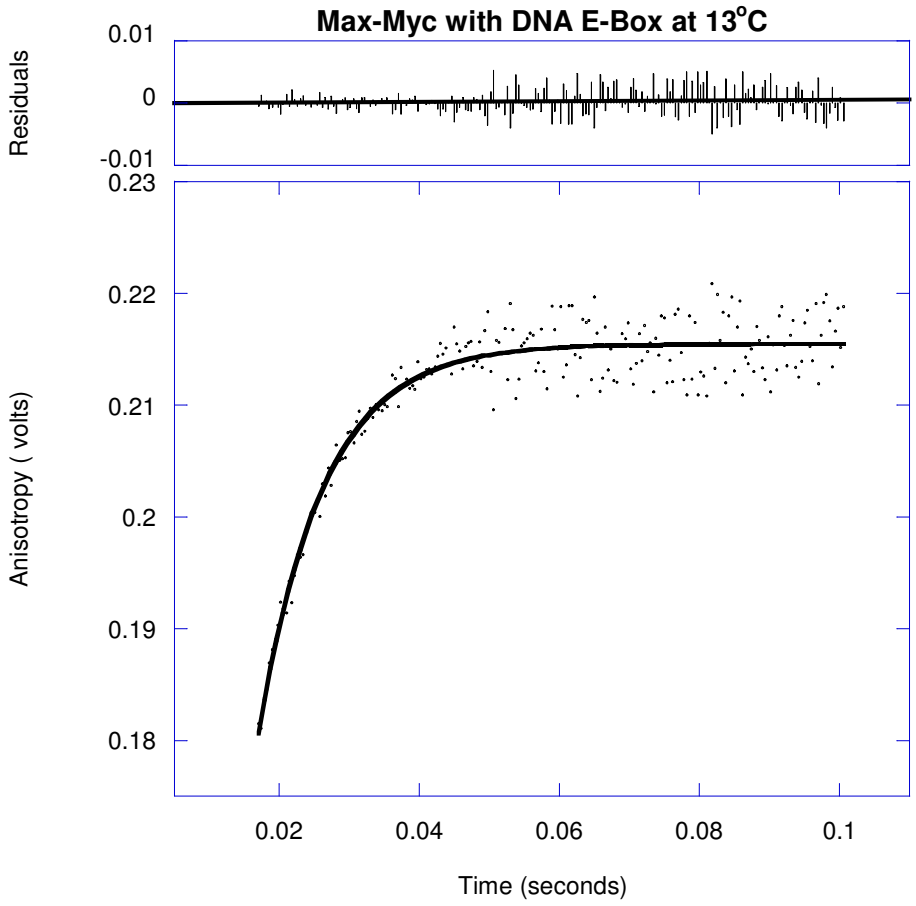

Figure 44: Stopped- flow kinetic binding measurement of Myc-Max to DNA E-Box

Kinetic data shows the time dependent increase in anisotropy after mixing 50 nM DNA oligonucleotide with 3 µM Myc-Max heterodimer at 13 °C

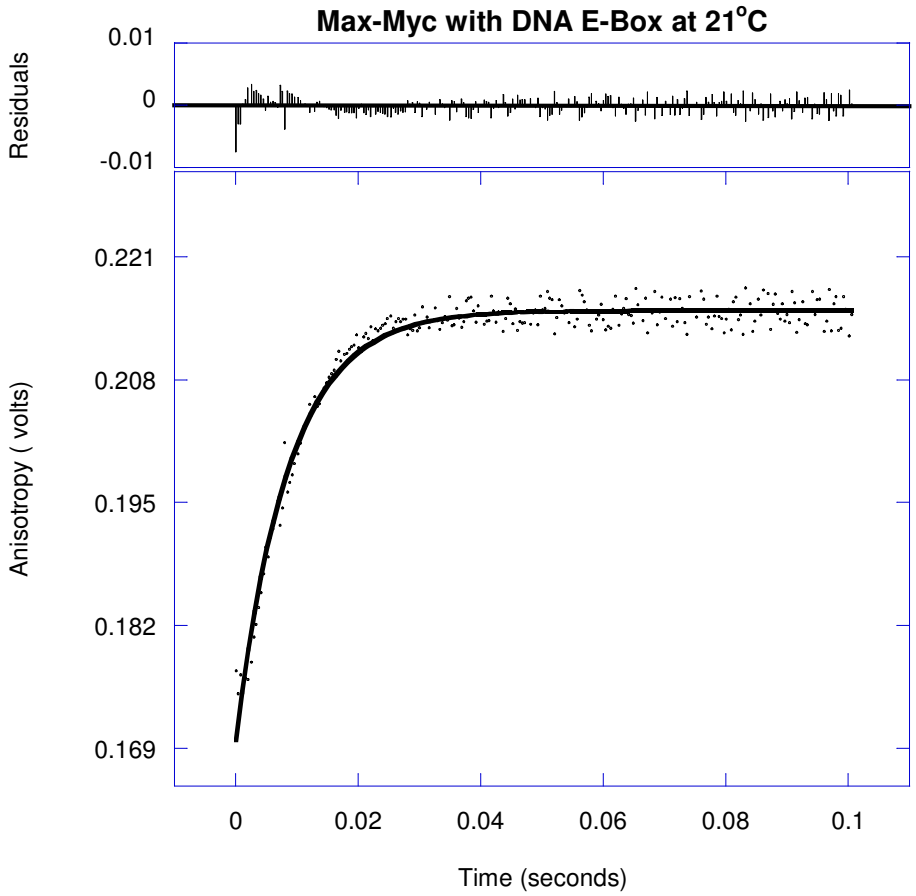

Figure 45: Stopped- flow kinetic binding measurement of Myc-Max to DNA E-Box

Kinetic data shows the time dependent increase in anisotropy after mixing 50 nM DNA oligonucleotide with 3 µM Myc-Max heterodimer at 21 °C

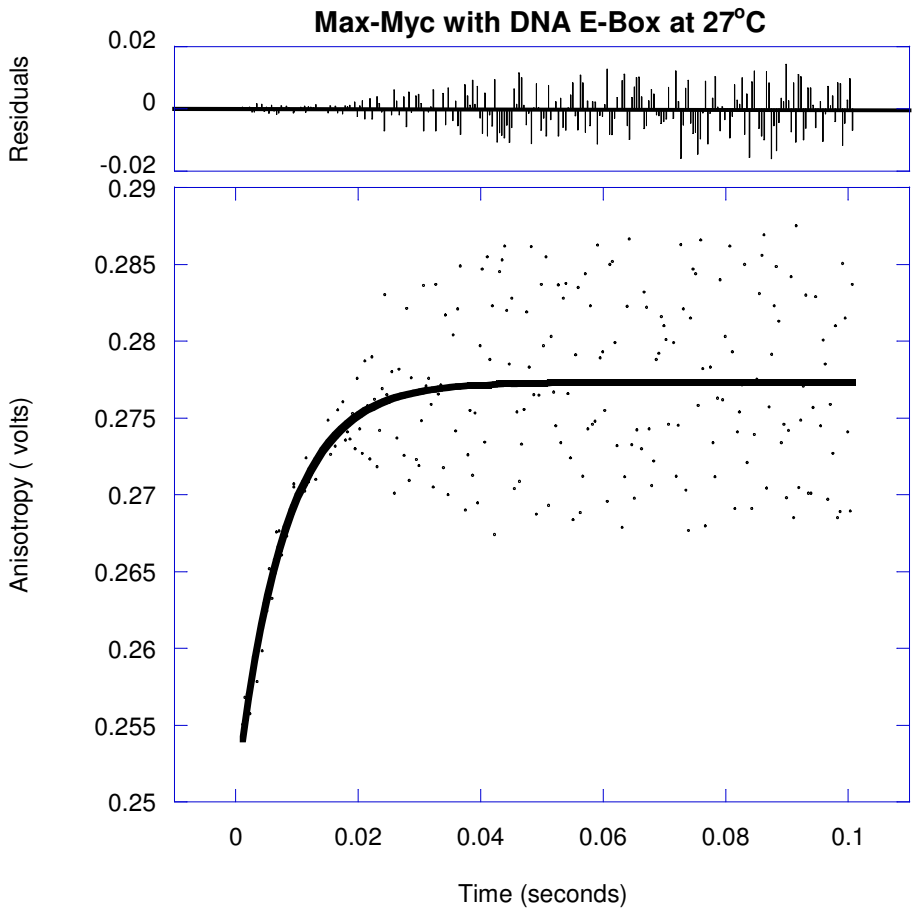

Figure 46: Stopped- flow kinetic binding measurement of Myc-Max to DNA E-Box

Kinetic data shows the time dependent increase in anisotropy after mixing 50 nM DNA oligonucleotide with 3 µM Myc-Max heterodimer at 27 °C

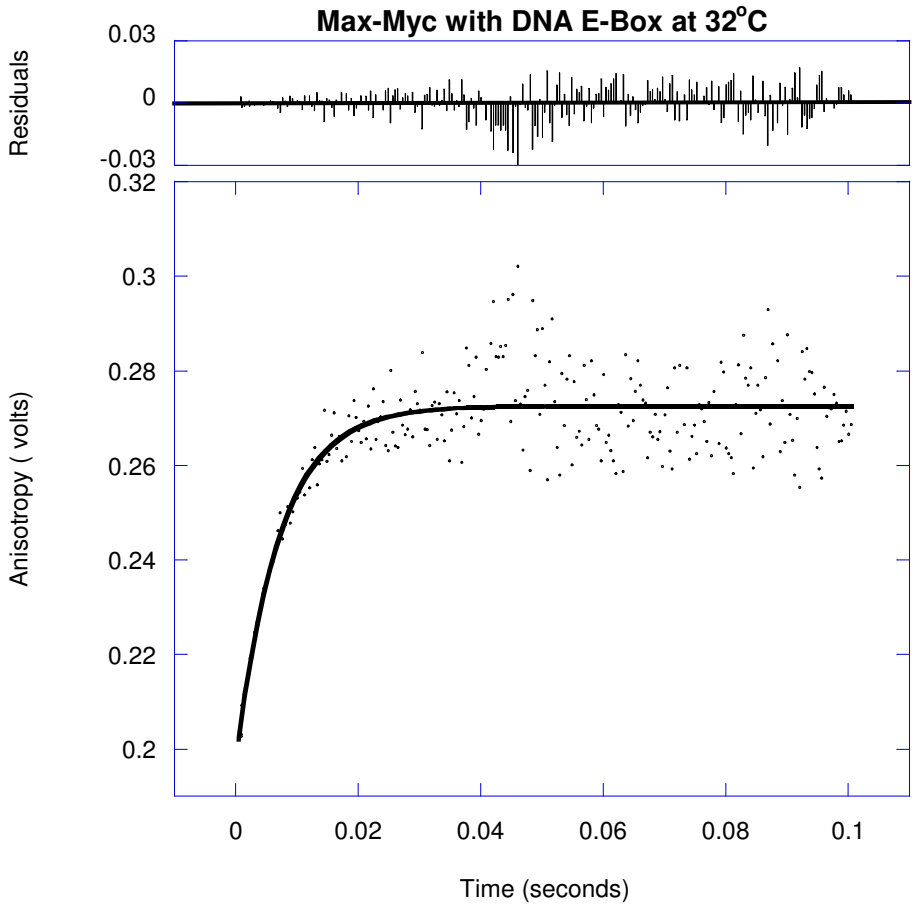

Figure 47: Stopped- flow kinetic binding measurement of Myc-Max to DNA E-Box

Kinetic data shows the time dependent increase in anisotropy after mixing 50 nM DNA oligonucleotide with 3 µM Myc-Max heterodimer at 32 °C

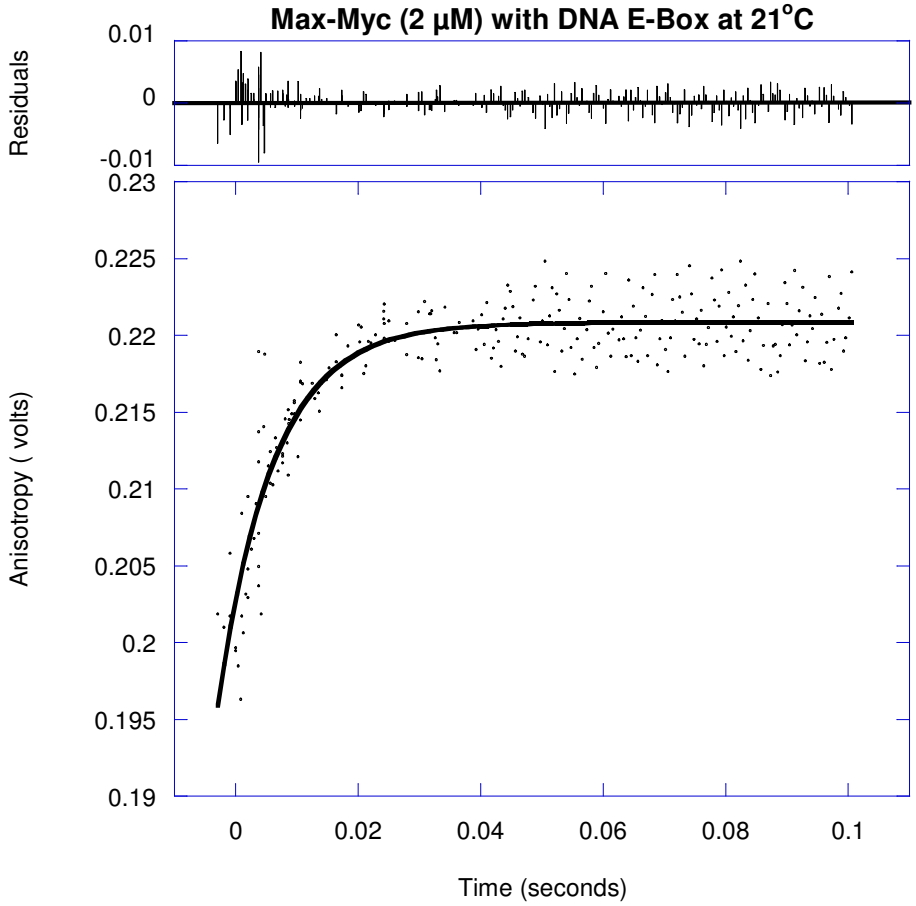

Figure 48: Stopped- flow kinetic binding measurement of Myc-Max to DNA E-Box

Kinetic data shows the time dependent increase in anisotropy after mixing 50 nM DNA oligonucleotide with 2 µM Myc-Max heterodimer at 21 °C

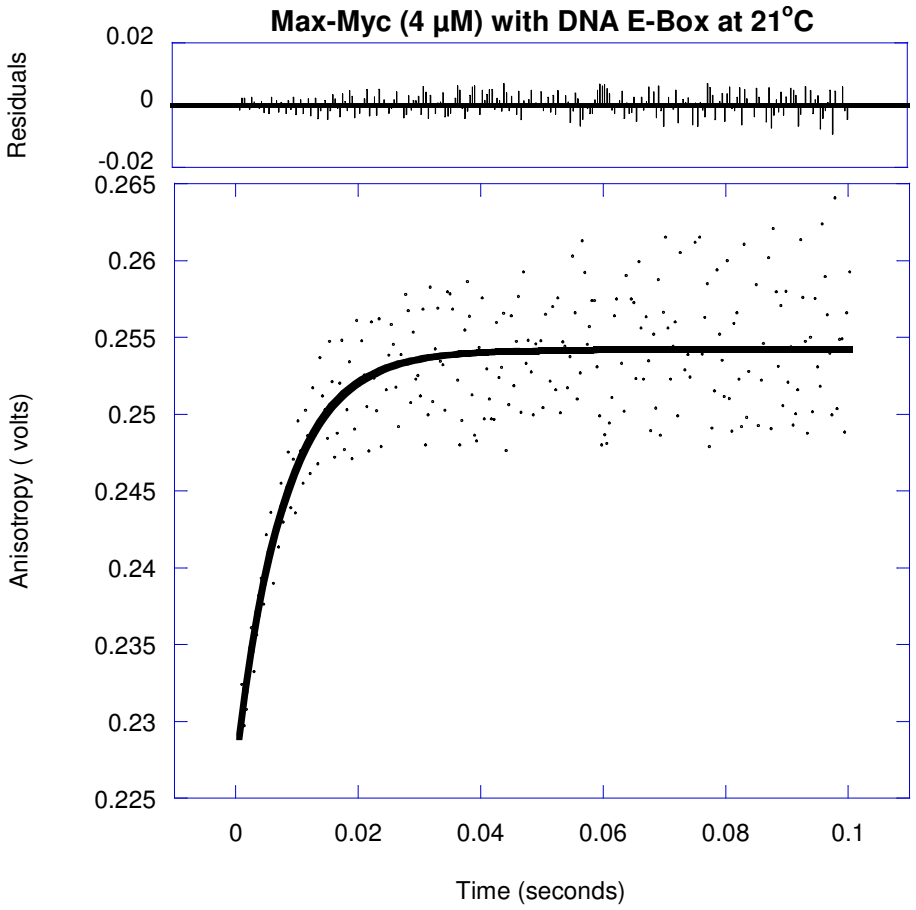

Figure 49: Stopped- flow kinetic binding measurement of Myc-Max to DNA E-Box

Kinetic data shows the time dependent increase in anisotropy after mixing 50 nM DNA oligonucleotide with 4 µM Myc-Max heterodimer at 21 °C

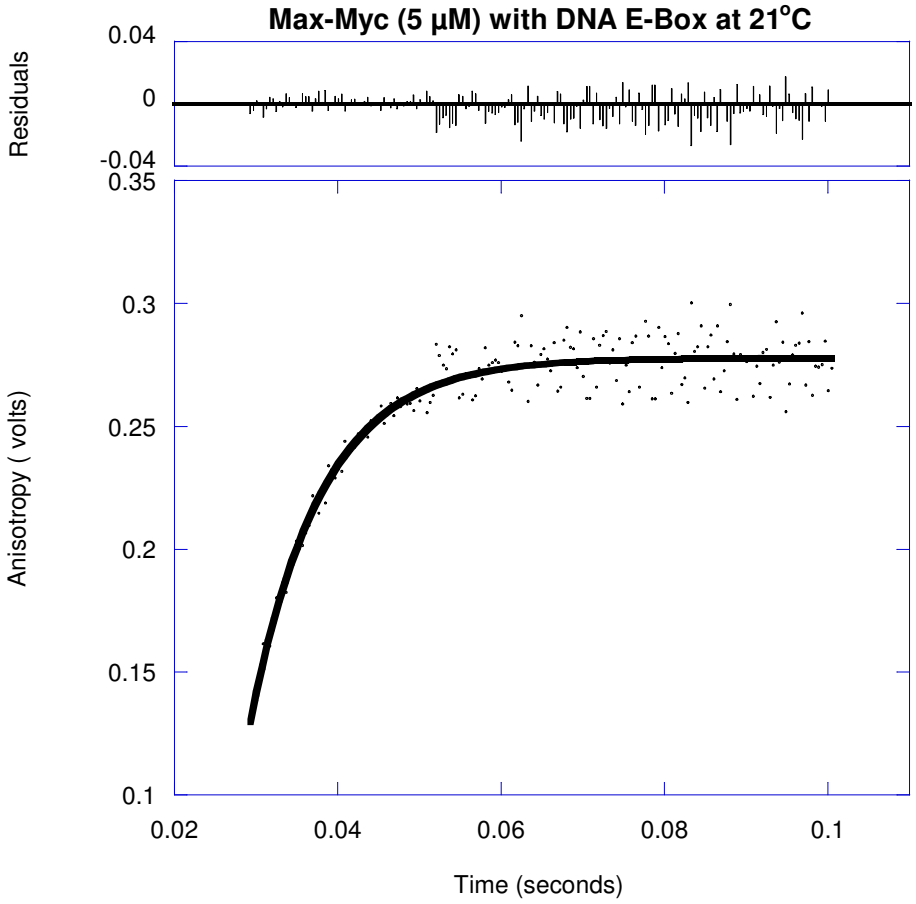

Figure 50: Stopped- flow kinetic binding measurement of Myc-Max to DNA E-Box

Kinetic data shows the time dependent increase in anisotropy after mixing 50 nM DNA oligonucleotide with 5 µM Myc-Max heterodimer at 21 °C

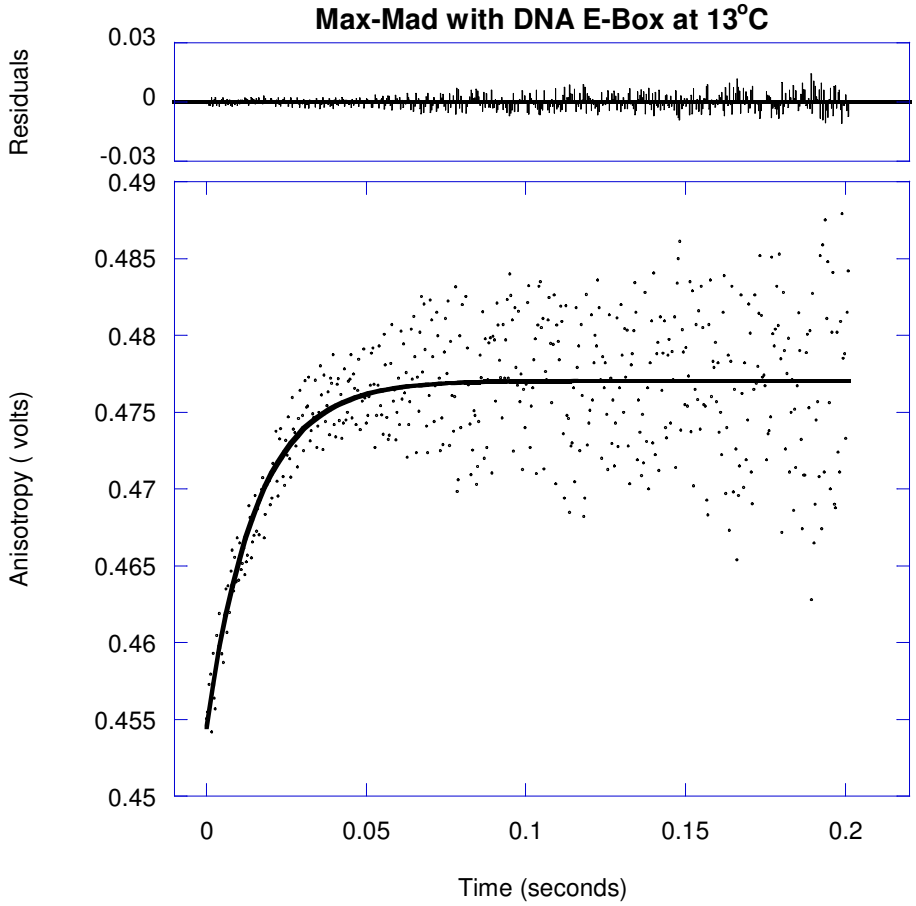

Figure 51: Stopped- flow kinetic binding measurement of Mad-Max to DNA E-Box

Kinetic data shows the time dependent increase in anisotropy after mixing 50 nM DNA oligonucleotide with 3 µM Mad-Max heterodimer at 13 °C

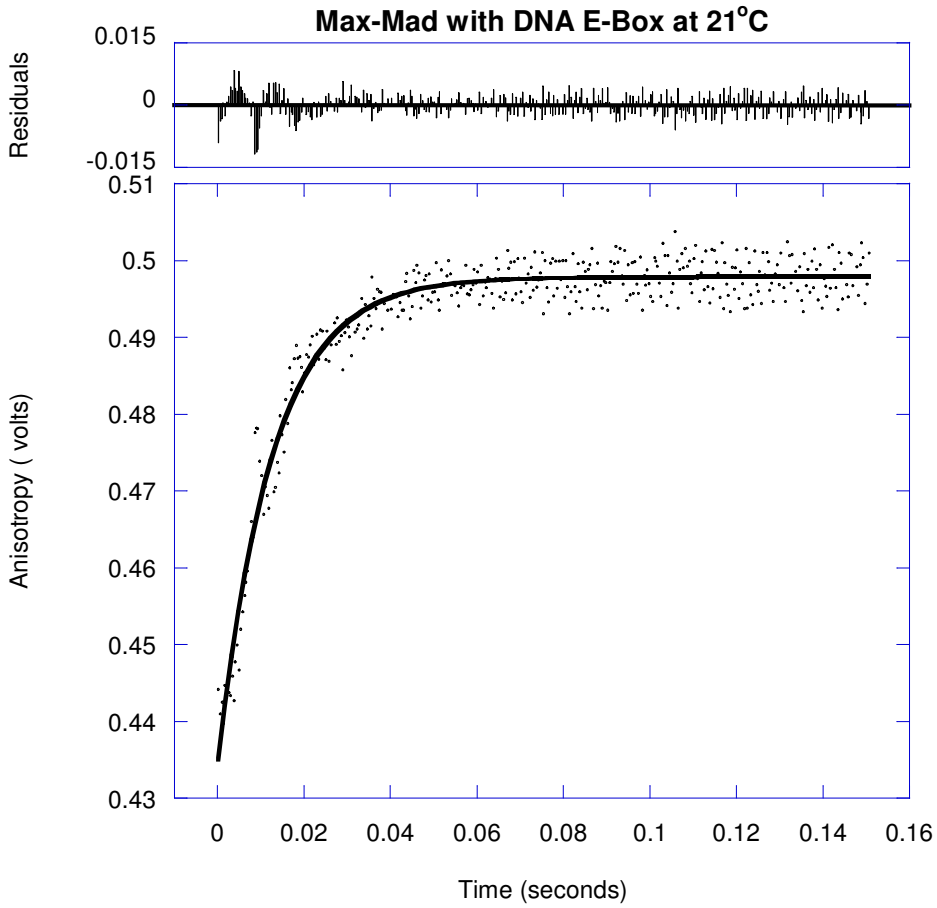

Figure 52: Stopped- flow kinetic binding measurement of Mad-Max to DNA E-Box

Kinetic data shows the time dependent increase in anisotropy after mixing 50 nM DNA oligonucleotide with 3 µM Mad-Max heterodimer at 21 °C

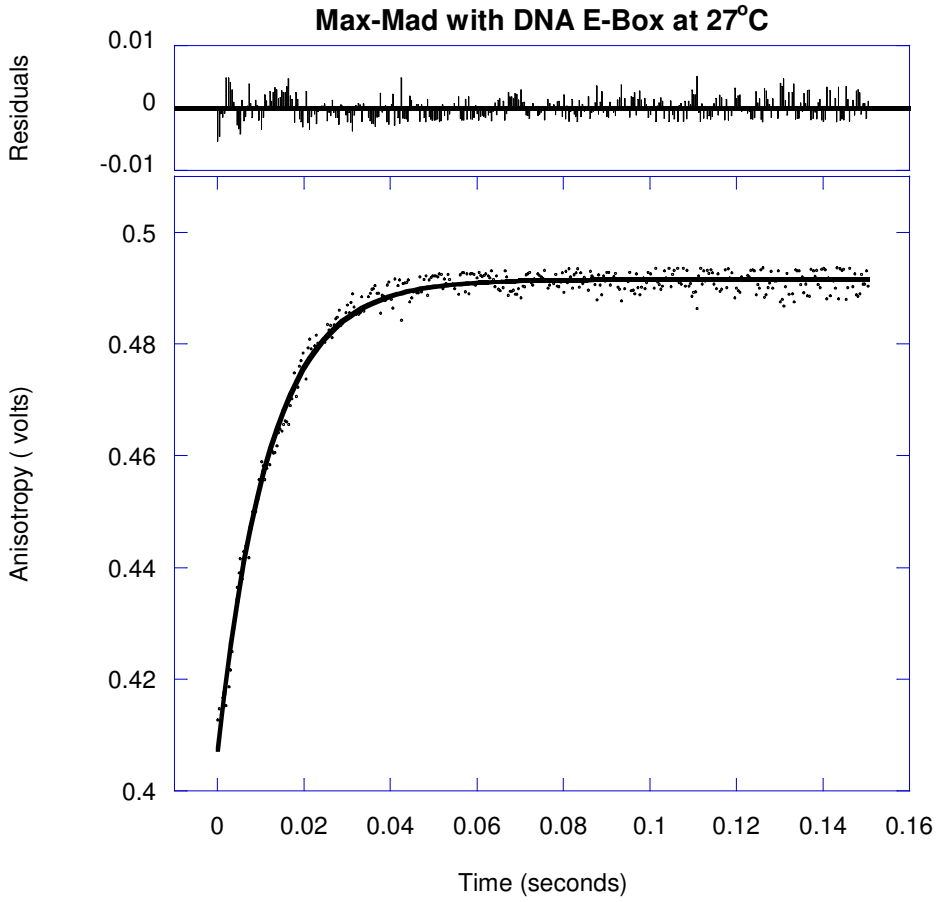

Figure 53: Stopped- flow kinetic binding measurement of Mad-Max to DNA E-Box

Kinetic data shows the time dependent increase in anisotropy after mixing 50 nM DNA oligonucleotide with 3 µM Mad-Max heterodimer at 27 °C

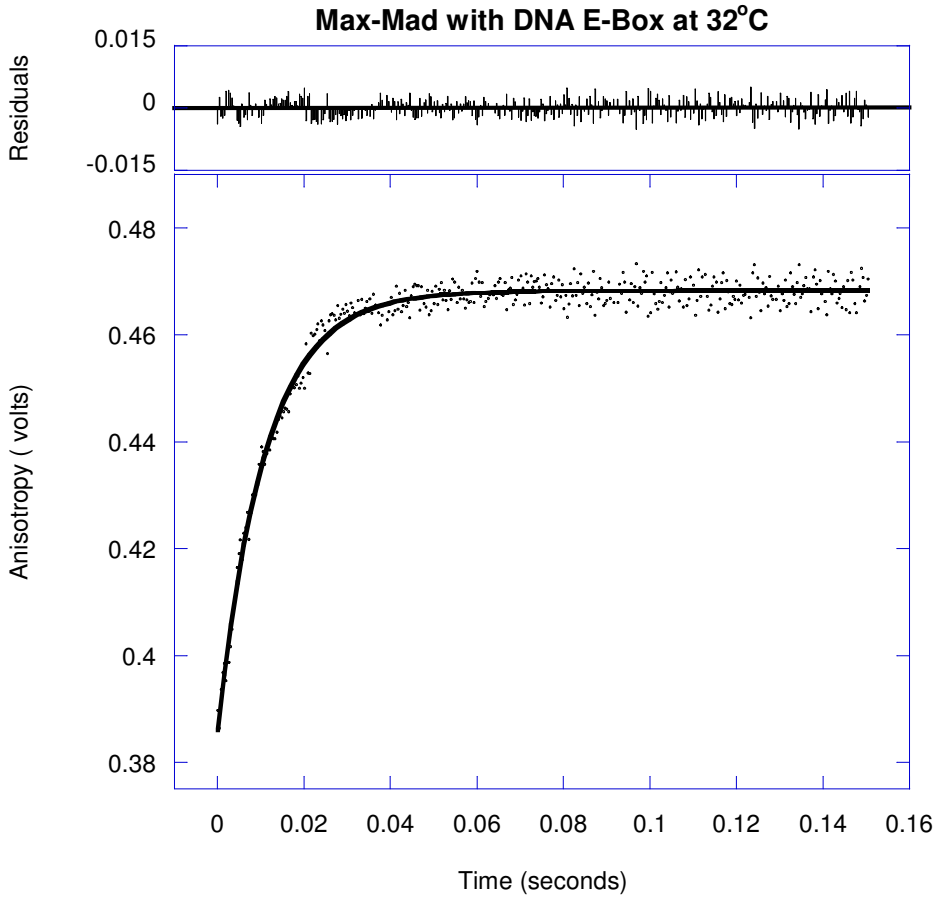

Figure 54: Stopped- flow kinetic binding measurement of Mad-Max to DNA E-Box

Kinetic data shows the time dependent increase in anisotropy after mixing 50 nM DNA oligonucleotide with 3 µM Mad-Max heterodimer at 32 °C

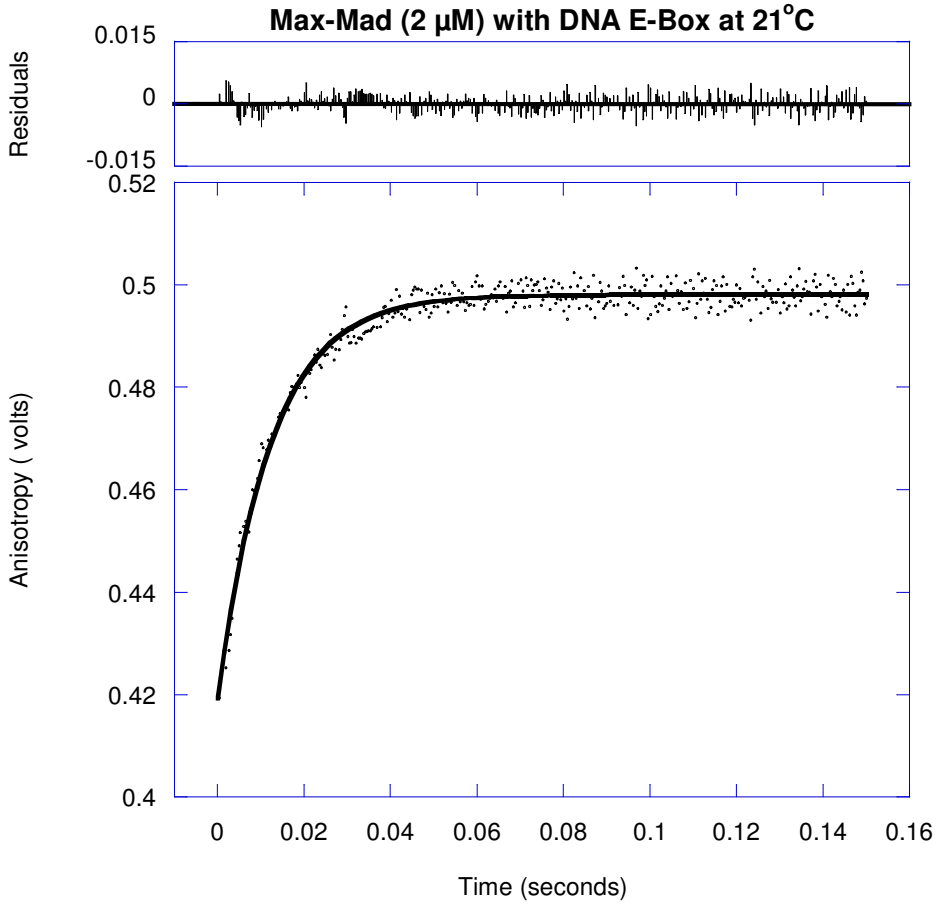

Figure 55: Stopped- flow kinetic binding measurement of Mad-Max to DNA E-Box

Kinetic data shows the time dependent increase in anisotropy after mixing 50 nM DNA oligonucleotide with 2 µM Mad-Max heterodimer at 21 °C

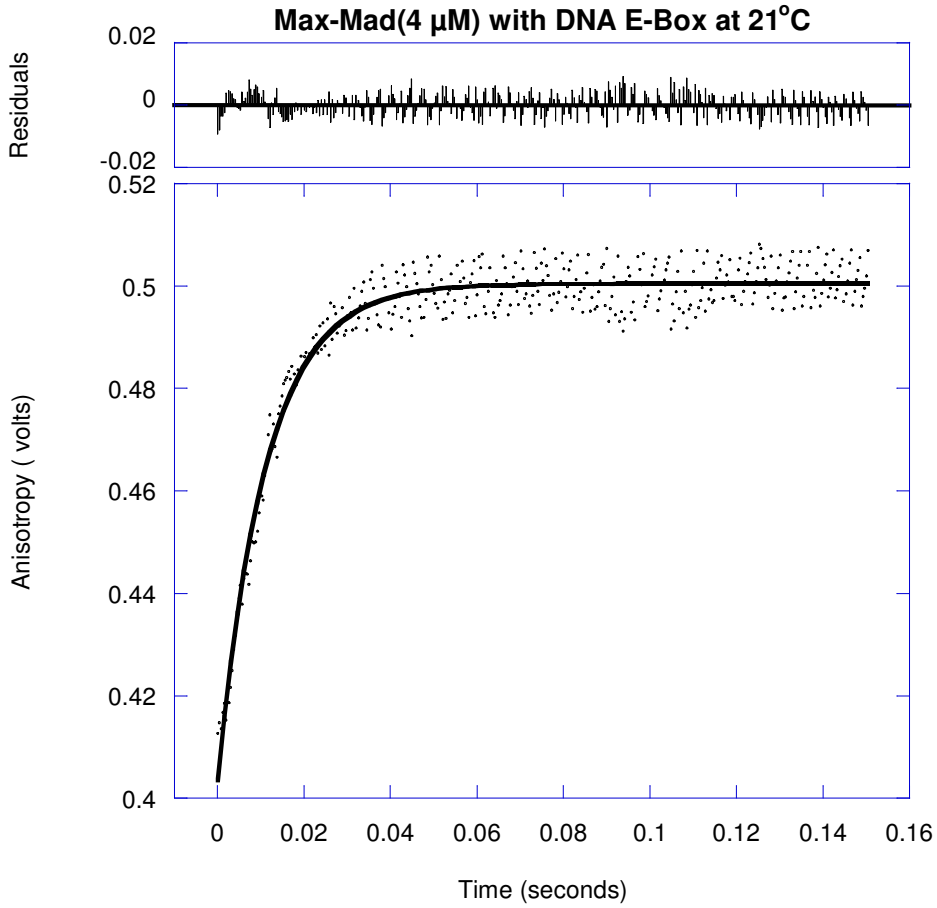

Figure 56: Stopped- flow kinetic binding measurement of Mad-Max to DNA E-Box

Kinetic data shows the time dependent increase in anisotropy after mixing 50 nM DNA oligonucleotide with 4 µM Mad-Max heterodimer at 21 °C

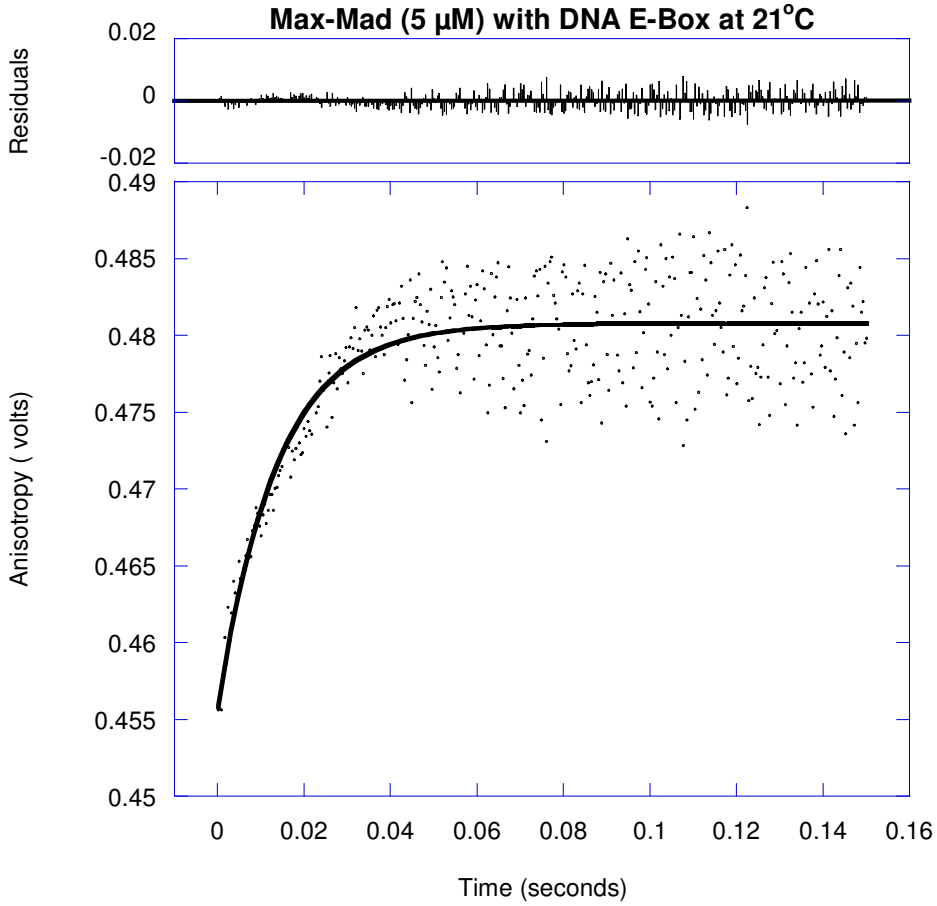

Figure 57: Stopped- flow kinetic binding measurement of Mad-Max to DNA E-Box

Kinetic data shows the time dependent increase in anisotropy after mixing 50 nM DNA oligonucleotide with 5 µM Mad-Max heterodimer at 21 °C

Table 4: Kinetic binding constants for the interaction of Max-Max, Myc-Max and Mad-Max with DNA E-Box

Rate Constants $k_2(s^{-1})$

Temp	Max-Max-DNA	Myc-Max-DNA	Mad-Max-DNA
13°C	106±5.0	108±4.6	64.8±5.6
21°C	127±7.4	117±2.4	79.7±1.9
27°C	138±8.0	126±8.4	84.0±1.0
32°C	146±4.9	141±6.2	90.5±1.5
E_a(kJ/mol)	***12.3±0.2***	***9.8±0.2***	***12.4±0.2***

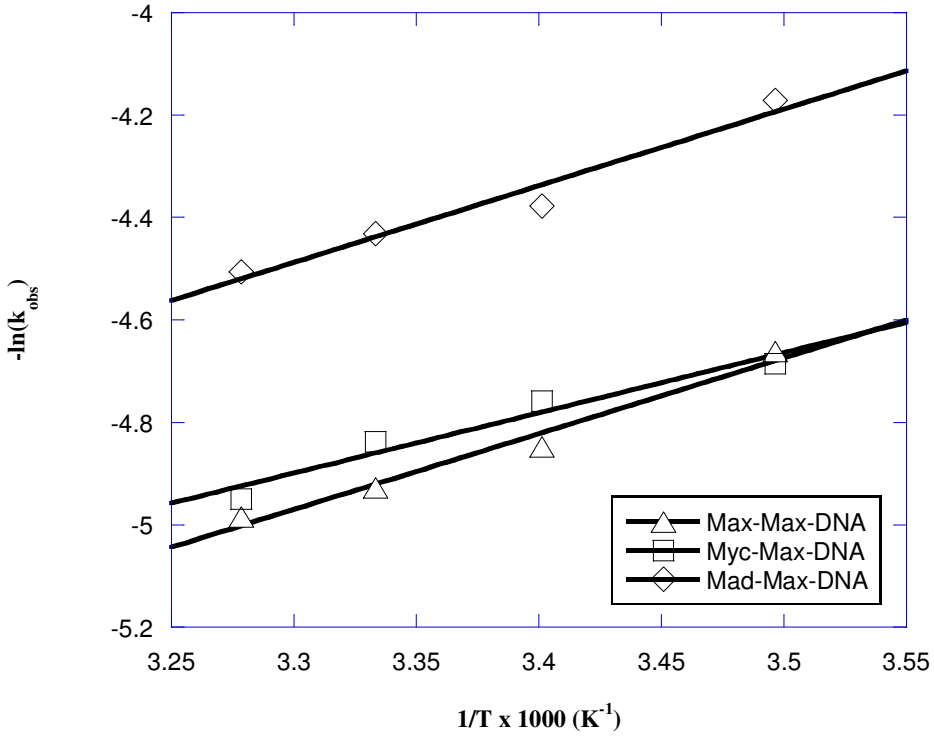

Figure 58: Arrhenius plots for the interaction of Max-Max, Myc-Max and Mad-Max with DNA E-Box

Table 5: Kinetic binding constants for the interaction of Max-Max, Myc-Max and Mad-Max with DNA E-Box

	Rate Constants $k_2(s^{-1})$		
[C] of protein dimers [µM]	**Max-Max-DNA**	**Myc-Max-DNA**	**Mad-Max-DNA**
2	134±5.0	111±6.5	81.3±1.3
3	127±4.9	117±2.4	79.7±1.9
4	136±8.1	121±6.1	84.0±2.1
5	128±4.4	114±4.7	78.3±4.6

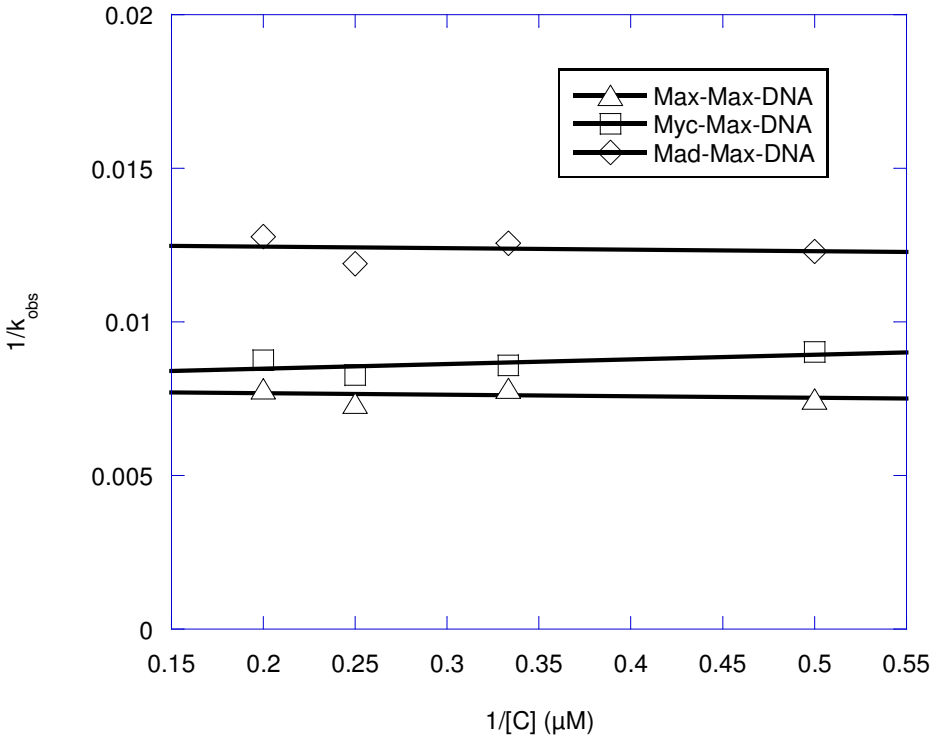

Figure 59: Kinetic plots of 1/ k_{obs} versus 1/ [C] for the interaction of Max-Max, Myc-Max and Mad-Max with DNA E-Box

3.3 Monomer-DNA Kinetics

Figure 1 shows the formation of b/HLH/Z transcription factors (Max, Myc and Mad) - DNA complex via a monomer and a dimer pathway. Equilibrium 1 followed by equilibrium 2 is the dimer pathway. Equilibria 3 and 4 represent the monomer pathway. The monomer and dimer pathways are energetically equivalent (thermodynamic cycle) and preference for one or the other is kinetic.

In order to compare the formation rates of transcription factor-DNA complex along the two pathways, we studied the monomer pathway separately. Max is the only protein among the three b/HLH/z family transcription factors Myc, Max and Mad, which has a significant affinity for DNA. The other two proteins, Myc and Mad, in the form of monomers, have a very low affinity for DNA [7]. As also stated earlier in this dissertation, they form homodimers weakly and bind DNA poorly. Therefore, binding of initial binding of monomeric Myc and Mad to DNA can be neglected. To avoid the DNA binding of dimeric Max proteins, we determined the most suitable experimental conditions using the previously published equilibrium data [46].

According to the equilibrium data of Hu et al. [46], binding of Myc, Max and Mad to DNA occurs in the nanomolar range and monomer-dimer association occurs in the micromolar range. In their work, they suggest that there is no dimer present initially when DNA is titrated with protein, and that the initial binding must be a monomer. By titration of DNA with low concentrations of Max, followed by Myc, they were able to obtain the fluorescence titration curve for both steps in the monomer pathway. We studied the kinetic mechanism of the monomer pathway

under similar experimental conditions. The first step of the monomer pathway, which is the initial binding of Max protein to DNA, was investigated by mixing labeled Max protein at low nanomolar concentrations with excess DNA. Low nanomolar concentrations of Max assured that most of the protein is in the monomeric form. The reason for using excess DNA in this experiment lies in the findings by Kohler and Schepartz [48]. They showed that protein monomer-DNA complexes are favored at high DNA concentrations. At low DNA concentrations and high protein concentrations, mostly dimer-DNA complexes were formed. Since dimer-DNA complexes have higher molecular weights and since they have a structured interface, a high polarization was observed. However, the molecular weight of monomer-DNA complexes is lower and the region to which FITC is attached is unstructured. Thus, they produced lower fluorescence polarization compared to dimer-DNA complexes.

The time course of binding of Max monomer with the DNA E-box complex was measured. To ensure that 90% of Max protein is in the monomeric form not dimeric, the required concentration of Max protein was calculated using the K_D value [46] for monomer-dimer equilibrium. 50 nM purified Max protein, 1 μM 5'-FITC labeled 16mer DNA oligonucleotide were mixed, and fluorescence anisotropy changes were monitored. To determine the binding of the Myc monomer to the Max-E-Box complex, 5'-FITC labeled 16mer DNA oligonucleotide and Max protein were kept at room temperature for 30 min. to bind. Then, 50 nM Max-DNA and 2 μM Myc protein were mixed in the stopped-flow mixing chamber and the association rates were observed.

Like the dimer-DNA and monomer-dimer kinetics, the monomer-DNA association experiments were performed under pseudo first order conditions. Measurements were made at 21°C and kinetic traces of 6-10 different experiments were averaged. The best fit for all of the association kinetics data was to the single-exponential equation. (Eq.5)

The obtained rate constant for the binding of the Myc to the Max-E-Box complex (step 4 in Fig.1) was 138 s^{-1}. The association rate constant for DNA binding of monomeric Max protein (step 3 in figure 1) is close to that of step 4 (148 s^{-1}). It is also interesting to note that the rate constants for the monomer pathway are similar to those of dimer-DNA interaction.

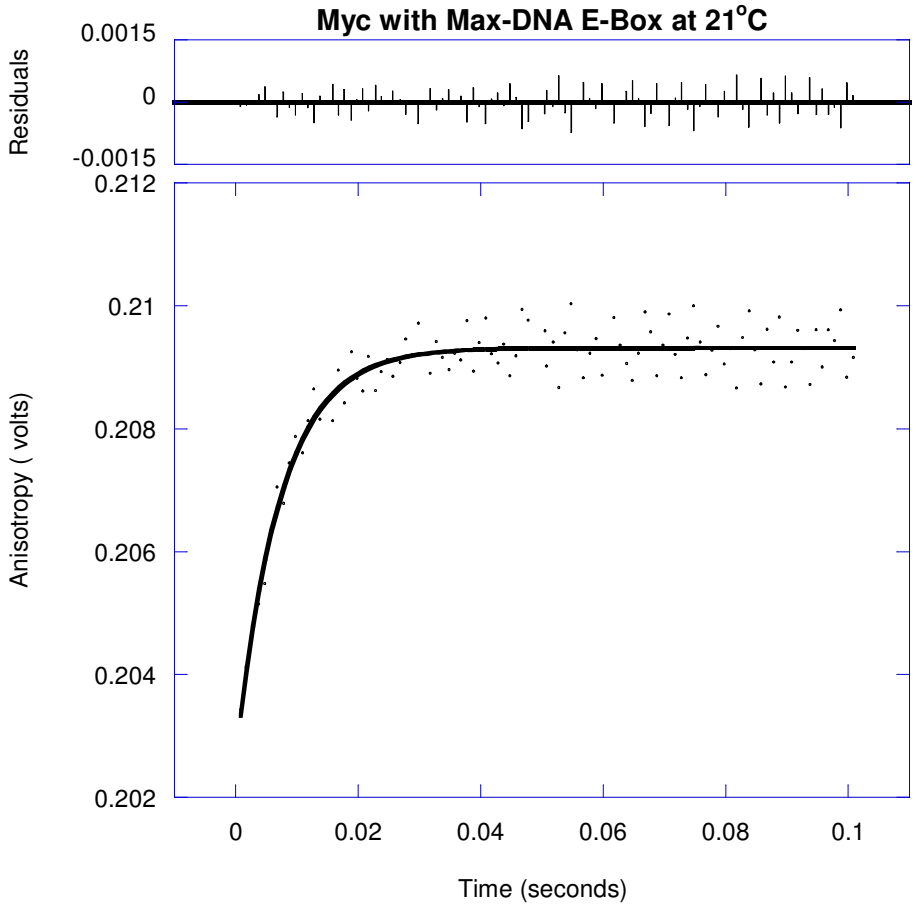

Figure 60: Stopped- flow kinetic binding measurement of Myc to Max-DNA E-Box

Kinetic data shows the time dependent increase in anisotropy after mixing 2 µM Myc with 50 nM Max DNA E-Box at 21 °C

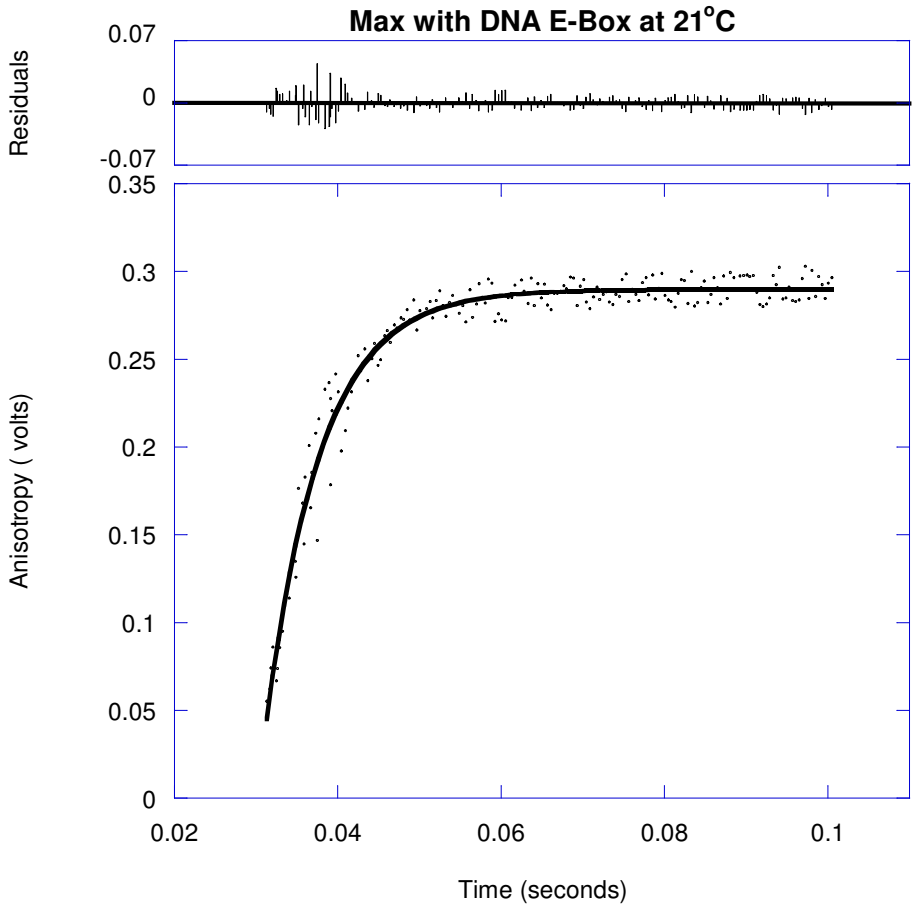

Figure 61: Stopped- flow kinetic binding measurement of Max to DNA E-Box

Kinetic data shows the time dependent increase in anisotropy after mixing 50 nM Max with 1 µM DNA E-Box at 21 °C

4.0 DISCUSSION

Our work here provides details of dimeric-DNA proteins which form complexes with DNA via the monomer pathway. Previously, proteins belonging to b/Z [44, 49] and b/HLH [50], nuclear hormone receptor [14] families, Arc [51], and LexA [52] repressors have been shown to bind DNA using the monomer pathway.

For example, stopped-flow fluorescence resonance energy transfer (FRET) studies conducted on cFos and cJun by Kohler and Schepartz [44] showed that although the dimerization of these proteins occurred rapidly in the absence of DNA, the rate of dimerization was enhanced in the presence of DNA. Their explanation of why the DNA binding is accelerated is based on electrostatic interactions between the proteins and DNA. Charge-charge interactions between the negatively-charged DNA and positively charged proteins are the main attractive forces which form the monomer-DNA interface [48]. For Coulombic electrostatic interactions, the force between two molecules of opposite charges is proportional to the inverse of the separation distance squared. Thus, in the case of basic protein monomers and acidic DNA, one expects an accelerated binding.

The conclusion of our study is consistent with the one reached by Kohler and Schepartz [44]. The rate of protein dimerization (step 1 in Fig.1) is limiting the overall rate of the dimer pathway (step 1 followed by step 2 in Fig.1) (Table 2, 3, 4 and 5). Therefore, the monomer pathway provides a faster route to the final complex.

Another reason of the preference of the monomer pathway lies in the fact that unfolded proteins (monomeric Max) have a bigger capture radius than folded proteins (dimeric b/HLH/Z proteins) [48]. Because of this larger capture radius, monomeric Max recognizes DNA with an increased rate.

Conclusions of a previous study utilizing computer simulations also support our results. Kohler and Schepartz showed through simulations of binding kinetics using the Dynafit software that binding of monomeric Fos and monomeric Jun to DNA provides a better fit to the experimental data than the dimer pathway [44].

In a previous work published by Park et al [53], the association kinetic constants of the interaction of truncated Max-Max and Myc-Max dimers with DNA were determined. Their results are also in good agreement with ours in terms of similarity of the rate constants of Myc-Max and Max-Max binding to DNA. They found that the Max-Max dimer recognized DNA at almost the same rate as Myc-Max, which was also the case in our present study.

Fig. 1 shows the formation of a b/HLH/Z family transcription factor-DNA complex through a monomer and a dimer pathway. Monomer-monomer binding (Step 1 in Fig.1.) followed by DNA binding (Step 2 in Fig.1.) is the dimer pathway. In the monomer pathway, two protein monomers bind DNA sequentially (steps 3 and 4 in Fig. 1). These two pathways are energetically equivalent. This means that they form a thermodynamic cycle. The equilibrium affinity will be the same whether a monomer or a dimer pathway is followed. However, as Kohler and Schepartz showed, there is a kinetic preference for the monomer pathway [44]. They attached different fluorophores to the leucine zipper region of Jun and Fos and measured the resonance

energy transfer in the presence and absence of DNA. They concluded that dimerization of Jun and Fos is more rapid in the presence of DNA, that Jun-Fos-DNA complex is extremely stable and that the monomer pathway is preferred for the complex formation.

We have previously analyzed the thermodynamics of Max, Myc, Mad-DNA associations [45, 46]. In order to fully understand the forces involved in protein-DNA recognition, the kinetics of Myc, Max, Mad-DNA interactions were studied. In the work presented here, we report the pre-steady state kinetic results on the interactions of the b/HLH/Z family transcription factors, Max, Myc and Mad with each other and also with DNA using stopped-flow anisotropy.

The concentration dependencies of the observed rates of these processes correspond with a two-step reaction model in which initial fast formation of dimer-DNA complex is followed by a conformational change of the complex in a rather fast step, but with a measurable rate.

4.1 Dimer Pathway

The temperature and concentration dependence of formation of Max-Max, Myc-Max and Mad-Max dimers in the absence of DNA was studied in detail. The formation of all three dimeric proteins follows Arrhenius kinetics, and the Arrhenius activation energies for the interaction of Max, Myc and Mad with FITC-labeled Max were 14.8 ± 0.2; 27.6 ±0.8 and 31.9 ± 0.6, respectively. In the case of formation of Max-Max homodimer, the activation energy was lower compared to Myc-Max and Mad-Max heterodimers. This reduced temperature dependence suggests that Max-Max interaction is accelerated and a substantially lower energy barrier is provided. The lower activation energy of the Max-Max dimerization suggests an intermediate that more easily achieves a stable conformation.

Binding of Myc to Max monomer has higher rate constants at all temperatures than Max-Max and Mad-Max formation. This suggests that Myc-Max complex is more able to rapidly change conformation.

The rate constants for the monomer-dimer equilibrium were found to be concentration independent, suggesting that the conformational changes are rate-limiting.

The rate constants for the DNA binding of Max-Max homodimer, Myc-Max and Mad-Max heterodimers (second step of the dimer pathway) were also studied as a function of temperature and concentration.

It was observed that dimer-DNA interaction is concentration independent. Binding of dimeric transcription factors to a 16-mer oligonucleotide exhibits two

kinetic phases: initial rapid phase and a rather fast, concentration independent phase. The reaction is interpreted as the concentration-dependent initial complex, which rearranges in a concentration-independent step to a thermodynamically stable complex.

The rate for the interaction of the dimeric proteins with E-Box DNA is faster than the rate of the formation of the protein dimers, at all temperatures. The rates for the formation of Myc-Max-DNA and Max-Max-DNA complexes were higher than the Mad-Max –DNA complex.

The Arrhenius activation energies for the binding of Max-Max, Myc-Max and Mad-Max to E-Box DNA were close to each other. They were in the range of 10-12 kJ/mol, almost half as the activation energies for the dimer formation.

4.2 Monomer Pathway

To compare the monomer and dimer pathways, we also studied the DNA binding rates of monomeric Max and Myc (step 3 and 4 in Fig. 1). The DNA binding rate of the first monomeric protein is almost the same as that of the second monomer.

It is also interesting to note that the rates of step 3 and 4 (the monomer pathway) is similar to the DNA binding rate of the dimeric transcription factors (step 2 in Fig.1).

The results of this study demonstrate that in the isolated system examined here, which is composed of a 16-mer double stranded DNA containing the E-Box and three b/HLH/Z family transcription factors, Myc, Max and Mad, both monomeric and

dimeric transcription factors recognize the palindromic E-Box at the same rate. Since the rate of formation of the dimers (step 1 in fig 1) is slower than the DNA binding rates (steps 2, 3 and 4), the monomer pathway is more rapid than the dimer pathway.

The conclusions of a similar study by Kohler and Schepartz [44] suggest that assembly of the dimeric transcription factors Jun-Fos and specific DNA follows the monomer pathway. However, Kohler and Schepartz preferred an experimental condition, in which the dimer-DNA complex was formed from monomeric Jun, monomeric Fos and DNA. However, in cellular environment there are monomeric and also dimeric proteins present which may compete for DNA. We found here that the DNA binding rates for both monomeric and dimeric transcription factors are similar to each other. In such a case, the ratio of monomeric proteins to dimeric ones may be a crucial factor for determining the choice of the pathway.

It is important to recognize that the assembly of transcription factor-DNA complexes in vivo is more intricate than in vitro. There are many factors affecting DNA recognition in vivo. In cellular environment, the transcription factors discriminate between specific and a lot of non-specific DNA. There are also a large excess of other proteins with which the transcription factors have to compete for DNA.

The most commonly discussed theory for DNA-binding proteins to recognize their specific sequences is “facilitated diffusion” [47]. According to this theory, proteins find their target by sliding along the DNA. This is a one dimensional diffusion during which the protein remains in contact with the DNA for long enough periods so that appreciable diffusive motion occurs in either direction along the chain

contour. DNA binding strength of proteins is another factor affecting the diffusion rates of monomeric and dimeric proteins along the DNA. Since the unspecific DNA binding of a monomeric protein is weak compared to a dimeric one due to more interactions between the DNA, it may slide faster along the DNA. The diffusion rate of a monomeric protein may be more rapid because it is sterically less hindered. Therefore one of the reasons why the monomer pathway is preferred over the dimer pathway may be the fast diffusion rate of the monomeric transcription factor along the DNA.

Another factor affecting the rate of target recognition is the stability of protein-DNA complex. Accessory proteins may influence the stability of these complexes by binding to monomeric or dimeric transcription factors. Hence, the rate of DNA binding through a monomer or dimer pathway may differ depending on whether such accessory proteins bind to the monomeric or dimeric transcription factors.

In conclusion, many factors play a role in choosing a monomer or dimer pathway in vivo. Future experiments should be extended such that the effect of accessory proteins on the stability of these complexes and the diffusion rates of monomeric and dimeric transcription factors along the DNA can be determined.

APPENDIX

A1.0 BUFFERS AND SOLUTIONS USED IN THE EXPERIMENTS

A1.1 Cell media

1 L Luria-Bertani (LB) media

NaCl	10 g
Yeast Extract	5 g
Peptone	10 g
dd H_2O	1000 ml

200 ml LB agar

NaCl	2 g
Yeast Extract	1 g
Peptone	2 g
dd H_2O	200 ml

A1.2 Reagents and solutions for cell cultivation

50 mg/ml Ampicillin: 0.5 g Ampicillin in 10 ml dd H_2O

50 mg/ml Kanamicin: 0.5 g Kanamicin in 10 ml dd H_2O

0.5 M isopropyl-beta-D-thiogalactopyranoside (IPTG): 1.62 g IPTG in 12 ml dd H_2O

100mM phenylmethylsulphonyl fluoride (PMSF): 440mg PMSF in 25ml isopropanol

25ml 100xProtease inhibitor stock

Benzamidine HCl	40 mg
Phenanthroline	25 mg
Aprotinin	25 mg
Pepstatin A	25 mg
Leupeptin	25 mg
1 x HEPES buffer	25 ml

A1.3 Buffers for Protein purification and titrations

10X HEPES Buffer, pH 7.6

HEPES	59.5 g
KCl	74.6 g
$MgCl_2$	2.0 g
* DTT	
dd H_2O	900 ml

- Adjust the pH to 7.6 with potassium hydroxide (KOH), then add dd H_2O to 1 l
- * Add DTT fresh before use to a final concentration of 10 mM

Phosphate-buffered Saline (PBS)

NaCl	8 g
KCl	0.2 g
Na_2HPO_4	1.44 g
K_2HPO_4	0.24 g
dd H_2O	800 ml

- Adjust the pH to 7.4 with Hydrochloric acid (HCl), then add dd H_2O to 1 l

100 ml Lysis Buffer

10X HEPES Buffer, pH 7.6	10 ml
Glycerol	10 ml
Protease inhibitor stock	1 ml
100 mM PMSF	1 ml
dd H_2O	78 ml

Dialysis Buffer (1 X HEPES Buffer)

A1.4 Buffers for Electrophoresis

10xTank buffer pH 8.3

Tris Base	30.28 g
SDS	10 g
Glycine	144.13 g
dd H_2O	to 1L

4x Running Gel buffer (1.5 M Tris-Cl, pH 8.8)

4x Stacking Gel buffer (0.5M Tris-Cl, pH 6.8)

10 ml 2x Treatment Buffer

4xStacking Gel buffer	2.5 ml
10 % SDS	4.0 ml
Glycerol	2 ml
Bromphenol blue	2.0 mg
DTT	0.31 g
dd H_2O	to 10 ml

A2.0 PROTEIN PURIFICATION AND DETECTING

A2.1 Max protein purification by using Hightrap SP column

Gradient Buffers for Hightrap SP column

	Buffer A	Buffer B
2M KCl	6.25 ml	100 ml
10X HEPES Buffer, 7.6	50 ml	20 ml
0.5 M EDTA, pH 8.0	0.5 ml	0.2 ml
100 mM PMSF	1 ml	1 ml
Glycerol	50 ml	20 ml
dd H_2O	to 500 ml	to 200 ml

- Wash the column with buffer A and B and apply the protein sample in the following order
    i. 20 ml Buffer A, 5 ml/min
    ii. 50 ml Buffer A, 2 ml/min
    iii. 50 ml Buffer A + 1M NaCl, 2 ml/min
    iv. 50 ml buffer A, 2 ml/min
    v. Protein Sample, 2 ml/min
    vi. 30 ml Buffer A (+ Octyl Glycoside, + PMSF), 2 ml/min
    vii. 30 ml 70% Buffer A(21ml) and 30% Buffer B(9 ml) , 2 ml/min

viii. 140 ml 40% Buffer A (56 ml) and 60% Buffer B (84 ml), 2 ml/min

ix. 40 ml 20% Buffer A (8 ml) and 80% Buffer B (32 ml), 5 ml/min

x. 65 ml Buffer A + 1M NaCl, 5 ml/min

xi. 50 ml Buffer A, 5 ml/min

- Collect the desired fractions
- Transfer the fractions to dialysis tubing and dialyze against 1 X HEPES buffer overnight at 4 ^{o}C.
- Estimate the protein concentration and detect the purity by SDS-PAGE
- Transfer the protein to Centricon Tubes and centrifuge at 5000 rpm for 3 hours
- Determine the final protein concentration by using Bradford assay

A2.2 Mad protein purification by using the His-tag affinity column

Binding Buffer: 0.5 M NaCl, 20 mM Tris-HCl, 5 mM imidazole, pH 7.9

Wash Buffer: 0.5 M NaCl, 60 mM imidazole, 20 mM Tris-HCl, pH 7.9

Elute Buffer: 1 M imidazole, 0.5 M NaCl, 20 mM Tris-HCl, pH 7.9

Strip Buffer: 0.5 M NaCl, 100 mM EDTA, 20 mM Tris-HCl, pH 7.9

Charge Buffer: 50 mM $NiSO_4$

- Pack a 5ml chromatography column with 1ml His-Bind resin (from Novagen)
- Wash the column with 10 ml binding buffer
- Wash the column with 5 ml charge buffer to charge the column with Ni^{2+}
- Wash the column with 10 ml of binding buffer
- Apply the protein sample to the Ni^{2+} charged His-trap column
- Wash the column with 10 ml binding buffer
- Wash the column with 10 ml wash buffer
- Elute the column with 10 ml elute buffer and collect the fractions
- Estimate the protein concentration and detect the purity by SDS-PAGE.
- Transfer desired fractions to dialysis tubing and dialyze against 1X HEPES buffer (without DTT) overnight at $4^{o}C$.
- Transfer proteins to Centricon Tubes and centrifuge at 5000 rpm for 3 hours.
- Determine the final protein concentration by using Bradford assay

A2.3 Myc protein purification by GST affinity column

10 x GST Bind/Wash Buffer: 43 mM Na_2HPO_4, 14.7 mM KH_2PO_4, 1.37 M NaCl, 27 mM KCl, pH 7.3

10x GST Elution Buffer: 500 mM Tris-HCl, 100mM reduced glutathione, pH 8.0

- Pack a small polypropylene column (5ml) with 1ml GST•Bind Resin (from Amersham)
- Wash the column with 10ml of GST Bind/Wash Buffer
- Apply the protein sample to the column
- Wash the column with 10ml 1X GST Bind/Wash Buffer.
- Elute the bound protein with 5ml 1X GST Elution Buffer. Collect the fractions
- Estimate protein concentration and detect the purity by SDS-PAGE.
- Transfer the desired fractions to dialysis tubing and dialyze against 1X HEPES buffer (without DTT) overnight at 4^{o}C.
- Transfer the protein to Centricon tubes and centrifuge at 5000 rpm for 3 hours.
- Determine the final protein concentration by using Bradford assay

A2.4 Quantitation of Protein Using the Bradford Assay

For protein quantitation, a well-known colorimetric method-Bradford coomassie binding- was used. When coomassie dye binds protein in an acidic medium, an immediate shift in absorption maximum occurs from 465 nm to 595 nm with a color change from brown to blue.

A2.4.1 Preparation of Diluted BSA Standards

Prepare a fresh set of protein standards by diluting the 2.0 mg/ml BSA stock standard as illustrated in the table below.

Preparation of the Diluted BSA Standards (Working Range = 100 - 1500 µg/ml)

Volume of the BSA	Volume of Diluent	Final BSA Concentration
300 µl of (Stock)	0 µl	2,000 µg/ml (A)
375 µl of (Stock)	125 µl	1,500 µg/ml (B)
325 µl of (Stock)	325 µl	1,000 µg/ml (C)
175 µl of (B)	175 µl	750 µg/ml (D)
325 µl of (C)	325 µl	500 µg/ml (E)
325 µl of (E)	325 µl	250 µg/ml (F)
325 µl of (F)	325 µl	125 µg/ml (G)
100 µl of (G)	400 µl	25 µg/ml (H)
0	400 µl	0 µg/ml (I)

A2.4.2 Mixing of the Coomassie® Plus Protein Assay Reagent

Allow the Coomassie® Plus Reagent to come to room temperature. Mix the Coomassie® Plus Reagent solution just prior to use by gently inverting the bottle several times. Do not shake.

A2.4.3 Reaction

Pipette 0.05 ml of each standard or unknown sample into appropriately labeled UV cuvettes. Use 0.05 ml of the diluent for the blank. Add 1.5 ml of the Coomassie® Plus Reagent to each cuvette, mix well.

A2.4.4 Detection

Measure the absorbance at 595 nm of blank and zero the spectrophotometer. Measure the absorbance at 595 nm of each sample. Prepare a standard curve by plotting the average corrected 595 nm reading for each BSA standard versus its concentration. Using the standard curve; determine the protein concentration of each unknown sample.

A2.5 SDS Polyacrylamide Gel Electrophoresis (SDS-PAGE)

A2.5.1 Running Gel

Gel concentration of 15 % in 0.25 M Tris-HCl pH 8.8

Monomer solution*	5 ml
DD H_2O	2.4 ml
4X Running gel buffer	2.5 ml
10% SDS	0.1 ml
10% Ammonium Persulfate	50 µL
TEMED	3.3 µL

* Monomer solution

acrylamide	60 g
bisacrylamide	1.6 g
dd H_2O	to 200 ml

- Mix the reagents in a small side-arm vacuum flask leaving out the ammonium persulfate and the TEMED.
- Stopper the flask and apply vacuum for several minutes to deaerate the solution.

- Add the TEMED and ammonium persulfate.
- Pour the solution into gel unit.
- Overlay gel with n-butanol to ensure a flat surface and to exclude air.
- Wash off n-butanol with water after gel has polymerized (about15 min).

A2.5.2 Stacking Gel

Gel concentration of 4 % in 0.125 M Tris-HCl pH 6.8

Monomer solution	0.44 ml
DD H_2O	2.03 ml
4X Stacking gel buffer	0.83 ml
10% SDS	33 µL
10% Ammonium Persulfate	16.7 µL
TEMED	1.7 µL

- Mix the reagents in a small side-arm vacuum flask leaving out the ammonium persulfate and the TEMED.
- Stopper the flask and apply vacuum for several minutes to deaerate the solution.
- Add the TEMED and ammonium persulfate.

- Pour the solution on top of running gel, insert comb, allow polymerizing (about 30 minutes)
- Remove comb, and fill each well with 1 X tank buffer.
- Put the lid on the gel unit. Fill the assembly with 1X tank buffer(1-6).

A2.5.3 Loading and running the gels

- Combine equal parts of protein sample and 2X treatment buffer in an eppendorf tube
- Place the tube in a boiling water bath for 90 seconds.
- Keep the samples on ice until ready for use.
- Load every well with same volume of sample.
- Turn on the power supply and run the gel under appropriate conditions.

A2.5.4 Staining and destaining the gels

Staining Solution

Coomassie Brilliant Blue R250	0.5 g
Methanol	800 ml
Acetic acid	140 ml
dd H_2O	1060 ml

- Cover gel with staining solution, seal in plastic box and leave overnight on shaker at room temperature or for 2 to 3 hours at 37 °C.

Destaining Solution

Methanol	800 ml
Acetic acid	140 ml
dd H_2O	1060 ml

- Decant staining solution, replace with distaining solution and shake gel for several hours until gel has a clear background

BIBLIOGRAPHY

1. Sauer, R.T., *Transcriptional control. Scissors and helical forks.* Nature, 1990. **347**(6293): p. 514-5.

2. Schwabe, J.W. and D. Rhodes, *Beyond zinc fingers: steroid hormone receptors have a novel structural motif for DNA recognition.* Trends Biochem Sci, 1991. **16**(8): p. 291-6.

3. Prendergast, G.C., D. Lawe, and E.B. Ziff, *Association of Myn, the murine homolog of max, with c-Myc stimulates methylation-sensitive DNA binding and ras cotransformation.* Cell, 1991. **65**(3): p. 395-407.

4. Duesberg PH, B.K., Vogt PK, *The RNA of avian acute leukemia virus MC29.* Proc Natl Acad Sci U S A, 1977. **74**(10): p. 4320-4324.

5. Bouchard, C., et al., *Regulation of cyclin D2 gene expression by the Myc/Max/Mad network: Myc-dependent TRRAP recruitment and histone acetylation at the cyclin D2 promoter.* Genes Dev, 2001. **15**(16): p. 2042-7.

6. Amati, B., et al., *The c-Myc protein induces cell cycle progression and apoptosis through dimerization with Max.* Embo J, 1993. **12**(13): p. 5083-7.

7. Grandori, C., et al., *The Myc/Max/Mad network and the transcriptional control of cell behavior.* Annu Rev Cell Dev Biol, 2000. **16**: p. 653-99.

8. Ayer, D.E., L. Kretzner, and R.N. Eisenman, *Mad: a heterodimeric partner for Max that antagonizes Myc transcriptional activity.* Cell, 1993. **72**(2): p. 211-22.

9. Hurlin, P.J., et al., *Mad3 and Mad4: novel Max-interacting transcriptional repressors that suppress c-myc dependent transformation and are expressed during neural and epidermal differentiation.* Embo J, 1995. **14**(22): p. 5646-59.

10. Zervos, A.S., J. Gyuris, and R. Brent, *Mxi1, a protein that specifically interacts with Max to bind Myc-Max recognition sites.* Cell, 1993. **72**(2): p. 223-32.

11. Nair, S.K. and S.K. Burley, *X-ray structures of Myc-Max and Mad-Max recognizing DNA. Molecular bases of regulation by proto-oncogenic transcription factors.* Cell, 2003. **112**(2): p. 193-205.

12. Choy, B. and M.R. Green, *Eukaryotic activators function during multiple steps of preinitiation complex assembly.* Nature, 1993. **366**(6455): p. 531-6.

13. Li, X.Y., et al., *Enhancement of TBP binding by activators and general transcription factors.* Nature, 1999. **399**(6736): p. 605-9.

14. Holmbeck, S.M., H.J. Dyson, and P.E. Wright, *DNA-induced conformational changes are the basis for cooperative dimerization by the DNA binding domain of the retinoid X receptor.* J Mol Biol, 1998. **284**(3): p. 533-9.

15. Shuai, K., et al., *Interferon activation of the transcription factor Stat91 involves dimerization through SH2-phosphotyrosyl peptide interactions.* Cell, 1994. **76**(5): p. 821-8.

16. Foley, K.P. and R.N. Eisenman, *Two MAD tails: what the recent knockouts of Mad1 and Mxi1 tell us about the MYC/MAX/MAD network.* Biochim Biophys Acta, 1999. **1423**(3): p. M37-47.

17. Solomon, D.L., B. Amati, and H. Land, *Distinct DNA binding preferences for the c-Myc/Max and Max/Max dimers.* Nucleic Acids Res, 1993. **21**(23): p. 5372-6.

18. Kohler, J.J., et al., *DNA specificity enhanced by sequential binding of protein monomers.* Proc Natl Acad Sci U S A, 1999. **96**(21): p. 11735-9.

19. Nesbit, C.E., J.M. Tersak, and E.V. Prochownik, *MYC oncogenes and human neoplastic disease.* Oncogene, 1999. **18**(19): p. 3004-16.

20. Erisman, M.D., et al., *Deregulation of c-myc gene expression in human colon carcinoma is not accompanied by amplification or rearrangement of the gene.* Mol Cell Biol, 1985. **5**(8): p. 1969-76.

21. Hann, S.R. and R.N. Eisenman, *Proteins encoded by the human c-myc oncogene: differential expression in neoplastic cells.* Mol Cell Biol, 1984. **4**(11): p. 2486-97.

22. Amati, B., et al., *Transcriptional activation by the human c-Myc oncoprotein in yeast requires interaction with Max.* Nature, 1992. **359**(6394): p. 423-6.

23. McMahon, S.B., M.A. Wood, and M.D. Cole, *The essential cofactor TRRAP recruits the histone acetyltransferase hGCN5 to c-Myc.* Mol Cell Biol, 2000. **20**(2): p. 556-62.

24. Gaubatz, S., et al., *Transcriptional activation by Myc is under negative control by the transcription factor AP-2.* Embo J, 1995. **14**(7): p. 1508-19.

25. Peukert, K., et al., *An alternative pathway for gene regulation by Myc.* Embo J, 1997. **16**(18): p. 5672-86.

26. Bao, J. and A.S. Zervos, *Isolation and characterization of Nmi, a novel partner of Myc proteins.* Oncogene, 1996. **12**(10): p. 2171-6.

27. Blackwood, E.M. and R.N. Eisenman, *Max: a helix-loop-helix zipper protein that forms a sequence-specific DNA-binding complex with Myc.* Science, 1991. **251**(4998): p. 1211-7.

28. Cerni, C., et al., *Differential effects by Mad and Max on transformation by cellular and viral oncoproteins.* Oncogene, 1995. **11**(3): p. 587-96.

29. Lahoz, E.G., et al., *Suppression of Myc, but not E1a, transformation activity by Max-associated proteins, Mad and Mxi1.* Proc Natl Acad Sci U S A, 1994. **91**(12): p. 5503-7.

30. Roussel, M.F., et al., *Inhibition of cell proliferation by the Mad1 transcriptional repressor.* Mol Cell Biol, 1996. **16**(6): p. 2796-801.

31. Littlewood, T.D., et al., *Max and c-Myc/Max DNA-binding activities in cell extracts.* Oncogene, 1992. **7**(9): p. 1783-92.

32. Berberich, S., et al., *max encodes a sequence-specific DNA-binding protein and is not regulated by serum growth factors.* Oncogene, 1992. **7**(4): p. 775-9.

33. Yin, X., L. Grove, and E.V. Prochownik, *Lack of transcriptional repression by max homodimers.* Oncogene, 1998. **16**(20): p. 2629-37.

34. Meroni, G., et al., *Rox, a novel bHLHZip protein expressed in quiescent cells that heterodimerizes with Max, binds a non-canonical E box and acts as a transcriptional repressor.* Embo J, 1997. **16**(10): p. 2892-906.

35. Blackwell, T.K., et al., *Binding of myc proteins to canonical and noncanonical DNA sequences.* Mol Cell Biol, 1993. **13**(9): p. 5216-24.

36. Schreiber-Agus, N., et al., *An amino-terminal domain of Mxi1 mediates anti-Myc oncogenic activity and interacts with a homolog of the yeast transcriptional repressor SIN3.* Cell, 1995. **80**(5): p. 777-86.

37. Ayer, D.E. and R.N. Eisenman, *A switch from Myc:Max to Mad:Max heterocomplexes accompanies monocyte/macrophage differentiation.* Genes Dev, 1993. **7**(11): p. 2110-9.

38. Larsson, L.G., et al., *Expression of mad, mxi1, max and c-myc during induced differentiation of hematopoietic cells: opposite regulation of mad and c-myc.* Oncogene, 1994. **9**(4): p. 1247-52.

39. Ayer, D.E., Q.A. Lawrence, and R.N. Eisenman, *Mad-Max transcriptional repression is mediated by ternary complex formation with mammalian homologs of yeast repressor Sin3.* Cell, 1995. **80**(5): p. 767-76.

40. Patikoglou, G. and S.K. Burley, *Eukaryotic transcription factor-DNA complexes.* Annu Rev Biophys Biomol Struct, 1997. **26**: p. 289-325.

41. Ferre-D'Amare, A.R., et al., *Recognition by Max of its cognate DNA through a dimeric b/HLH/Z domain.* Nature, 1993. **363**(6424): p. 38-45.

42. Ellenberger, T., et al., *Crystal structure of transcription factor E47: E-box recognition by a basic region helix-loop-helix dimer.* Genes Dev, 1994. **8**(8): p. 970-80.

43. Dang, C.V., et al., *Discrimination between related DNA sites by a single amino acid residue of Myc-related basic-helix-loop-helix proteins.* Proc Natl Acad Sci U S A, 1992. **89**(2): p. 599-602.

44. Kohler, J.J. and A. Schepartz, *Kinetic studies of Fos.Jun.DNA complex formation: DNA binding prior to dimerization.* Biochemistry, 2001. **40**(1): p. 130-42.

45. Banerjee, A., J. Hu, and D.J. Goss, *Thermodynamics of protein-protein interactions of cMyc, Max, and Mad: effect of polyions on protein dimerization.* Biochemistry, 2006. **45**(7): p. 2333-8.

46. Hu, J., A. Banerjee, and D.J. Goss, *Assembly of b/HLH/z proteins c-Myc, Max, and Mad1 with cognate DNA: importance of protein-protein and protein-DNA interactions.* Biochemistry, 2005. **44**(35): p. 11855-63.

47. Halford, S.E. and J.F. Marko, *How do site-specific DNA-binding proteins find their targets?* Nucleic Acids Res, 2004. **32**(10): p. 3040-52.

48. Kohler, J. J., and Schepartz, A. (2001) *Bioorg Med Chem* **9**(9), 2435-2443

49. Metallo, S. J., and Schepartz, A. (1997) *Nat Struct Biol* **4**(2), 115-117

50. Wendt, H., Thomas, R. M., and Ellenberger, T. (1998) *J Biol Chem* **273**(10), 5735-5743

51. Rentzeperis, D., Jonsson, T., and Sauer, R. T. (1999) *Nat Struct Biol* **6**(6), 569-573

52. Kim, B., and Little, J. W. (1992) *Science* **255**(5041), 203-206

53. Park, S., Chung, S., Kim, K. M., Jung, K. C., Park, C., Hahm, E. R., and Yang, C. H. (2004) *Biochim Biophys Acta* **1670**(3), 217-228